Volcanism and tectonism across the inner solar system: an overview

T. PLATZ^{1,2*}, P. K. BYRNE^{3,4}, M. MASSIRONI⁵ & H. HIESINGER⁶

¹Planetary Science Institute, 1700 East Fort Lowell Road, Tucson, AZ 85719-2395, USA

²Freie Universität Berlin, Institute of Geological Sciences, Planetary

Sciences & Remote Sensing, Malteserstrasse 74-100, 12249 Berlin, Germany

³Lunar and Planetary Institute, Universities Space Research Association, 3600 Bay Area Boulevard, Houston, TX 77058, USA

⁴Department of Terrestrial Magnetism, Carnegie Institution of Washington, 5241 Broad Branch Road NW, Washington, DC 20015-1305, USA

⁵Dipartimento di Geoscienze, Universita' degli Studi di Padova, via G. Gradenigo 6, 35131 Padova, Italy

⁶Institut für Planetologie, Westfälische Wilhelms-Universität Münster, Wilhelm-Klemm-Strasse 10, 48149 Münster, Germany

*Corresponding author (e-mail: platz@psi.edu)

Abstract: Volcanism and tectonism are the dominant endogenic means by which planetary surfaces change. This book, in general, and this overview, in particular, aim to encompass the broad range in character of volcanism, tectonism, faulting and associated interactions observed on planetary bodies across the inner solar system – a region that includes Mercury, Venus, Earth, the Moon, Mars and asteroids. The diversity and breadth of landforms produced by volcanic and tectonic processes are enormous, and vary across the inventory of inner solar system bodies. As a result, the selection of prevailing landforms and their underlying formational processes that are described and highlighted in this review are but a primer to the expansive field of planetary volcanism and tectonism. In addition to this extended introductory contribution, this Special Publication features 21 dedicated research articles about volcanic and tectonic processes manifest across the inner solar system. Those articles are summarized at the end of this review.

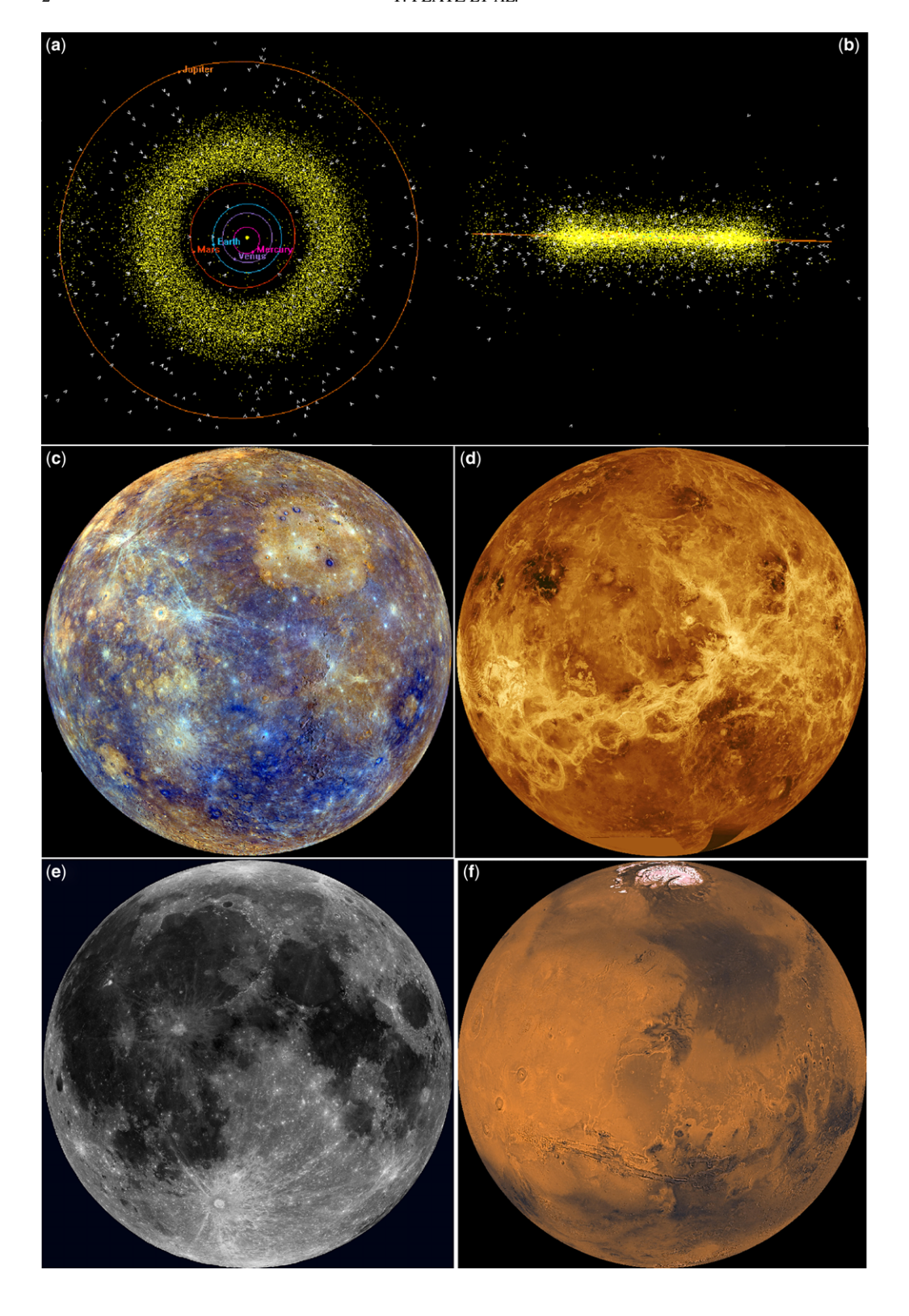
Volcanic and tectonic processes have profoundly shaped the surfaces of terrestrial planets in the inner solar system. Even minor bodies such as asteroids and small moons, where volcanism and tectonism have not played dominant roles, are still affected by fracturing and faulting as a result of other processes like dynamic loading and gravitational collapse. This Special Publication aims to encompass the broad range in character of volcanism, tectonism, faulting and associated interactions observed on planetary bodies across the inner solar system. By collating observations of the Earth and other planetary bodies, the interpretations of extraterrestrial landforms and their formational processes are appraised in the light of our current understanding of comparable processes on Earth.

The inner solar system comprises our star, the Sun, and the four terrestrial planets, Mercury, Venus, Earth and Mars, as well as Mars' moons Phobos and Deimos, and Earth's companion, the Moon (Fig. 1). Although the main asteroid belt, located

between the orbits of Mars and Jupiter, divides our solar system into inner and outer portions, it itself is composed of asteroidal and cometary objects of which a large number enter the inner solar system. Some asteroids have received attention as the result of spacecraft flybys or orbital operations, and for that reason are included briefly in this volume.

In this Special Publication, the journey across the inner solar system begins at the planet closest to the Sun. From Mercury we move to Venus; Earth and its Moon are next, before we move yet further out, to Mars. This celestial journey terminates at the main asteroid belt (Fig. 1).

The first part of this introductory chapter highlights the current knowledge of, and recent discoveries regarding, volcanic and tectonic features and their formational processes on the Moon, Mars, Mercury and Venus. The second part is dedicated to summarizing the major conclusions of articles presented in this volume. In its writing, we have sought not to compose a comprehensive review



per se but, rather, to provide a detailed introduction to the diversity of observed volcanic and tectonic processes present throughout the inner solar system, from which the interested reader may explore further – and farther.

Mercury

Until very recently, Mercury (Fig. 1c) was the most enigmatic of the inner solar system's planets. Its proximity to the Sun rendered telescopic observations of Mercury from Earth difficult, and the planet's location in the Sun's gravity well challenged mission designers. It was not until NASA's Mariner 10 spacecraft flew past the planet in the 1970s that the surface of Mercury was imaged directly for the first time and, even then, only a single hemisphere was observed. Those early data showed the planet's surface to resemble superficially that of the Moon, with ancient, cratered plains interspersed with expanses of younger smooth plains. Yet, unlike its larger terrestrial counterparts, Mercury does not have primary volcanic features, such as the giant shield volcanoes that dominate the Tharsis province on Mars. The volcanic character of Mercury, therefore, remained an open question until the planet was visited by the MErcury Surface, Space Environment, GEochemistry, and Ranging (MESSENGER) mission. However, the tectonics of Mercury were readily visible from the outset of its exploration by spacecraft. Long, clifflike escarpments were observed across the Mariner 10 hemisphere, with wrinkle ridges akin to those in lunar maria populating the planet's smooth plains units. Even so, the spatial extent, styles and amount of tectonic deformation of Mercury are questions that could only be fully explored from orbit. This section describes the current state of knowledge of Mercury's volcanic and tectonic character, places these findings in the context of how our understanding of the innermost planet has evolved, and highlights key aspects of the geological development of Mercury that have yet to be answered.

Volcanism

The three flybys of Mercury by the Mariner 10 spacecraft in 1974–1975 returned images that raised the prospect of volcanism on the innermost planet. Smooth plains deposits were identified across the approximately 45% of the planet observed during that mission; some workers interpreted their large volumes, together with their embayment relationships with, and spectral distinctiveness from, surrounding terrain, as evidence for a volcanic origin for these deposits (Murray et al. 1975; Strom et al. 1975; Dzurisin 1978; Kiefer & Murray 1987; Robinson & Lucey 1997). Yet, others argued that Mercury's smooth plains units were morphologically similar to lunar highland plains, which were shown to have been emplaced as fluidized ejecta (Wilhelms 1976; Oberbeck et al. 1977). The provenance of smooth plains on Mercury therefore remained unresolved until the three flybys of the MESSENGER spacecraft in 2008-2009 (Fig. 1c).

Smooth plains. MESSENGER imaged almost the entire surface of Mercury during its flybys, and showed the smooth plains to be a globally present unit, the majority of which is volcanic in nature (Fig. 2). This inference is based on superposition relations indicative of the sequential embayment of impact basins and ejecta, as well as spectral homogeneity but colour variation, partially buried impact structures, and thicknesses of hundreds to thousands of metres (Head et al. 2008, 2009; Denevi et al. 2009). Observations made after MESSENGER entered orbit about the planet in March 2011 have allowed for the spatial extent of Mercury's smooth plains to be quantified (Denevi et al. 2013): these plains are now known to occupy some 27% of the surface of Mercury (Fig. 2). Notably, the single largest contiguous smooth plains unit on the planet has been identified at high northern latitudes (Head et al. 2011). Occupying around 6% of the total planet surface, this region has been termed the northern volcanic plains (NVP) (Fig. 3a).

Fig. 1. The principal components of the inner solar system include the four terrestrial planets, Mercury, Venus, Earth and Mars, as well as Earth's moon and the two moons of Mars. The main asteroid belt separates the inner and outer portions of the solar system. On a yet smaller scale are objects that come close to Earth's neighbourhood (on astronomical scales) or cross Earth's orbit; these are collectively termed Near Earth Objects (NEO). At time of writing, there are 11 057 NEAs, of which 861 are larger than 1 km in diameter. (a) View of the inner solar system from above the ecliptic plane. The yellow dots denote Near Earth Asteroids; white triangles denote Near Earth Comets (courtesy of P. Chodas; 1 April 2014; NASA/JPL; http://neo.jpl.nasa.gov). (b) View of the inner solar system from the edge of the ecliptic plane. The orange line represents Jupiter's orbit (courtesy of P. Chodas; 1 April 2014; NASA/JPL; http://neo.jpl.nasa.gov). (c) Enhanced colour mosaic of Mercury in orthographic projection centred at 0° (wide-angle camera of the Mercury Dual Imaging System; NASA/John Hopkins University Applied Physics Laboratory/Carnegie Institution of Washington). (d) Global view of Venus centred at 180°E (Magellan Synthetic Aperture Radar Mosaic; NASA/JPL). (e) Nearside view of the Moon (Lunar Reconnaissance Orbiter wide-angle camera mosaic; NASA/JPL/USGS).

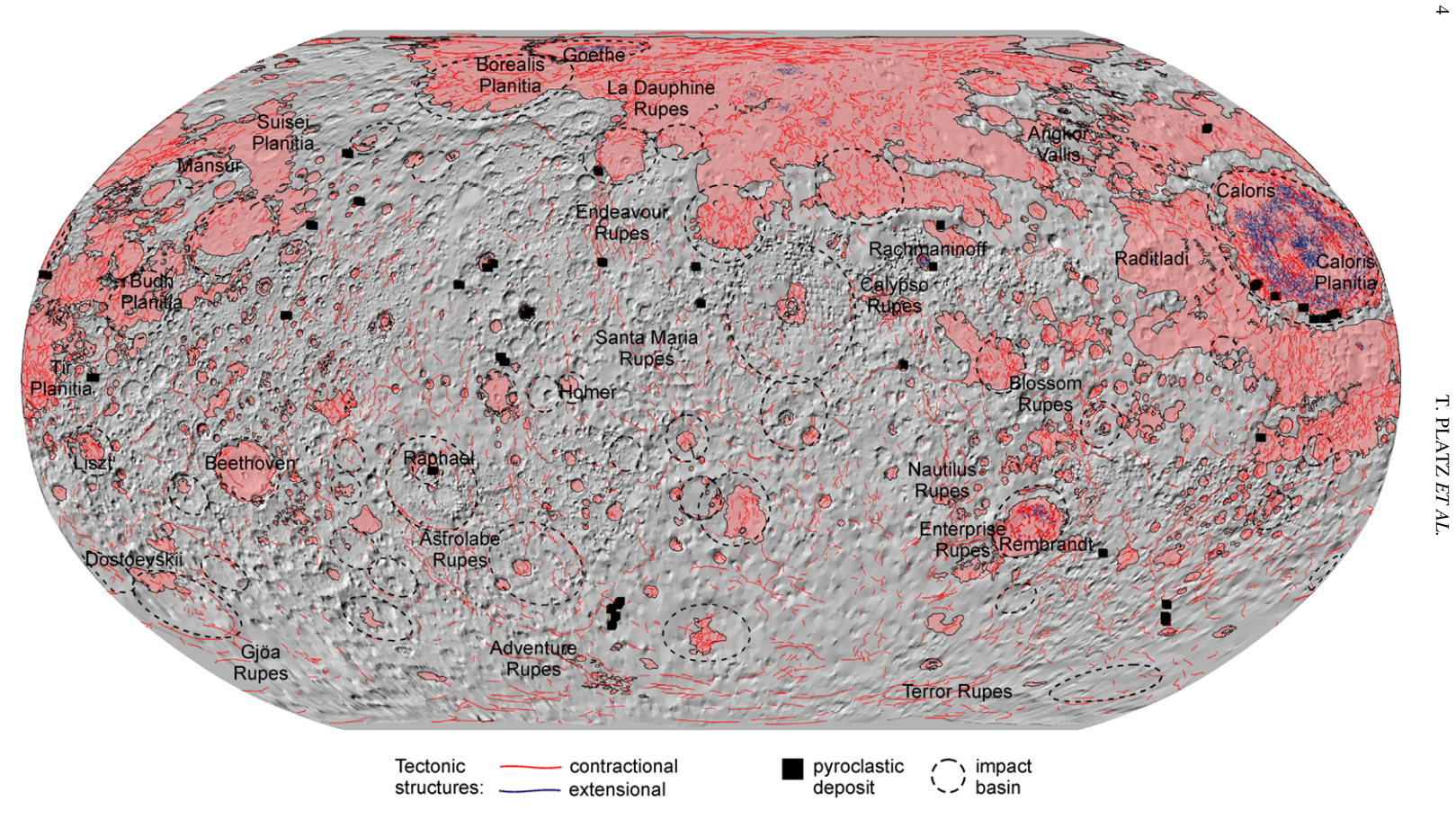


Fig. 2. All mapped tectonic structures on Mercury. Contractional (red lines: Byrne *et al.* 2014*b*) and extensional (blue lines: Byrne *et al.* 2013*d*) are shown, as well as the smooth plains units mapped by Denevi *et al.* (2013). Black squares represent the locations of pyroclastic deposits (Kerber *et al.* 2011*a*). Only impact basins > 300 km in diameter (dashed ellipses) are highlighted for clarity (Fassett *et al.* 2011). Topography is from the controlled Mercury Dual Imaging System (MDIS) wide-angle camera global base map (2.7 km/px; Becker *et al.* 2012). The map is shown in a Robinson projection, centred at 0°E.

The NVP is not obviously related to one or more large impact basins, although an origin due to impact cannot be discounted (Byrne et al. 2013b). Nevertheless, these plains, emplaced near the end of the Late Heavy Bombardment (LHB) of the inner solar system at around 3.7-3.8 Ga, were likely to have formed in a single, voluminous event associated with extensive partial melting of Mercury's mantle (Head et al. 2011). The NVP hosts a variety of landforms characteristic of the planet's physical volcanological character in general. Numerous 'ghost craters', impact structures that predate the emplacement of the plains and that are partially to almost entirely filled with lava, are widespread throughout the NVP. Features interpreted to be lava flow fronts have also been identified throughout the region, often as linear, lobate contacts that embay older, more heavily textured terrain (Head et al. 2011).

Valles. One of the most notable types of landform spatially associated with the NVP is a set of five broad channels (or 'valles') located to the SE of the region. These channels, morphologically distinct from any other trough-like depression identified on Mercury, connect regions of smooth plains through surrounding older terrain, and are typified by steep, linear edges and smooth floors that feature rounded islands aligned with the long axes of the channels (Byrne *et al.* 2013c). In one case, at the end of Angkor Vallis, a group of such islands forms a 'splay'-like pattern as the channel opens into the adjoining Kofi basin (Fig. 3b). Four of the valles are orientated approximately radial to the 1640 kmdiameter Caloris basin, and may have originally been impact-sculpted furrows carved by ballistically emplaced ejecta during the formation of that basin (Byrne et al. 2013c). Some combination of thermal and mechanical lava erosion, probably by voluminous, high-temperature, low-viscosity flows, then probably shaped the troughs to the forms the channels have today (Byrne et al. 2013c; Hurwitz et al. 2013b).

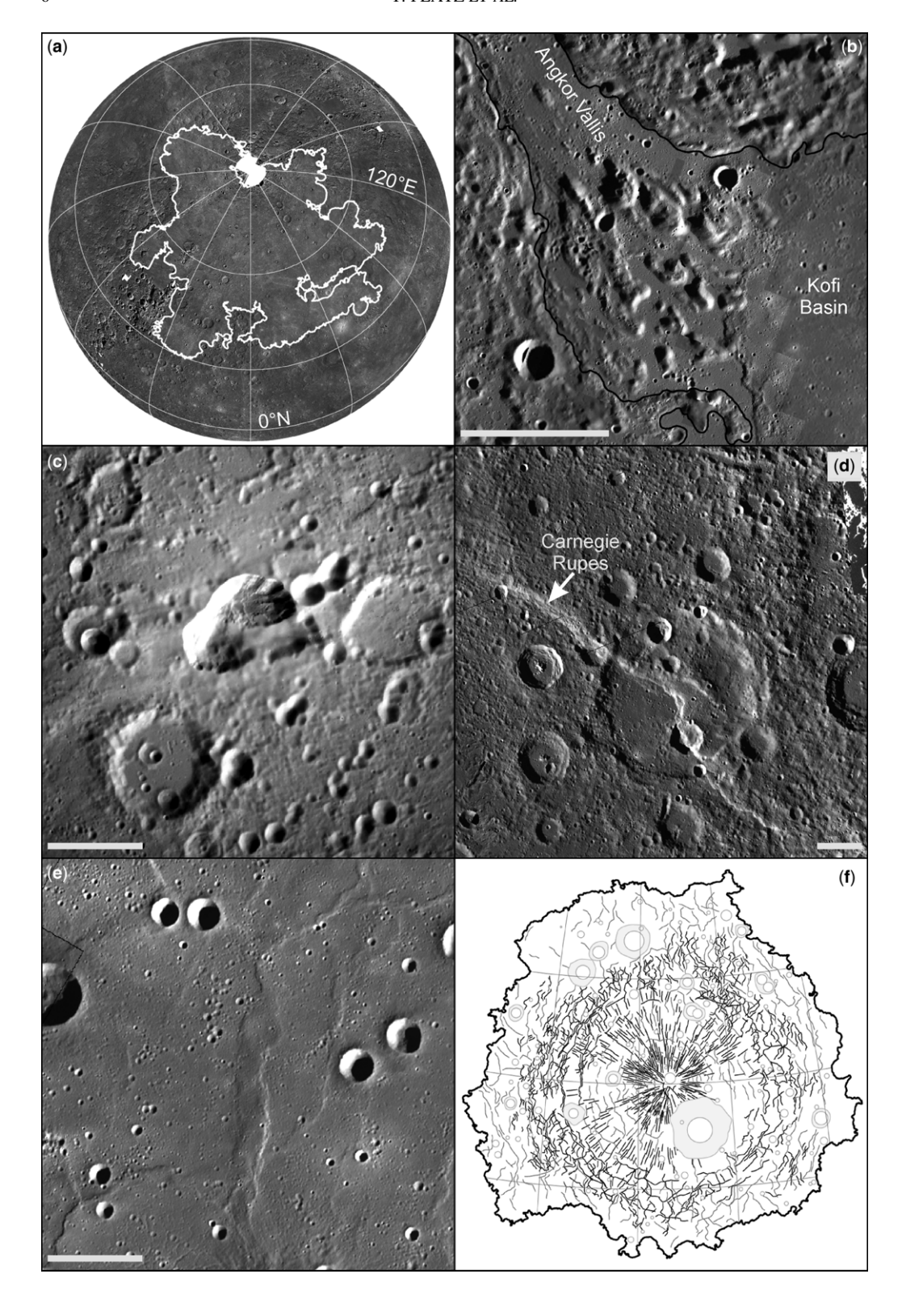
Taken together, these observations attest to a predominance of flood-mode lava emplacement for the majority of Mercury's smooth plains units. This inference is consistent with geochemical data returned by MESSENGER's X-ray spectrometer (XRS) instrument, which indicate that the planet's surface is relatively rich in Mg but poor in Al, Ca and Fe, relative to terrestrial and lunar basalts (Nittler *et al.* 2011). Mercury's surface therefore probably has a bulk composition intermediate between low-Fe basalt and high-Mg ultramafic lithologies. Moreover, on-going XRS observations suggest a compositional difference between the NVP and the surrounding plains (Stockstill-Cahill *et al.* 2012; Weider *et al.* 2012). The last widespread

volcanism on Mercury was therefore effusive, with MESSENGER observations indicating that some such activity, albeit highly spatially localized, may have occurred as recently as around 1 Ga (Prockter *et al.* 2010; Marchi *et al.* 2011).

Pyroclastic volcanism. Mercury is not without explosive volcanism. Evidence for pyroclastic activity has been identified at numerous sites across the planet, in the form of irregularly shaped depressions without raised rims that are often located atop low, broad rises. These features frequently appear to be coalesced from smaller, overlapping depressions and are typically encircled by haloes of high-reflectance material with a steeper spectral slope over visible to near-infrared wavelengths (and so they appear redder) than most of Mercury's surface. These haloes have been interpreted as proximal deposits of fine-grained pyroclastic material (Head et al. 2009; Kerber et al. 2009, 2011a) (Figs 2 & 3c). The Caloris basin hosts a number of such 'red'-haloed depressions, particularly along its southern margin (Head et al. 2009). Some of these depressions may, in fact, be long-lived loci of explosive eruptive activity, whose locations have been influenced by the underlying structural fabric of the Caloris basin (Rothery et al. 2014).

It should be noted that irregular, coalesced depressions occur across Mercury without red halos. For example, numerous impact craters across the planet host central 'pits' on their floors (and so are termed pit-floor craters), which appear unrelated to the impact process itself. Gillis-Davis et al. (2009) investigated the morphology, structural association, relative age and proximity to smooth plains units of seven such pit craters, and concluded that they formed through collapse into underlying magma chambers. A similar mechanism has been inferred for the origin of several non-impact craterhosted depressions within the broad channel network proximal to the NVP (Byrne et al. 2013c). Such pits therefore represent a third form of surficial igneous activity on Mercury, in addition to pyroclastic and effusive eruptions (Gillis-Davis et al. 2009).

Cratered plains. What of Mercury's older terrain? Trask & Guest (1975) classified Mercury's non-smooth plains surface portions as either 'intercrater plains' or 'heavily cratered terrain'. Intercrater plains were interpreted to be the oldest surviving surface unit, its emplacement even predating the end of the LHB, whereas heavily cratered terrain described large craters, basins and their deposits. Despite the lack of primary volcanic landforms on Mercury (e.g. large shield volcanoes), Strom et al. (1975) considered their great volumes as evidence that these plains were formed by volcanism.



Indeed, there is a lower density of 100 km-diameter craters on Mercury than on the Moon (Strom & Neukum 1988; Fassett *et al.* 2011), and the oldest surviving terrain on Mercury is no older than 4.1 Ga (Marchi *et al.* 2013). These findings reinforce a geological history for the innermost planet that features global resurfacing due to volcanism before the end of the LHB. If so, then the majority of Mercury's surface – that portion consisting of smooth plains, intercrater plains and heavily cratered terrain – is dominantly volcanic.

A further observation is that the majority of smooth plains deposits are collocated with impact structures (Byrne et al. 2013b). This is best expressed by the expansive interior Caloris smooth plains deposits (Strom et al. 1975), and by smooth plains within other large impact basins such as Rembrandt, Beethoven and Tolstoj (Fig. 2). Although there is no consensus as to the existence of a causal link between the impact process and volcanism (Ivanov & Melosh 2003; Elkins-Tanton & Hager 2005), the impact process removes overburden, introducing thermal energy to the lithosphere, and resets pervasive regional- or global-scale stresses (see the next section) (Byrne et al. 2013b). This last point is particularly relevant to Mercury, since the global contraction of the planet (see the next section) will put the lithosphere into a pervasive state of net compression, inhibiting voluminous surface volcanism (e.g. Solomon 1977; Klimczak 2013). Whatever the mechanism responsible for the generation of large volumes of partial melt that then pools within impact structures - even if such structures penetrate to existing magma chambers or asthenospheric melts, or simply represent the shortest path for ascending magma to reach the surface the presence of large craters and basins may have played a key role in the last phase of extensive volcanic resurfacing on Mercury.

Tectonism

A key observation made of Mercury with Mariner 10 data was the extent to which the planet's surface has been tectonized. Evidence for both crustal shortening and lengthening was identified,

with the former process the overwhelmingly dominant style of deformation (Strom *et al.* 1975). Although Mariner 10 viewed less than half of Mercury's surface, the inference that such deformation was global in nature was confirmed when MESSENGER imaged the entire planet (Figs 1c & 2). To first order, crustal shortening has occurred universally across all surface units of the innermost planet and is manifest as one of two primary classes of structure (lobate scarp or wrinkle ridge) (e.g. Strom *et al.* 1975; Watters *et al.* 2009), whereas extension, in the form of graben, is restricted to volcanically flooded impact structures (e.g. Strom *et al.* 1975; Byrne *et al.* 2013*d*).

Lobate scarps. Lobate scarps are, in terms of overall length and accumulated relief, the larger of the two principal expressions of crustal shortening on Mercury. Like their counterparts on Mars and the Moon (e.g. Mueller & Golombek 2004), they are characterized by a steeply sloping scarp face and a gently sloping back limb (Fig. 3d), and probably represent a monocline or asymmetrical hangingwall anticline atop a blind or surface-breaking thrust fault. Mercury's lobate scarps range in length from 9 to 900 km, and in places have accumulated some 3 km of relief (Byrne et al. 2014b). Although lobate scarps are superficially similar in morphology to inferred lava flow fronts (Head et al. 2011), their generally linear plan form, transection relationships with craters and surrounding terrain, and their cross-cutting of craters with orthogonal horizontal offsets support a tectonic origin for the overwhelming majority of such scarps (e.g. Strom et al. 1975). A less commonly observed form of scarp, termed a high-relief ridge, also occurs on Mercury (Dzurisin 1978; Watters et al. 2009). High-relief ridges are generally narrower than, but often transition into, lobate scarps, such that delineating these ridges from other structures is difficult.

Wrinkle ridges. Wrinkle ridges, by comparison, are substantially smaller landforms. Like on other terrestrial worlds, they are typically manifest on Mercury as broad, low-relief arches with opposite-facing leading edges, often superposed by a

Fig. 3. Examples of key volcanic and tectonic landforms on Mercury. (a) The northern volcanic plains (NVP) on Mercury (outlined in white) occupy some 6% of the planet's surface (Head *et al.* 2011). (b) Several valles occur proximal to the NVP, shaped by high-temperature, low-viscosity lavas. Here, lava flowing through Angkor Vallis into the Kofi basin has formed a 'splay'-like pattern of erosional remnants (Byrne *et al.* 2013*c*). (c) An example of an irregular depression, surrounded by a halo of high-albedo, fine-grained material interpreted as a pyroclastic vent (Kerber *et al.* 2009). This example lies between the Rachmaninoff and Copland basins. (d) A prominent lobate scarp, Carnegie Rupes, in Mercury's northern hemisphere; contrast its size and morphology with that of the wrinkle ridge, situated in the NVP, shown in (e). (f) Structural sketch of the tectonic structures within the Caloris basin (Byrne *et al.* 2013*d*). Ridges and scarps are shown in black, whereas graben are shown in grey. Superposed craters and their ejecta deposits are also shown. Azimuthal equidistant projections centred as follows: (a) 0°N, 70°E; (b) 57°N, 124.2°E; (c) 35.7°N, 64.1°E; (d) 59.1°N, 304.5°E; (e) 61.4°N, 49.9°E; and (f) 30°N, 161°E. Scale bar in (b)–(e) is 30 km.

narrow ridge (Fig. 3e). Although the dimensions of wrinkle ridges across the planet vary, they are usually tens to hundreds of metres in height and several kilometres in length, and occur in long, subparallel groups or in complex map patterns (Byrne et al. 2014b). Wrinkle ridges are likely to form due to some combination of faulting and folding but the orientations and depths of the causative faults, and the contribution to ridge formation played by folding, remain open questions (e.g. Golombek et al. 1991; Plescia 1993; Zuber 1995; Schultz 2000). Moreover, although wrinkle ridges appear to accommodate small amounts of shortening relative to lobate scarps (e.g. Plescia 1993) on all planets, debate continues regarding their subsurface structure and whether their faults penetrate to tens of kilometres (i.e. 'thick-skinned deformation': Zuber 1995; Golombek et al. 2001; Montési & Zuber 2003) or only the upper few kilometres of the lithosphere (i.e. 'thin-skinned deformation': Watters 1991; Mangold et al. 1998).

Graben. Where it has occurred, crustal lengthening on Mercury has been accommodated by linear, topographical troughs that are interpreted as graben (i.e. sets of antithetic normal faults) (e.g. Strom et al. 1975). Graben are typically 5-10 km long and up to 1 km wide, although some examples are larger (Klimczak et al. 2012; Watters et al. 2012). Some graben appear isolated and show no evidence of having interacted with other such structures, and display a characteristic continuous deepening of their floor towards the centre, whereas others are segmented or linked (Klimczak et al. 2012). Most graben show a generally constant displacement along their lengths, implying that the development of their component-normal faults was confined to a mechanical layer of limited thickness (Klimczak et al. 2012, 2013).

Distribution of tectonics. The tectonic deformation of Mercury is global but the distribution of different classes of structure is far from uniform (Fig. 2). In their global survey of contraction on the innermost planet, Byrne et al. (2014b) characterized shortening structures according to the primary terrain type in which they occur. Adopting the nomenclature of Trask & Guest (1975), the surface of Mercury can be described as consisting of smooth plains and cratered plains (the latter term incorporating both the intercrater plains and heavily cratered terrain units described from images returned by Mariner 10). Smooth plains structures overwhelmingly consist of wrinkle ridges, and represent about two-thirds of the almost 6000 shortening structures mapped on the planet. Over 1500 ridges were identified in the NVP alone, with the remainder situated within the circum-Caloris

plains or in smaller smooth plains deposits that occur in more heavily cratered terrain. In contrast, cratered plains structures are almost entirely lobate scarps, and represent about one-third of all mapped shortening structures.

In some cases, shortening structures demarcate volcanically filled or buried impact features. For example, wrinkle ridges can delineate the rims of buried craters (i.e. the Type-1 'ghost craters' described by Klimczak *et al.* 2012), particularly in the NVP, whereas lobate scarps situated within impact basins can follow, and verge outwards in the direction of, the basin perimeter (Byrne *et al.* 2014*b*). Moreover, approximately 100 lobate scarps border areas of high-standing terrain on Mercury and verge onto surrounding lows; these structures have some of the greatest accumulated relief of any tectonic landform on Mercury (Byrne *et al.* 2014*b*).

Earlier studies of Mercury's tectonics suggested that Mercury's lithospheric fracture pattern might contain evidence for ancient global stress states resulting from, for example, tidal despinning (Melosh & Dzurisin 1978; Melosh & McKinnon 1988). Byrne et al. (2014b) did not identify such a globally coherent pattern but did note that in places their structural survey was probably influenced, in part, by lighting geometry (Mercury has a remarkably low obliquity of c. 2 arcmin). Even so, in places there are systematic patterns of regionalscale deformation, where ridges and scarps form laterally contiguous, narrow bands of substantial length. These narrow zones of concentrated crustal shortening are Mercury's equivalent to the foldand-thrust belts of Earth (Byrne et al. 2014b).

Planetary radius change. The widespread distribution of lobate scarps on Mercury implies that their formation is linked to a process that is global in scale. Thermal models for the innermost planet require a substantial contraction in response to secular cooling of the planet's interior (e.g. Solomon 1977; Schubert et al. 1988). It is this contraction, and the resultant horizontal compression of the planet's lithosphere, that probably formed the lobate scarp population observed today. Importantly, the morphology of lobate scarps can be used to estimate their contribution to planetary radius change (a direct measure of planetary contraction), wherein their relief is related to their horizontal component of shortening using an assumed fault dip.

There has been a long-standing disagreement between estimates of radius change made from photogeological studies of Mercury's brittle structures (e.g. Strom *et al.* 1975; Watters *et al.* 1998, 2009; Di Achille *et al.* 2012) and those predicted by thermal evolution models (e.g. Solomon 1977; Dombard & Hauck 2008), with those from the first

approach typically about 1–3 km but those from modelling of the order of 5–10 km. The availability of global imaging and topographical data for Mercury from the MESSENGER mission, however, has enabled this issue to be resolved: Byrne *et al.* (2014*b*) have shown that the portion of radius change accommodated by tectonic structures is at least 5–7 km, bringing into accord photogeological observations and thermal history models. This finding is of importance to on-going studies of Mercury's bulk silicate abundances of heat-producing elements, mantle convection, and the cooling and present-day structure of the planet's large metallic core.

The provenance of Mercury's wrinkle ridges is not as obviously linked to global contraction as are its lobate scarps. Because they are generally associated with volcanic units within impact structures, subsidence of volcanic infill may play a dominant role in their formation (e.g. Watters *et al.* 2009; Byrne *et al.* 2013*d*), as has been suggested for wrinkle ridges within volcanic units on the Moon (e.g. Melosh 1978) and on Mars (e.g. Zuber & Mouginis-Mark 1992). However, given their small size relative to lobate scarps, removing the contribution of wrinkle ridges to Mercury's global contraction results in a change in radius only around 10% lower than that calculated for all structures.

Tectonics within impact structures. Whereas the widespread smooth and cratered plains structures attest to global crustal shortening, extension on Mercury is almost exclusive to volcanically in-filled craters and basins (Murchie et al. 2008; Watters et al. 2009; Byrne et al. 2013d). However, the complexity of extensional deformation varies considerably, and increases within progressively larger impact structures. For example, many ghost craters on Mercury, tens of kilometres across, contain sets of graben in their interior that have no preferred orientation and so form polygonal block patterns; these ghost craters may also feature graben superposed on (and following the strike of) the wrinkle ridges that outline the ghost crater rim (Klimczak et al. 2012). Several medium-sized basins on the planet also feature interior graben that show no preferred orientations, such as the 230 km-diameter Mozart basin, although some graben in this basin appear concentric to its perimeter (Blair et al. 2013). Yet, with an increase in basin diameter, the pattern of interior extension becomes even more complex: the 750 km-diameter Rembrandt basin features collocated basin-radial graben and wrinkle ridges, which are bound to the north by circumferential graben (and ridges) (Byrne et al. 2013d).

However, the greatest structural complexity of all occurs within the Caloris basin, where a prominent set of radial graben (termed Pantheon Fossae) dominates the basin interior, is superposed by basincircumferential ridges and is bound by a nearcomplete annulus of circumferential graben located at about half a basin radius from the centre of Caloris (Byrne *et al.* 2013*d*). Beyond this annulus, graben once more lack a preferred orientation, and, forming a polygonal map pattern, steadily decrease in width, depth and length towards the basin rim (Fig. 3f).

Finite-element models show that the thermal contraction of thick, rapidly emplaced lava flows produces quasi-isotropic horizontal stresses that promote the formation of graben with mixed orientations, such as those observed within ghost craters and medium-sized basins on Mercury (Freed et al. 2012; Blair et al. 2013). This process may also account for the mixed orientations of graben within Caloris. Moreover, such models also show that graben can nucleate atop ghost-craterdelineating wrinkle ridges (Freed et al. 2012) and over buried basin rings (Blair et al. 2013), which may account for the circumferential graben within Caloris. As yet, however, there is no consensus for the origin of the remarkable Pantheon Fossae (Klimczak et al. 2013), although previous studies suggested that they may have formed due to dyke propagation (Head et al. 2008) or to flexural uplift of the basin centre, in response either to the volcanic emplacement of the circum-Caloris smooth plains (Freed et al. 2009) or to the inward flow of the lower crust (Watters et al. 2005).

Venus

The major findings on Venus' composition, volcanic forms and tectonic structures have been obtained mainly by analysing data from the late 1970s and 1980s, together with Magellan radar images (Figs 1d & 4). Nevertheless, Venus has always been of particular interest due to its Earth-like size, mass and internal structure, despite great differences between the physiography of the two planets. The main reason for this discrepancy is probably the apparent lack of plate tectonics on Venus, which is interpreted to be due to the planet's water-depleted bulk composition. For that reason, the following subsection starts by addressing Venus' general geodynamics, which serve as a basis from which to cover specific aspects of its tectonic and volcanic character.

Tectonics

Venus as a one-plate planet. Water, and its capacity to weaken rock, is essential in governing lithospheric rheology on Earth. Together with temperature, water is the major actor responsible for

defining the thickness and strength of the elastic lithosphere, its decoupling from the deeper asthenosphere and, hence, plate tectonic onset and development. The absence of water on Venus' surface due to the high surface temperatures (460 °C on average: e.g. Lewis 2004), coupled with the dehydrated character of its interior as a result of extensive volcanic degassing (Kaula 1990; Grinspoon 1993; Smrekar & Sotin 2012), precludes plate tectonics on the planet (e.g. Smrekar *et al.* 2007; McGill *et al.* 2010).

The lack of Venusian plate tectonics is also implied by the global dominance of a basaltic composition of the crust, with limited possible exceptions on the highlands (Terrae) (Surkov 1983; Hashimoto et al. 2008; Helbert et al. 2008). A dehydrated, stiff diabasic crust prevents the onset of lithospheric break-up and ensuing subduction; moreover, dry systems possess a highly viscous and water-depleted mantle, which precludes any asthenosphere-lithosphere decoupling (Kohlstedt & Mackwell 2010; Huang et al. 2013), a process that modulates relative plate motions on Earth (e.g. McKenzie 1967; Isacks et al. 1968; Morgan 1968; Ranalli 1995, 1997; Gung et al. 2003; Scoppola et al. 2006; Anderson 2007; Doglioni et al. 2007, 2014; Fischer et al. 2010). The main consequence of a globally continuous lithosphere are a conductive stagnant lid on top of a convective and viscous deep mantle (Moresi & Solomatov 1998; Reese et al. 1999; Solomatov & Moresi 2000; O'Rourke & Korenaga 2012; Smrekar & Sotin 2012), and planetary tectonics that directly reflect underlying mantle processes (e.g. Smrekar & Phillips 1991; Herrick & Phillips 1992; Bindschadler et al. 1992; Kohlstedt & Mackwell 2010; Huang et al. 2013).

On Venus then, planetary cooling is achieved through both conduction across a stagnant lid and advection by mantle plumes, whose surface expressions are well represented by a great variety of volcanic forms (e.g. volcanic rises, coranae and shield volcanoes) (Solomon & Head 1982; Morgan & Phillips 1983; Smrekar & Parmentier 1996; Schubert et al. 1997; Hansen & Olive 2010). Compared with plate tectonics, however, near-surface conduction and deep advection are regarded as less efficient than mantle convection in cooling a terrestrial planet whose mass and heat production is thought to be more or less equal to that of Earth. The result, therefore, is the heating up of the mantle, with a consequent increase in mantle dynamics and volcanism that may ultimately lead to periodical global resurfacing and overturn (e.g. Parmentier & Hess 1992; Turcotte 1993; Nimmo & McKenzie 1998; Reese et al. 1999; Turcotte et al. 1999), as suggested by the low-density and nearly uniform distribution of craters on the surface of Venus.

These craters give an average age of between 500 and 800 Ma for almost the entire surface of Venus (Schaber *et al.* 1992; Strom *et al.* 1994; McKinnon *et al.* 1997; Campbell 1999), far younger than the scarred surfaces of Mercury or the Moon.

The topography of Venus is one of the principal pieces of evidence for the absence of modern plate tectonics on that planet. Unlike Earth, which is characterized by the classic ocean-continent bimodal hypsometry, Venus shows a unimodal hypsometric function, with over 80% of the surface covered by plains (Planitiae) and only 8% of the surface at elevations greater than 2 km above the datum. These uplands are in turn subdivided into Terrae and Regiones, with Regiones having more moderate relief than the Terrae (Fig. 4) (Banerdt et al. 1997; Tanaka et al. 1997).

Also, unlike Earth, the strong correlation between free-air gravity and topography, and the high gravity anomaly/relief ratios of some positive topographical features, indicate that topographical variations on Venus are deeply compensated through upwelling and downwelling processes within the mantle (e.g. Smrekar & Phillips 1991; Solomon 1993; McGill et al. 2010). This implies the absence of an Earth-like asthenosphere-lithosphere decoupling, as predicted for a dehydrated planetary lithosphere, and points to a direct correlation between crustal deformation and the upwellingdownwelling convective motions of the mantle (e.g. Kiefer & Hager 1991; Smrekar & Phillips 1991; Solomon 1993). Hence, dome-shaped Regiones (i.e. elevated expanses) associated with broad free-air gravity anomalies (e.g. Beta, Atla and Eislta Regiones), together with great compensation depths, have been interpreted as volcanic rises directly related to underlying mantle plumes. Moreover, the enigmatic Artemis, a feature 2400 km in diameter, may be the largest mantle-plume-derived landform in the solar system (Hansen & Olive 2010). Therefore, Venus is thought to be essentially dominated by vertical tectonism (e.g. Phillips & Malin 1983; Campbell et al. 1984; Kiefer & Hager 1991; Senske et al. 1992; Smrekar 1994; Solomon 1993; Smrekar & Parmentier 1996; Smrekar et al. 1997).

On the other hand, some extensive and highly deformed highlands on Venus, termed crustal plateaux (e.g. Ishtar and Aphrodite Terrae and Alpha, Ovda, Thetis, Phoebe and Tellus Regiones), are associated with low gravity anomalies and a low gravity/topography ratio, which are indicative of a shallow depth of compensation and a thickened, low-density crust (Bindschadler *et al.* 1992; Smrekar & Phillips 1991; Kucinskas *et al.* 1996; Simons *et al.* 1997). The two main hypotheses proposed to explain such peculiar geophysical signatures invoke either downwelling or upwelling mantle flows. According to the downwelling model,

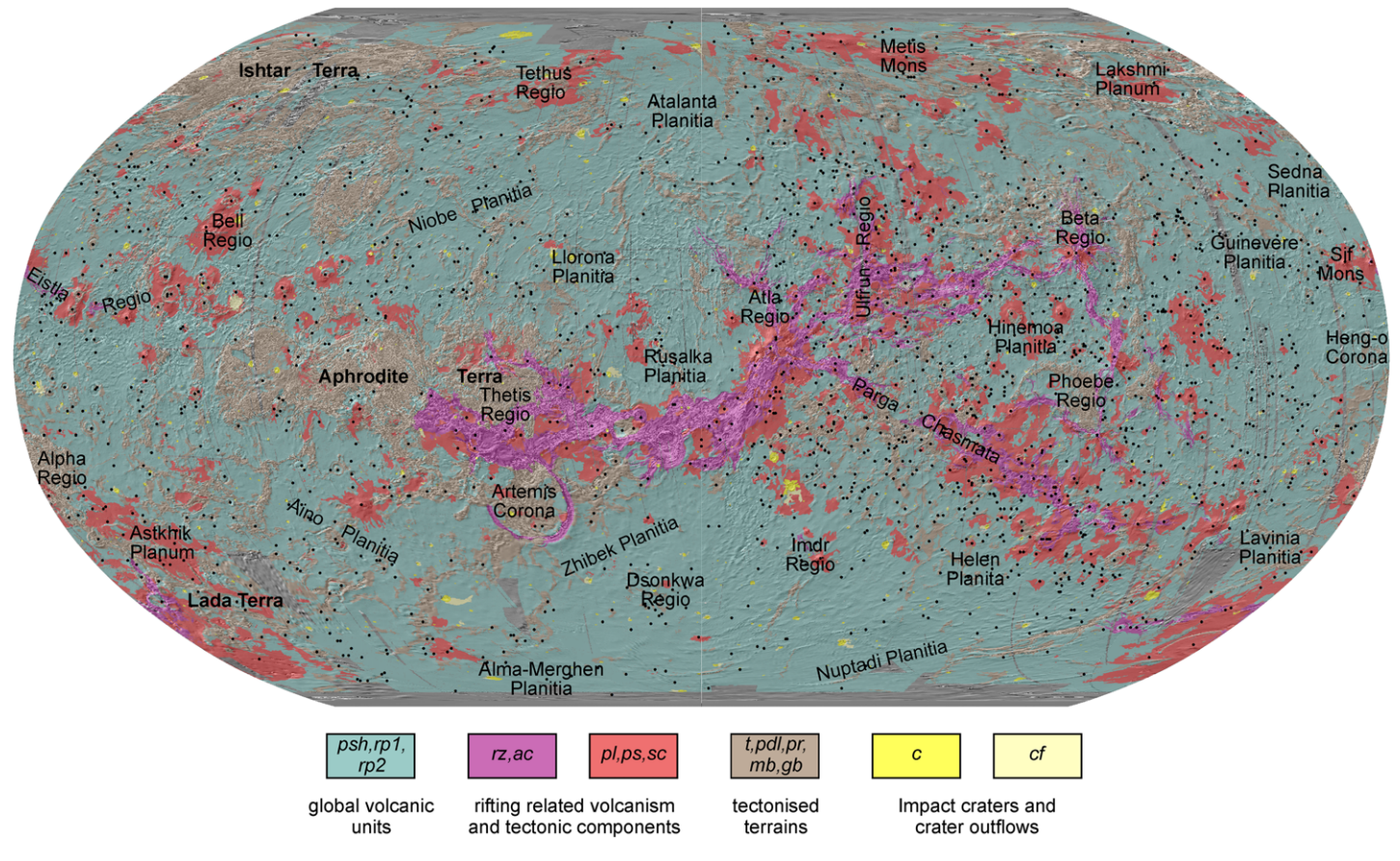


Fig. 4. Simplified geological map of Venus, modified after Ivanov & Head (2011). From that original source, the following units were merged to represent: (1) tectonized terrains – units t (tessera, Fortuna Formation), pdl (densely lineated plains, Atropos Formation), pr (ridged plains, Lavinia Formation), mb (mountain belts, Akna Formation) and gb (groove belts, Agrona Formation); (2) global volcanic terrains – units psh (shield plains, Accruva Formation), rpl (regional plains 1, Rusalka Formation) and rp2 (regional plains 2, Ituana Formation); (3) rifting-related terrains – units pl (lobate plains, Bell Formation), ps (smooth plains, Gunda Formation) and sc (shield clusters, Boala Formation); and (4) tectonic components related to (3) – units rz (rift zones, Devana Formation) and ac (Artemis Canyon materials). Impact craters and crater outflows are shown as units c and cf, respectively. Individual tectonic structures are omitted for clarity. Black dots represent the locations of volcanic edifices (Head et al. 1992). Grey areas correspond to the radar-based hillshade (i.e. no mapping data available). The geological map is superimposed on a Magellan Global Topography Data Record shaded relief map (4.6 km/px) shown here in a Robinson projection, centred at 0°E.

crustal thickening and plateau formation is achieved through accretion of a thin primordial lithosphere by downwelling of a cold mantle diapir (Bindschadler & Parmentier 1990; Bindschadler & Head 1991; Bindschadler et al. 1992; Gilmore & Head 2000; Marinangeli & Gilmore 2000). In contrast, upwelling may accomplish crustal thickening and plateau formation through magmatic underplating above a laterally spreading hot plume (Grimm & Phillips 1991; Phillips et al. 1991; Hansen & Willis 1998; Phillips & Hansen 1998; Ghent & Hansen 1999). The latter hypothesis is consistent with the evidence of low-density felsic rocks within crustal plateaux (Basilevsky et al. 1986, 2012; Nikolaeva et al. 1992; Jull & Arkani-Hamed 1995; Arkani-Hamed 1996; Hashimoto et al. 2008; Helbert et al. 2008; Mueller et al. 2008; Harris & Bédard 2014a), which could have been generated by hightemperature plumes in an earlier, wetter environment on Venus (McGill et al. 2010; Shellnutt 2013). Upwelling in response to bouyant melt formed by the impact of large bolides (c. 20–30 km in diameter) may have contributed to the formation of crustal plateaux and tesserated terrain (Hansen 2006).

However, the upwelling model cannot explain the widespread contractional tectonics observed at some plateau margins nor the complex compressional-extensional deformation recorded on crustal plateaux within so-called tesserae terrains (Ivanov & Head 1996; Gilmore et al. 1998; Romeo et al. 2005; Hansen & López 2010). On the other hand, the downwelling hypothesis fails to explain the flat-topped topography of plateaux, and, further, it requires an excessive amount of time for crustal thickening (Lenardic et al. 1995; Kidder & Phillips 1996). Interestingly, a recent model suggests that crustal plateaux (and tesserae terrains across Venus' surface) might represent buoyant continental crust remnants that were spared from catastrophic overturns due to their inherent buoyancy, and that thereafter were involved in cycles of compressional and extensional tectonism as a function of the evolving continental crust/lithosphere mantle thickness ratio (Romeo & Turcotte 2008). This last model is not strictly an alternative to the upwelling hypothesis as it still allows that the continental crust on Venus could have originated, and then be developed, through felsic magma production atop hot mantle plumes.

Rift systems and extensional deformation. Despite the absence of plate tectonics on Venus, the planet still hosts Earth-like rift systems called chasmata that extend for several thousand kilometres across its surface (e.g. Devana, Ganis, Daiana/Dali, Hecate and Parga Chasmata) (Fig. 4). These structures have been interpreted as linear zones of mantle

upwelling and lithospheric extension, in several cases punctuated by single plumes or plume clusters manifest as volcanic rises, shield volcanoes, coronae and radiating graben–fissure systems (e.g. Schaber 1982; Head & Crumpler 1987; Hansen & Phillips 1993; Baer *et al.* 1994; Hamilton & Stofan 1996; Aittola & Kostama 2000; Magee & Head 2001; Stofan *et al.* 2001; Krassilnikov & Head 2003; Harris & Bédard 2014*a*). On the basis of structural observations and gravitational data, further major extensional rifts have been proposed to follow plains' depressions that were later covered by volcanic materials (Sullivan & Head 1984; Harris & Bédard 2014*b*).

Extensional deformation is widespread on planitiae, and commonly manifest as graben that appear generally associated with plume diapirism and volcanic centres (McGill *et al.* 2010). Graben that form polygonal patterns are also present on Venus, with that pattern being attributed variously to cooling–heating cycles induced by subsurface dynamics (Johnson & Sandwell 1992) or to climate changes (Anderson & Smrekar 1999; Smrekar *et al.* 2002).

Mountain belts. The large number of Venusian rift systems, and their corresponding lithospheric extension, is not compensated by a comparable cumulative length of compressive mountain belts (montes). Mountains are, instead, limited to crustal plateau boundaries, such as the Montes encircling Laksumi Planum at Isthar Terra (Danu, Akna, Freya and Maxwell Montes: Fig. 5a). This has been taken as further evidence for the lack of plate tectonics on Venus, where contractional deformation is widely distributed throughout the entire lithosphere rather than at discrete sites (Solomon et al. 1992; Solomon 1993). Indeed, folds and faults are particularly pervasive in the tesserated terrains, which are expressions of multiple deformations on highrelief crustal plateaux and crustal remnants within plains (Bindschadler & Head 1991; Hansen & Willis 1996; Hansen et al. 1999, 2000; Romeo & Turcotte 2008). Folds and faults are also common in the planitiae, either concentrated in narrow contractional ridge belts or in widely distributed wrinkle ridges (Tanaka et al. 1997; McGill et al. 2010).

Contractional deformation. The ridge belts are up to 20 km wide and several hundreds to thousands of kilometres long (Ivanov & Head 2001; Rosenberg & McGill 2001). As for terrestrial foldand-thrust systems, these Venusian features are also thought to have formed due to long-lived tectonic stress fields. The most widely distributed contractional landforms are wrinkle ridges (e.g. Tanaka et al. 1997; Ivanov & Head 2008). The origin of these structures has been variously ascribed

to gravitational spreading on shallow slopes (McGill 1993), rock thermal expansion induced by a hotter atmosphere than at present after global resurfacing (Solomon *et al.* 1991) or regional tectonics controlled by a stress state centred on the planetary geoid, with compression at the geoid's low-standing regions and extension at the geoid's high-standing regions, respectively (Sandwell *et al.* 1997; Bilotti & Suppe 1999).

Strike-slip tectonics. On a planet dominated by vertical tectonism and characterized by widely distributed deformations, there is no space for strikeslip shear belts that have traditionally been highly underconsidered on Venus (e.g. Solomon 1993; McGill et al. 2010) despite the apparently straightforward evidence collected so far (Raitala 1994; Brown & Grimm 1995; Ansan et al. 1996; Koenig & Aydin 1998; Tuckwell & Ghail 2003; Kumar 2005; Romeo et al. 2005; Chetty et al. 2010; Fernàndez et al. 2010: Harris & Bédard 2014a, b). For example, Brown & Grimm (1995) highlighted en echelon fractures and folds along and within Artemis Chasma. Koenig & Aydin (1998) and Fernàndez et al. (2010) showed horse-tail terminations, en echelon folds, contractional bends and strike-slip offsets in Lavinia Planitia. Finally, Romeo et al. (2005) and Chetty et al. (2010) identified conjugate shear zones in Ovda Regio associated with tear-folds and imbricate duplexes. Continental drift may account for the substantial horizontal tectonism required by prominent strikeslip belts (Harris & Bédard 2014b).

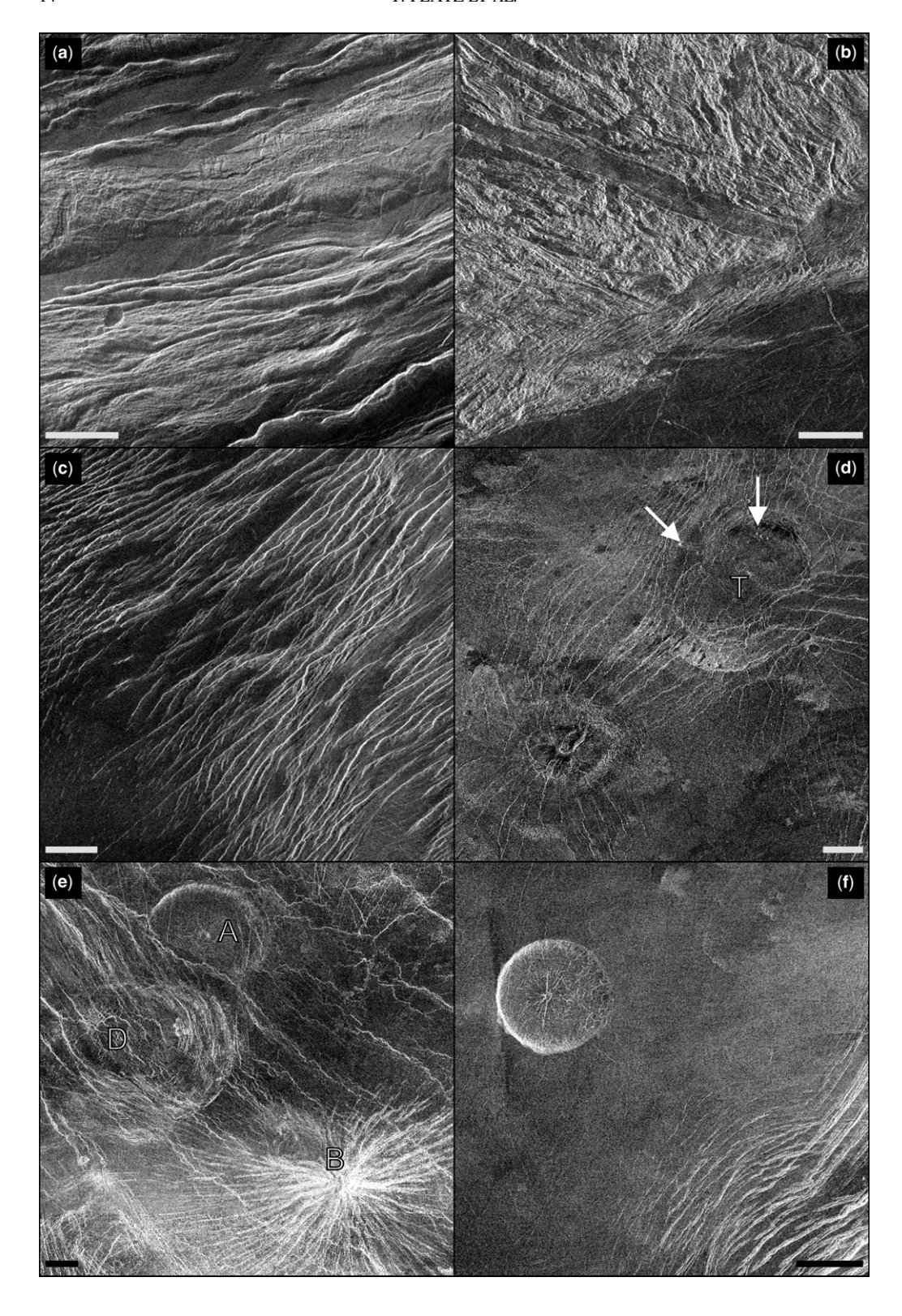
Volcanism

On a geodynamically active planet that lacks modern-day plate tectonics, upwelling plumes and their related surface expressions are its dominant volcanic traits. The volcanic landforms on Venus largely depend on the dimensions of the blooming head of such mantle plumes, which are mostly responsible for the development of volcanic rises ranging from 1400 to 2500 km in diameter and up to 2.5 km in elevation (e.g. Beta, Atla, Bell; Eistla, Luafey, Imdr, Themis and Dione Regiones). The enigmatic coronae, also attributed to volcanism, display variable diameters (with 250 km being the average). Other types of volcanic landform include shield volcanoes, which normally range between 100 and 600 km in diameter (and which rarely exceed 700 km in breadth: see Stofan et al. 1995; Glaze et al. 2002; Crumpler & Aubele 2000; Ivanov & Head 2013 for size distributions). These landforms are typically accompanied by smaller volcanic features (<100 km in diameter), such as small and intermediate volcanoes known as tholi and steep-sided domes ('pancakes': Fig. 5f).

Volcanic rises. Volcanic rises, corresponding to Venus' regions, have been classified either as volcano-dominated, coronae-dominated or riftdominated (Stofan et al. 1997). Whereas in the first case volcanic rises are representative of major plume sites along rift zones, in the latter two cases the plume heads could have been broken up into a swarm of smaller upwelling diapirs (although not necessarily simultaneously) (Stofan et al. 1995). Smrekar & Stofan (1999) noted that the volcanic construction typical of volcano-dominated rises requires large volumes of pressure-release melting due to vigorous hot plumes generated at the coremantle boundary, whereas corona-dominated rises are more likely to be associated with smaller plumes from shallower depths.

Coronae, novae and arachnoids. Coronae (Fig. 5d & e) are annular forms dominated by either positive or negative topography, and which are encircled by concentric systems of fractures and ridges (Type 1 coronae) or by a rim alone (Type 2) (Basilevsky et al. 1986; Head et al. 1992; Squyres et al. 1992; Stofan et al. 1992, 2001). Coronae are often associated with radiating, graben-fissure systems (Fig. 5d) that converge towards the coronas' rims and that in some cases reach their centres (with such structures being termed novae) (Barsukov et al. 1986; Crumpler & Aubele 2000; Aittola & Kostama 2000, 2002; Krassilnikov & Head 2003; Basilevsky et al. 2009; Studd et al. 2011). Indeed, radiating graben-fissure systems can also be associated with large volcanoes (e.g. Keddie & Head 1994; Galgana et al. 2013) or can occur individually, following rift zones (Grosfils & Head 1994; Aittola & Kostama 2000). The structures within radiating graben-fissure systems can extend for up to 2000 km. In places, they may become subparallel to each other, or they may form systems perpendicularly orientated to the prevailing maximum regional horizontal stress (Grosfils & Head 1994). Based on their appearance and lateral extent, radiating graben-fissure systems have been compared with giant radiating dyke swarms on Earth, such as the Proterozoic Mackenzie and Matachewan swarms in Canada, the Tertiary Sky Isle swarm in Scotland, and the Mesozoic central Atlantic reconstructed swarm (Ernst et al. 1995). The Venusian systems also resemble radiating extensional systems on Mars (Ernst et al. 2001; Wilson & Head 2002).

Arachnoids are characterized by ridges that converge towards annular depressions (Aittola & Kostama 2000; Crumpler & Aubele 2000; Frankel 2005). These landforms have often been considered as a subtype of coronae (Head *et al.* 1992; Price & Suppe 1995; Hamilton & Stofan 1996). Indeed, coronae, radiating graben–fissure systems (novae) and arachnoids may represent different



evolutionary stages of mantle plume upwellings (Hamilton & Stofan 1996). Under such a scenario, corona evolution begins with lithospheric updoming and radial fracturing due to mantle plume (or diapir) impingement, followed by the gravitational collapse of the central dome due to radial spreading and thinning of the plume (Squyres et al. 1992; Stofan et al. 1991, 1992; Hamilton & Stofan 1996). Recent finite-element modelling indicates that radial fractures form during early mantle diapir impingement, with an outward propagation of dykes occurring at a later stage due to loadinginduced downward lithospheric flexure (Galgana et al. 2013). Together with novae, then, coronae with a topographically positive central dome and radial fracture system may represent the first stage of mantle plume upwelling, and coronae with a central annular depression might be typical of the final stage (Stofan et al. 1992; DeLaughter & Jurdy 1999). In another analysis, however, Gerya (2014) proposed a variation of this general process. Gerya suggested a scenario in which novae and coronae structures are not directly related to astenospheric plume impingement but, instead, are the result of magma-assisted convection of a weak ductile crust, induced by decompressional melting of hot rising mantle plumes. Under this scenario, novae represent the initial stage of this convection, with coronae corresponding to the intermediate and final stages.

Whether arachnoid structures are a somewhat intermediate phase between novae and coronae (Hamilton & Stofan 1996) is still the subject of debate, however, given the different geological contexts in which arachnoids have been documented. In particular, these structures are largely located in volcanic plains, and are rarely situated along the equatorial deformation zones where most novae and corona are situated (Aittola & Kostama 2000).

Volcanic products. The primary volcanic products on Venus are extensive tholeitic-alkali basalt

plains that cover about 70% of the planet. These plains differ in terms of the styles of deformation to which they have been subjected or their connection with small shield volcanoes (ridged, lineated, regional plains, lobate and shield plains) (e.g. Ivanov & Head 2011).

Typical volcanic landforms include lava flow fields, lava channels and steep-sided domes (Crumpler & Aubele 2000; Stofan et al. 2000; Magee & Head 2001). Lava flow fields are composed of very long (up to 1000 km) digitated flows, both with radar bright (interpreted to be aa-type lavas) or dark (pahoehoe-type lavas) surfaces, which erupted from shield volcanoes and fissures (including those of coronae). Their substantial lengths are attributed to endogenous spreading processes, such as inflation and lava tubes, which should be facilitated by an efficient cooling of the flow surface (due to convective processes within the dense atmosphere, whose pressure is c. 9.2 MPa), aided by a low cooling rate of the lava flow's inner core (due to the high surface temperature environment of c. 700°K) (Grosfils et al. 1999; Crumpler & Aubele

Remarkably long individual lava channels, of typical lengths of between 100 and 1000 km in general but in some cases extending to more than 5000 km, are explained by invoking very low-viscosity fluxes such as these expected for exotic lava types such as komatites, carbonatites and sulphur flows (Kargel *et al.* 1994; Baker *et al.* 1997; Williams-Jones *et al.* 1998; Komatsu *et al.* 2001; Lang & Hansen 2006).

There is evidence for highly viscous lavas on Venus, too. Such evidence includes steep-sided domes, which are circular, positive-relief landforms with diameters ranging between 20 and 100 km (e.g. Pavri *et al.* 1992), and flows with pronounced margins. The higher lava viscosities implied by these features could be due to a high silica content (i.e. evolved magmas), high crystal content or high

Fig. 5. Examples of volcanic and tectonic features on Venus. (a) Fold-and-thrust belt sequence of Akna Montes; note the presence of intra-mountain basins (image centre: 69°N, 318°E; Magellan full resolution radar mosaic archive MGN-RDRS FMAP: FL69n318). (b) Complex deformation in Sudice Tessera; at the lower right are the regional plains of Aino Planitia (37°S, 113°E; MGN-RDRS FMAP: FR37s113). (c) Tectonized ridge belt east of Aino Planitia (45°S, 116.5°E; MGN-RDRS FMAP: FR45s117). (d) Structural relations between Tituba corona (T), centred at 42.5°N, 214.5°E (termed Type 1, after Stofan et al. 2001) and the corona at 40.4°N, 212.4°E (Type 2, after Stofan et al. 2001). Note the concentric and radial features related to both the coronae and the small volcanic edifices at the NW margin of Tituba corona (white arrows). The radial fissures and graben between the coronae become parallel at a certain distance from the coronae centres, and are common to both the two main volcanic landforms (MGN-RDRS FMAP: Fl39n211, FL39n213, FL39n215, FL41n211, FL41n213, FL41n215, FL43n211, FL43n213, FL43n215). (e) Becuma radiating graben system (nova) (B) (34.13°N, 21.9°E), Dzudzdi corona (D) (35°N, 20.7°E) and the Aegina Farrum steep-sided dome (A) (35.54°N, 21.1°E) in the eastern Sedna Planitia. Note that Aegina Farrum is transected by a 220 km-long extensional fault. (MGN-RDRS FMAP: Fl35n021, FL35n023, FL33n021, FL33n023). (f) Steep-sided dome at 2.8°S, 150.9°E, to the west of Sella Corona (not shown) and its related graben system (lower right corner) (MGN-RDRS FMAP: FL03s151). The scale bar in all images is 20 km, except in (d) where it is 50 km. All images are shown with simple cylindrical projections, except (a), which has a stereographic projection.

vesicularity (Head *et al.* 1992; Pavri *et al.* 1992). It has been proposed that the considerable atmospheric pressure on Venus' surface prevents the formation of eruptive plumes due to explosive magmatic fragmentation and, instead, is conducive to outpourings of frothy lava domes.

16

It is widely accepted that the planet's high atmospheric pressure would strongly inhibit gas exsolution in magmas and, hence, would inhibit or preclude entirely explosive eruptions (e.g. Head & Wilson 1986). However, geomorphological evidence exists for an extensive pyroclastic flow deposit near Diana Chasma, which, if found to be a common form of volcanic deposit on Venus, would have implications for the mantle volatile content and the volcanic origin of atmospheric SO₂ on the planet (Ghail & Wilson 2013).

Global volcanic resurfacing. Global resurfacing models of Venus (e.g. Parmentier & Hess 1992; Turcotte 1993; Nimmo & McKenzie 1998; Reese et al. 1999) call for volcanic and tectonic events that are globally correlated throughout the planet's geological record. Indeed, according to several studies (e.g. Basilevsky & Head 1995, 1998, 2000; Basilevsky et al. 1997; Ivanov & Head 2011), all of the physiographical units recognized on the Venusian surface are expressions of a common sequence of events across the globe. The geological map of Ivanov & Head (2011) is currently the most complete and updated synthesis of this view, where each morphological unit is regarded as a stratigraphic unit of global significance and, when synthesized as such, describes a coherent Venusian geological history.

Under this scheme, all deformed terrains (tessera, densely lineated plains, ridged plains, mountain belts and groove belts) should belong to the earliest phase of tectonism, which was followed by extensive volcanic effusion manifest as regional and shield plains, and which was followed in turn by more spatially concentrated, long-lived rift volcanism, represented by morphological units such as lobate plains, smooth plains and shield clusters. The first phase of volcanism probably began with the construction of shield plains associated with small shield structures and steep-sided domes, the likely expression of shallow crustal melting. This form of volcanism was followed by the effusion and emplacement of huge volumes of lava, essentially mantle-derived, pressure-release melts as attested to by regional plains and extended lava channels. This second volcanic phase, well represented by lobate plains, is supposed to be dominated by voluminous volcanic effusions punctuated by long temporal gaps (Ivanov & Head 2013).

Guest & Stofan (1999) defined as a 'directional model' the view of a globally correlated geological

history, which contrasts with a 'non-directional model' in which the recognition of similar sequences of events in different regions of Venus does not imply their coeval occurrence. In favour of the first model are the globally distributed regional plains that were utilized as the main stratigraphic reference for the entire Venusian time system by Ivanov & Head (2011). These authors argued that the global presence of these plains supports the general 'directionality' of Venus' geological history but some authors have highlighted several exceptions to this hypothesized commonality in the geological record across the entire surface (Guest & Stofan 1999; Rosenberg & McGill 2001; McGill 2004; McGill et al. 2010). Of note, and supported by observations of where in terrestrial geology equivalent morphologies and geneses do not necessarily mean a coeval origin, McGill et al. (2010) proposed an intermediate view within which a general 'directional' framework predominated but in which tectonic and volcanic events might still have developed at different times and in diverse locations.

Nevertheless, the resurfacing of Venus continues to be viewed within the narrative of either 'catastrophic' (e.g. Schaber et al. 1992) or 'equilibrium' (e.g. Phillips et al. 1992) scenarios, both of which must satisfy the near-random spatial distribution of fewer than 1000 impact craters across the planet and the lack of many obviously modified such craters. Although catastrophic models more readily satisfy these constraints, recent work has also shown that equilibrium models, within a select parameter space, also meet these requirements (Bjonnes et al. 2012). Moreover, numerous further constraints introduced by careful geological mapping question the underlying assumptions of the catastrophic scenarios. It may be that a protracted period of resurfacing set against the backdrop of a globally thin lithosphere (e.g. the 'SPITTER' hypothesis: Hansen & Young 2007) accounts more fully for these observational constraints. This viewpoint is bolstered by recent mapping and modelling, which indicates that Venus' tesserae terrain probably predates extensive resurfacing of the planet (Romeo & Turcotte 2008; Hansen & López 2010).

The Moon

The Moon is a key planetary body with which to study diverse volcanic activity, as it has produced a variety of volcanic landforms over an extended period of time (Figs 6 & 7). As the Moon is lacking plate tectonics, an atmosphere, water and life, it allows us to study volcanic processes in an unobscured form (e.g. Hiesinger & Head 2006; Jaumann *et al.* 2012; Hiesinger & Jaumann 2014). Analyses

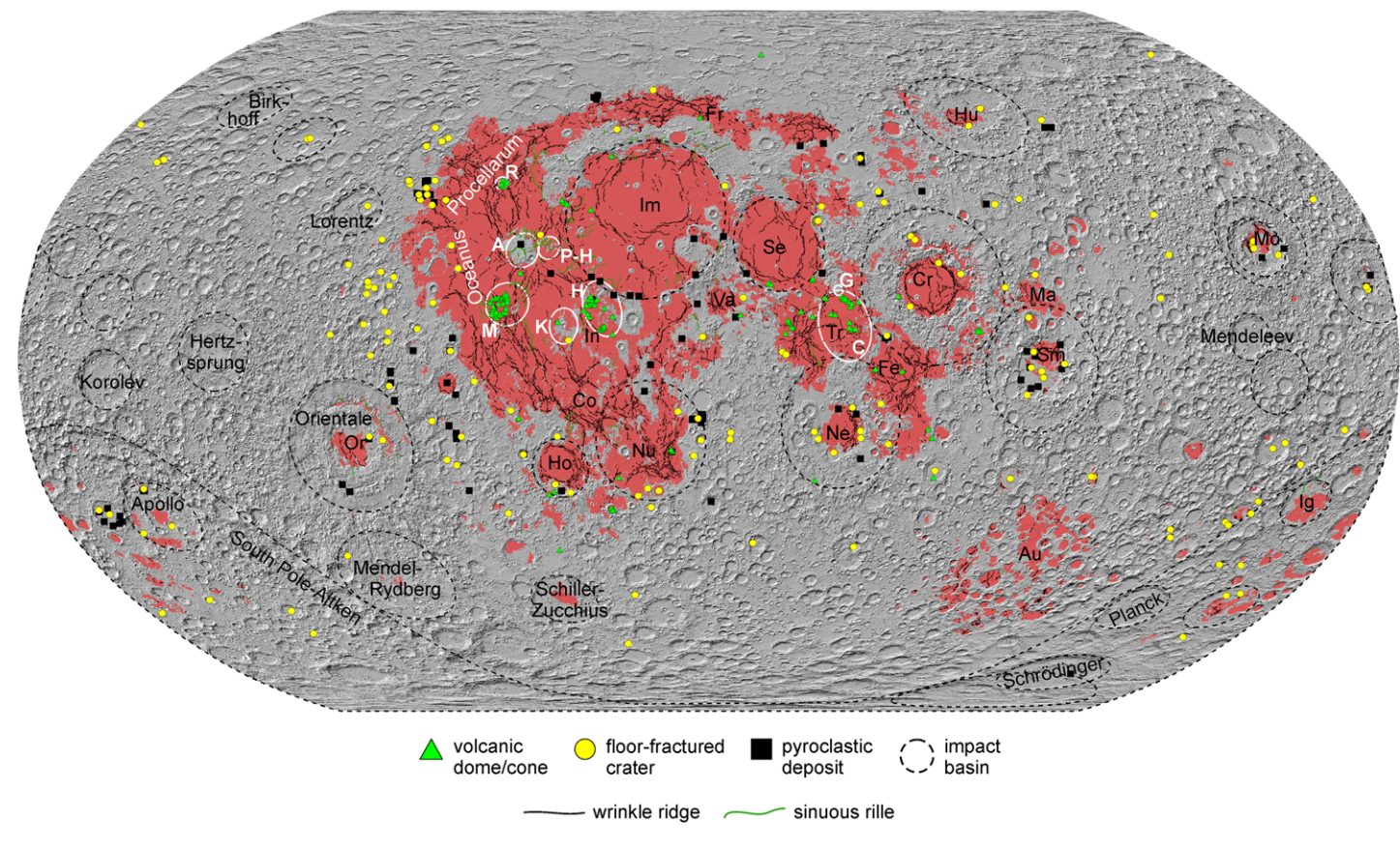
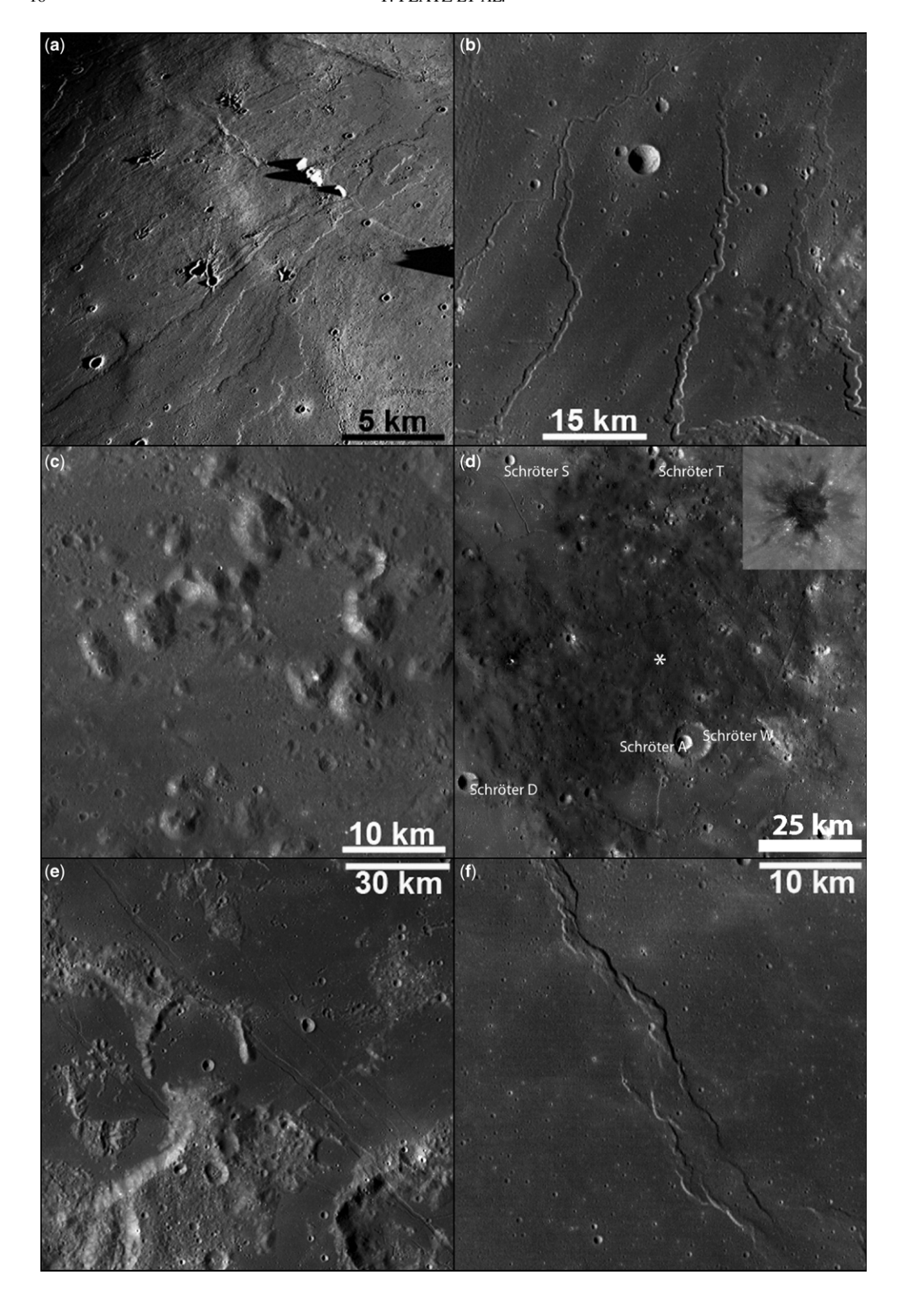


Fig. 6. The distribution of maria, volcanic edifices, sinuous rilles and selected tectonic structures on the Moon. The lunar maria are highlighted in red. Impact basins larger than 300 km in diameter are shown as dashed black ellipses (Kaddish *et al.* 2011). The locations of floor-fractured craters (yellow dots) are taken from Jozwiak *et al.* (2012). Identified pyroclastic deposits (black squares: Gaddis *et al.* 1998) and sinuous rilles (green lines: Gustafson *et al.* 2012; Hurwitz *et al.* 2012, 2013*a*) are shown. The approximate locations of the broad shield volcanoes identified by Spudis *et al.* (2013) are highlighted as white ellipses with bold white letters representing: A, Aristarchus; C, Cauchy; G, Gardner; H, Hortensius; K, Kepler; M, Marius; P–H, Prinz–Harbinger; and R, Rümker. The locations of the 118 domes and cones identified on the Moon are shown as green triangles (data from http://digilander.libero.it/glrgroup/consolidatedlunardomecatalogue.htm). Maria labels are abbreviated as follows: Au, Australe; Co, Cognitum; Cr, Crisium; Fe, Fecundidatis; Fr, Frigoris; Ho, Humorum; Hu, Humboldtianum; Ig, Ingenii; Im, Imbrium; In, Insularum; Ma, Marginis; Mo, Moscoviense; Ne, Nectaris; Nu, Nubium; Or, Orientale; Se, Serenitatis; Sm, Smythii; Tr, Tranquillitatis; Va, Vaporum. The background image is a Lunar Orbiter Laser Altimeter (LOLA)-based shaded-relief map (0.23 km/px) with a Robinson projection, centred at 0°E.



of lunar samples, coupled with remote-sensing investigations, have yielded detailed information on many aspects of lunar volcanism (i.e. extrusion) and, to a lesser amount, on lunar plutonism (i.e. intrusion). From those studies, it became apparent that magmatism has been a major crust-building and resurfacing process throughout the Moon's geological history (e.g. Lucey et al. 2006; Shearer et al. 2006). The available data also allow us to study the role of magmatic activity (both intrusive and extrusive) during the heavy bombardment, as well as during more recent lunar history (i.e. the mare stratigraphic record). Furthermore, the distribution of basalt types, and the implied spatial and temporal distribution of mantle melting, as well as volcanic volumes and fluxes, can be understood. Finally, the Moon is unique in that it allows us to assess a wide range of eruption styles, including pyroclastic activity, and their petrogenetic significance owing to the existence and preservation of an assorted suite of volcanic deposits (e.g. Hiesinger & Head 2006; Jaumann et al. 2012; Hiesinger & Jaumann 2014).

Igneous geochemistry

From the lunar sample collection it became apparent that lunar rocks can be classified, on the basis of texture and composition, into four distinct groups: (1) pristine highland rocks that are primordial igneous rocks, uncontaminated by impact mixing; (2) pristine basaltic volcanic rocks, including lava flows and pyroclastic deposits; (3) polymict clastic breccias, impact melt rocks and thermally metamorphosed granulitic breccias; and (4) the lunar regolith. In the following paragraphs we will only focus on highland rocks and mare basalts. Although breccias may contain igneous fragments, they are primarily produced by impacts and not by magmatic/volcanic processes.

On the basis of their molar Ca/(Ca + Na + K) content v. the molar Mg/(Mg + Fe) content of their bulk rock compositions, pristine highland rocks fall into two major chemical groups: ferroan anorthosites and magnesium-suite rocks (e.g. Warner *et al.* 1976; Papike 1998). These rocks appear to have different ages, with the ferroan anorthosites

being somewhat older (c. 4.56-4.29 Ga) than the magnesian-suite rocks (high Mg/Fe) (4.46-4.18 Ga) (Shearer et al. 2006). This latter group contains dunites, troctolites, norites and gabbronorites. Compared with these two rock types, the alkali suite is less abundant. Although this group contains similar rock types, they are enriched in alkali and other trace elements relative to, and are somewhat younger than (4.37-3.80 Ga), the ferroan anorthosites and the Mg-suite rocks (Shearer et al. 2006). This implies that the earliest Mg-suite rocks were formed contemporaneously with at least some ferroan anorthosite, which is not consistent with the idealized magma-ocean model, in which ferroan anorthosites form the oldest crust and are later intruded by younger, Mg-suite plutonic rocks. An alternative model to the magma-ocean scenario, which proposes a genesis of the lunar crust by intrusion of multiple magma bodies (i.e. serial magmatism) (e.g. Walker 1983; Longhi & Ashwal 1985; Longhi 2003; Shearer et al. 2006; Borg et al. 2011), appears to be more consistent with the observed age relationships of lunar pristine rocks.

From the Apollo samples, it is known that anorthosite is common in the lunar highlands. Compared with terrestrial rocks, the anorthosite abundances (An₉₆) of plagioclase in these rocks are much higher, ultimately reflecting the Moon's depletion in volatile elements such as sodium (Lucey et al. 2006 and references therein). The Mg# (i.e. Mg/ Mg + Fe) of pyroxene and olivine in lunar anorthosite is much more ferroan than in terrestrial rocks of such high Ca/Na ratios and any other non-mare lunar rocks (e.g. Lucey et al. 2006 and references therein). Thus, ferroan anorthosite refers to lunar anorthosite with plutonic or relict plutonic textures (e.g. Dowty et al. 1974a, b). The ferroan-anorthositic suite (Warren 1993) consists of ferroan anorthosites (>90% plagioclase), as well as their more mafic but less common variants, ferroan noritic anorthosite and ferroan anorthositic norite. Pyroxene usually predominates in the ferroan anorthosites, although some samples also contain olivine. Lunar ferroan anorthosites are coarse-grained intrusive igneous rocks, formed during slow cooling at some depth below the surface (Lucey et al. 2006). Because of the high concentration of plagioclase feldspar in

Fig. 7. Examples of volcanic and tectonic features on the Moon. (a) Basaltic lava flow in Mare Imbrium. Note also wrinkle ridges and secondary impact craters (Apollo 15 orbital photograph; AS15-M-1556). (b) Sinuous rille (Rima Prinz) in Mare Imbrium (Lunar Reconnaissance Orbiter Camera (LROC) wide-angle camera (WAC)). (c) Basaltic lava dome complex, situated within Mare Imbrium (LROC WAC). (d) Pyroclastic deposits located between Sinus Aestum and Schröter crater. Asterisk marks the location of the inset showing a 170 m-diameter crater, which excavated fresh pyroclastic material that is also termed dark mantle deposit (LROC WAC and NAC). (e) Rimae Goclenius graben system in Mare Fecunditatis. Faults cut the volcanic plains and pre-existing craters (LROC WAC). (f) Dorsa Whiston in Oceanus Procellarum represents a typical mare ridge (LROC WAC). Figures are adopted from Hiesinger & Jaumann (2014).

ferroan anorthosites, they are interpreted as cumulate rocks, produced by the separation and accumulation of crystals from the remaining melt. Compared with other lunar rocks, ferroan anorthosites are low in FeO and incompatible trace elements (e.g. Th) (e.g. Lucey et al. 2006 and references therein). The Apollo sample collection contains several large, nearly monomineralic plagioclase rocks (e.g. Warren 1990), and outcrops of 'pure' anorthosite have also been identified from Earth-based and spacecraft observations (Hawke et al. 2003; Ohtake et al. 2009). However, its perceived importance to lunar crustal formation has been challenged by Lucey et al. (2006) because, although ferroan anorthosite is the most common pristine rock type at the Apollo 16 site, it is uncommon or rare at other sites. On the basis of early inspection of the Apollo samples, it was concluded that the lunar highlands are dominated by ferroan anorthosite, and that the ferroan-anorthositic suite component of the crust is highly feldspathic. However, Lucey et al. (2006 and references therein) pointed out that the feldspathic lunar meteorites, geochemical observations taken from orbit, and regolith samples from Apollo 16 and Luna 20 suggest that highly feldspathic ferroan anorthosite is not necessarily typical of the highlands surface, at least not on the Moon's nearside. In fact, the majority of feldspathic lunar meteorites are more mafic than the feldspathic material of the Apollo 16 regolith (Korotev 1996, 1997; Korotev et al. 2003), and the high Mg# of the upper feldspathic crust (70 \pm 3) is at the high end for ferroan anorthosite. Together, this implies that magnesian feldspathic rocks contributed substantially to the make-up of the lunar highlands (e.g. Lucey et al. 2006).

The magnesian suite possibly represents the transition between magmatism associated with the magma ocean and serial magmatism that occurred between 30 and 200 Ma after the formation of that ocean (Solomon & Longhi 1977; Longhi 1980; Shearer & Newsom 2000). However, the exact duration of emplacement of the magnesian suite into the lunar crust is still debated due to the lack of deep sampling by impacts after 3.9 Ga, a function of a decreasing impact flux. Taylor et al. (1993) estimated that the magnesian rock suite constitutes approximately 20% of the uppermost 60 km of the crust, with the rest being composed of ferroan anorthosite. However, other studies suggest smaller amounts of magnesian- and alkali-suite rocks are present (e.g. Jolliff et al. 2000; Korotev 2000).

Probably the most prominent evidence of volcanic activity on the Moon is the emplacement of mare basalts that constitute the dark basin fills. In comparison to highland rocks, they are enriched in FeO and TiO₂, depleted in Al₂O₃, have higher CaO/Al₂O₃ ratios, contain more olivine and/or

pyroxene, especially clinopyroxene, but contain less plagioclase (e.g. Taylor et al. 1991). Mare basalts most probably formed from remelting of mantle cumulates produced by the early differentiation of the Moon. The origin of KREEP basalts (rich in K, Rare Earth Elements and P), however, is likely to be related to remelting or assimilation by mantle melts of a late-stage magma-ocean residuum, the so-called ur-KREEP (Warren & Wasson 1979). There are numerous ways to distinguish different basalt types, including through petrography, mineralogy and chemistry (e.g. Neal & Taylor 1992; Papike et al. 1998). Taylor et al. (1991) utilized their TiO₂ abundances to define three basalt types: very low-Ti (VLT) basalts (<1.5 wt% TiO₂), low-Ti basalts (1.5-9 wt% TiO₂) and high-Ti basalts (>9 wt% TiO₂). On the basis of extensive laboratory studies of TiO₂ abundances of the lunar samples and spectroscopy (e.g. Papike et al. 1976; Papike & Vaniman 1978; Neal & Taylor 1992; Papike et al. 1998), global maps of the major mineralogy-chemistry of the Moon with remote-sensing techniques have been derived (e.g. Charette et al. 1974; Pieters 1978; Johnson et al. 1991; Melendrez et al. 1994; Shkuratov et al. 1999; Giguere et al. 2000; Lucey et al. 2000). Because early interpretations of the Apollo and Luna data suggested that lunar mare volcanism began with high-TiO₂ basalts that are older than later Ti-poor basalts, models were proposed in which this perceived correlation was coupled to the depth of melting (e.g. Taylor 1982). However, remote-sensing data indicate that young basalts exist with high TiO₂ concentrations (e.g. Pieters et al. 1980); moreover, there are also old (mostly >3 Ga) lunar basaltic meteorites that are very low in Ti content (Cohen et al. 2000; Terada et al. 2007). Finally, a combination of iron and titanium maps (e.g. Lucey et al. 2000) and crater size-frequency distribution measurements across the nearside and farside did not reveal a distinct correlation between mare ages and composition (Hiesinger et al. 2001; Pasckert et al. 2014). Thus, FeO and TiO₂ concentrations varied independently with time, whereas TiO₂ (FeO)-rich and TiO₂ (FeO)-poor basalts erupted contemporaneously.

The geochemistry of returned lunar samples suggests that the ultramafic sources of mare basalts are complementary to the anorthositic crust (e.g. Wieczorek et al. 2006) and that the Moon is, therefore, differentiated. To explain these observations, the magma-ocean model was developed (e.g. Smith et al. 1970; Wood et al. 1970; Warren & Wasson 1979; Warren 1990). The model assumes that large parts of the Moon were initially molten, such that a global, several-hundred-metres-thick magma ocean formed. Although the details of the crystallization of such a magma ocean are not fully understood, it is likely that the early crystallization of

olivine and orthopyroxene produced cumulates in the deeper parts of the magma ocean because they were denser than coexisting melt (Shearer et al. 2006 and references therein). With time, early magnesium-rich cumulates became increasingly iron-rich. As a consequence of the early crystallization of Fe- and Mg-rich minerals, the melt became richer in Al and Ca, which in turn resulted in the crystallization of plagioclase after about 75-80% magma-ocean solidification. As plagioclase was less dense than its source melt, it eventually formed the anorthositic highland crust. Finally, continued crystallization of the magma ocean yielded a globally asymmetric distribution of KREEP elements. On the basis of lunar samples, it became apparent that the main phases of the magma ocean were completely crystallized by about 4.4 Ga. The KREEP residue was solid at about 4.36 Ga. In such a crystallization sequence, it is plausible that the laterformed, denser, iron-rich cumulate mantle overlying the earlier, less dense magnesium-rich mantle cumulates was gravitationally unstable, resulting in the development of an overturn of the cumulate mantle. Such an overturn might have delivered cold, dense, incompatible-element-rich material to the core-mantle boundary. Simultaneously, hot rising mantle plumes may have melted adiabatically to produce the first basaltic resurfacing crust of the Moon (i.e. the early mare basalts).

Volcanic landforms

The Moon hosts a wide variety of volcanic landforms, including lava flows, cones, domes, shield volcanoes, sinuous rilles, pyroclastic deposits and cryptomaria (e.g. Hiesinger & Head 2006; Spudis et al. 2013) (Fig. 7). Since the Russian Luna 3 mission in 1959, it has been known that lunar basalts are concentrated on the nearside. Many basalt deposits are located in the interiors of low-lying impact basins. Globally, mare basalts cover 7 × 10⁶ km², or 17%, of the total lunar surface – amounting to 1% of the lunar crustal volume (Head 1976; Wilhelms 1987; Hiesinger & Head 2006) (Fig. 6). Although the specific details of mare basalt petrogenesis are still not fully understood, the presence of radioactive elements (e.g. K, U and Th) most probably resulted in the formation of partial melts of ultramafic mantle material at depths of between about 60 and 500 km (e.g. Wilhelms 1987; Hiesinger & Head 2006).

Lava flows. Mare basalts were formed by large volumes of low-viscosity, high-temperature basaltic lava, which resurfaced vast areas (i.e. c. 30% of the lunar nearside) (Head 1976; Wilhelms 1987). In fact, laboratory measurements of molten lunar basalts indicate that their viscosity is only a few

tens of poise at 1200 °C, allowing them to flow for long distances across the surface before solidifying (Hörz et al. 1991). Lava flows several tens of metres thick extending for hundreds to thousands of kilometres across Mare Imbrium have been documented (Schaber 1973; Schaber et al. 1976) (Fig. 7a). Thin lava flows similar to those in Mare Imbrium have been observed elsewhere on the Moon: within the Hadley Rille at the Apollo 15 landing site, for example. However, many lunar lava flows lack distinctive flow fronts due to their very low viscosities, high eruption rates, ponding of lava in shallow depressions, subsequent destruction by impact processes and/or burial by younger flows. Similarly, volcanic vents in the mare regions are rare because they were probably covered by the erupting basalts or were degraded by subsequent impacts.

Sinuous rilles. Sinuous rilles (Figs 6 & 7b) are meandering channels that often start at a crater-like depression and end by grading downslope into the smooth mare surface (Greeley 1971). Most such rilles originate along the margins of the basins and trend towards the basin centre. These channels range in width from a few tens of metres to approximately 3 km, from a few kilometres to up to 300 km in length and are, on average, 100 m deep (Schubert et al. 1970; Hurwitz et al. 2012, 2013a). The Apollo 15 mission investigated one of these sinuous rilles, Rima Hadley, in detail. Despite early interpretations of sinuous rilles as lunar rivers (e.g. Lingenfelter et al. 1968; Peale et al. 1968), no evidence for water or pyroclastic flows was found and so it was concluded that sinuous rilles formed by thermal erosion, resulting in widening and deepening of channelled lava flows due to the melting of the underlying rock by very hot lavas (Hulme 1973; Coombs et al. 1987; Williams et al. 2000; Hurwitz et al. 2012, 2013a). Lower gravity, higher melt temperatures, lower viscosities and higher extrusion rates might be responsible for the much larger sizes of lunar sinuous rilles compared with lava tubes and channels on Earth. Bussey et al. (1997) and Fagents & Greeley (2001) showed that the process of thermal erosion is very sensitive to the physical conditions in the boundary layer between lava and solid substrate. They found that thermal erosion rates depend on the slopes, effusion rates and thermal conductivities of the liquid substrate boundary layer.

Cryptomaria. Cryptomaria are mare-like volcanic deposits that later were covered with lighter-coloured material (e.g. ejecta from craters and basins) (Head & Wilson 1992). These deposits can be studied with several techniques, including investigations of dark halo craters (e.g. Schultz & Spudis

1979, 1983; Hawke & Bell 1981), multispectral images (e.g. Head et al. 1993; Greeley et al. 1993; Blewett et al. 1995; Mustard & Head 1996) and orbital geochemical observations (e.g. Hawke & Spudis 1980; Hawke et al. 1985). These studies have shown that if cryptomaria are included, the total area covered by mare deposits exceeds 20% of the lunar surface, compared with about 17% of typical mare deposits alone (Head 1976; Antonenko et al. 1995). Thus, cryptomaria not only indicate a wider spatial distribution of ancient volcanic products but also reveal that mare volcanism was already active prior to the formation of the Orientale basin (i.e. the youngest basin on the Moon) and the emplacement of its ejecta, which is an important stratigraphic marker horizon. Although Giguere et al. (2003) and Hawke et al. (2005) reported that the buried basalts in the Lomonosov-Fleming and the Balmer-Kapteyn regions are very-low- to intermediate-Ti basalts, sampling and subsequent analyses are required to understand the true nature of cryptomaria.

Domes, cones and shields. A small fraction of the vast mare regions is covered by positive topographical surface features, such as domes, cones and shields, that measure up to several tens of kilometres across, are up to several hundred metres high and are basaltic in composition (Head & Gifford 1980). Lunar cinder cones are often associated with lunar sinuous rilles (e.g. in Alphonsus crater; Head & Wilson 1979), are less than 100 m high, 2–3 km wide, have summit craters of less than 1 km diameter and have very low albedos (Guest & Murray 1976).

Lunar mare domes are generally broad, convex, semi-circular landforms with relatively low topographical relief (Fig. 7c). For example, Guest & Murray (1976) mapped 80 mare domes with diameters of 2.5-24 km, 100-250 m heights and 2° 3° slopes; most of them occur in the Marius Hills complex. Some of the Marius Hills domes are characterized by steeper slopes $(7^{\circ}-20^{\circ})$ and some have summit craters or fissures. Most probably, the mare domes were formed by eruptions of more viscous (i.e. more silicic) lavas, intrusions of shallow laccoliths or mantling of large blocks of older rocks with younger lavas (e.g. Heather et al. 2003; Lawrence et al. 2005). Large shield volcanoes (>50 km) are common on Earth, Venus and Mars, and are constructive features: that is, they consist of a large number of small flows derived from a shallow magma reservoir where the magma reaches a neutral buoyancy zone (e.g. Ryan 1987; Wilson & Head 1990; Head & Wilson 1992). Thus, the presence of shield volcanoes and calderas implies shallow buoyancy zones, the stalling and evolution of magma there, leading to numerous eruptions

of small volumes and durations, and shallow magma migration that causes caldera collapse. However, no shield volcanoes larger than about 20 km in diameter have been identified on the Moon (Guest & Murray 1976). This observation indicates that shallow buoyancy zones do not occur on the Moon, and that lavas did not extrude in continuing sequences of short-duration, low-volume eruptions from shallow reservoirs. However, there is evidence that in a few locations magma may have stalled near the surface to form shallow sills or laccoliths, as possibly indicated by the formation of floor-fractured craters (Schultz 1976; Wichman & Schultz 1995, 1996) (see below).

Apart from the basaltic domes in the mare regions, there are also domes that are plausibly linked to non-mare volcanism. These landforms are much less abundant than those associated with basaltic volcanism, are characterized by slopes steeper than those of mare domes, and exhibit a high albedo and a strong absorption in the ultraviolet (Malin 1974; Wood & Head 1975; Head et al. 1978; Chevrel et al. 1999; Hawke et al. 2003). Braden et al. (2010) and Tran et al. (2011) used Lunar Reconnaissance Orbiter Camera (LROC) stereo images to study the topography of mare and non-mare domes. Volcanic constructs with shallow flank slopes (<10°) are associated with preferentially low-viscosity eruptions, whereas steeper slopes (>20°) tend to indicate high-viscosity, silica-rich eruptions of lava that are more viscous than mare basalts (Hawke et al. 2003; Wilson & Head 2003; Glotch et al. 2011). The Marius Hills complex is a key locality for the first type of dome; the Gruithuisen domes are excellent examples of the second type. However, some domes in the Marius Hills complex display relatively steep slopes (Tran et al. 2011), indicating that localized eruptions of higher-silicic lavas occurred, confirming the LROC and Chandrayaan-1 Terrain Mapping Camera (TMC) results of Lawrence et al. (2010) and Arya et al. (2011), respectively. Detailed morphological and spectral studies of non-mare domes (e.g. Gruithuisen and Hansteen Alpha), as well as domes associated with the Compton-Belkovich thorium anomaly, using LROC and LRO Diviner data are consistent with high-viscosity, silicic, non-mare volcanism (Braden et al. 2010; Glotch et al. 2011; Hawke et al. 2011; Jolliff et al. 2011). Lunar Prospector gamma-ray data revealed that several domes exhibit high Th concentrations (Lawrence et al. 2003; Hagerty et al. 2006), and in LRO Diviner data the domes are characterized by elevated silica contents (Glotch et al. 2011). Some of the non-mare domes show a very specific spectral behaviour in the ultraviolet spectrum and are known as 'red spots'. Red spots show a much wider range in morphology, and also include bright shields and bright smooth plains with little topographical expression (Bruno *et al.* 1991; Hawke *et al.* 2003). Because of their unique characteristics, it is thought that red spots have been formed by more viscous lava, comparable to, for example, terrestrial dacites or rhyolites (Hawke *et al.* 2003; Wilson & Head 2003).

Pyroclastic volcanism. There are two types of pyroclastic deposit that have been identified on the surface of the Moon: extensive regional pyroclastic deposits (>1000 km) located on the uplands adjacent to younger maria (e.g. Gaddis et al. 1985; Weitz et al. 1998); and smaller pyroclastic deposits that are more widely dispersed across the lunar surface (Head 1976; Hawke et al. 1989; Coombs et al. 1990). Most pyroclastic deposits are concentrated in localized areas but some may cover larger areas, in excess of 2500 km² (e.g. Head et al. 2002; Hiesinger & Head 2006) (Figs 6 & 7d). It has been proposed that regional dark-mantle deposits were formed by eruptions in which continuous gas exsolution in the lunar environment caused Hawaiian-style fire fountaining that distributed pyroclastic material over tens to hundreds of kilometres (Wilson & Head 1981, 1983). Substantial progress in understanding the ascent and eruption conditions of pyroclastic deposits has been made (e.g. Head et al. 2002; Shearer et al. 2006). The Apollo 17 orange glasses and black vitrophyric beads, for example, formed during lava fountaining of gas-rich, low-viscosity, Fe-Ti-rich basaltic magmas (Heiken et al. 1974). Crystallized black beads from the Apollo 17 landing site had cooling rates of 100 °C s⁻¹, which is much slower than expected from black-body cooling in a vacuum (Arndt & von Engelhardt 1987). Apollo 17 is not the only landing site where pyroclastic glass beads have been identified. Rather, the Apollo 15 green glasses are also volcanic in origin, as are other pyroclastic glasses found in the regolith of other landing sites (Delano 1986). In comparison to mare basalts, the volumes of pyroclastic deposits are trivial. However, they demonstrate that lava fountaining occurred on the Moon. In addition, because of the presumably fast ascent and cooling history of pyroclastic materials, they are thought to be unmodified by crystal fractionation. Thus, volcanic glass beads are plausibly the best samples for studying the lunar mantle. Pyroclastic eruptions resulted in the emplacement of dark mantled deposits that cover areas of the lunar surface large enough to be visible in remotely sensed data (e.g. Hawke et al. 1979, 1989; Head & Wilson 1980; Gaddis et al. 1985; Coombs et al. 1990; Greeley et al. 1993; Weitz et al. 1998; Weitz & Head 1999; Head et al. 2002). In remote-sensing data, it is apparent that pyroclastic deposits often tend to occur along the margins of impact basins, and in association with vents and sinuous rilles, implying that they were formed by sustained, large-volume eruptions. In addition, at least some of the observed dark-halo craters are volcanic (i.e. pyroclastic) in origin, whereas others are impact craters that excavated darker material from the subsurface. Commonly, the volcanic dark-halo craters preferentially occur along fractures and on the floors of larger craters. From studies of dark-halo craters within Alphonsus crater, it appears likely that they were formed by vulcanian-style eruptions (Head & Wilson 1979; Coombs *et al.* 1990).

Ages of volcanic deposits. On planetary surfaces, the number of impacts on a specific surface unit can be correlated with the time that this unit was exposed to bombardment by asteroids and comets: the higher the crater frequency, the greater the age of the unit (e.g. Öpik 1960; Baldwin 1964; Neukum et al. 1975a, b, 2001; Basaltic Volcanism Study Project 1981). Thus, the frequency of craters superimposed on a specific surface unit at a given diameter, or range of diameters, is a direct measure of the relative age of the unit (e.g. Arvidson et al. 1979; Basaltic Volcanism Study Project 1981; Neukum & Ivanov 1994; Neukum et al. 2001). The stratigraphic record of geological events on the Moon was studied in detail in preparation for, and following, the US and Russian lunar missions (e.g. Shoemaker & Hackman 1962; Wilhelms & McCauley 1971; Wilhelms 1979, 1987). Those studies, in concert with radiometric dating of lunar samples, revealed that the lunar highlands are generally older than the mare regions (e.g. Wilhelms 1987), that mare volcanism occurred over an extended period of time (e.g. Shoemaker & Hackman 1962; Carr 1966; Hiesinger et al. 2000, 2003, 2011) and that there is considerable variation in the mineralogy of basalts of different ages (e.g. Soderblom et al. 1977; Pieters et al. 1980; Hiesinger et al. 2000). Accurate mare basalt ages are important data as they help characterize the duration and the flux of lunar volcanism, the petrogenesis of lunar basalt and the relationship of volcanic activity to the thermal evolution of the Moon.

Hiesinger *et al.* (2000, 2003, 2011, 2012) dated basalts in Oceanus Procellarum, Imbrium, Serenitatis, Tranquillitatis, Humboldtianum, Australe, Humorum, Nubium, Cognitum, Nectaris, Frigoris and numerous smaller occurrences. They found that: (1) in the studied locations, lunar volcanism was active for almost 3 Ga, starting at about 4.0–3.9 Ga and ceasing at around 1.2 Ga; (2) most basalts were erupted during the late Imbrian Period, at about 3.8–3.6 Ga; (3) substantially fewer basalts were emplaced during the Eratosthenian Period (3.2–1.1 Ga); and (4) basalts of possible

Copernican age (<1.1 Ga) are found only in limited areas within Oceanus Procellarum (Hiesinger et al. 2000, 2003, 2011, 2012). From these results it is also apparent that older mare basalts preferentially occur in the eastern and southern lunar nearside, and in patches of maria peripheral to the larger maria, in contrast to the younger basalt ages on the western nearside, for example, those in Oceanus Procellarum. Although older basalts certainly also erupted in the western mare areas prior to the emplacement of younger flows, young volcanism only occurred in the western hemisphere, and has been related to the concentration of heatproducing elements there. Mare basalts on the central lunar farside erupted between 3.5 and 2.7 Ga, which is well within the range of ages found for the nearside mare basalts (Morota et al. 2011; Pasckert et al. 2014). However, farside mare volcanism ceased earlier than on the nearside, which might be a consequence of either a thicker crust or reduced abundances of radioactive elements in the farside mantle.

On the Moon, volcanism apparently resulted from the partial melting of mantle rocks. The decay of naturally radioactive elements resulted in the production of partial melts of mostly basaltic composition (45-55% SiO₂, and relatively high MgO and FeO content), requiring temperatures of >1100 °C and depths of >150-200 km (Hörz et al. 1991). Radiometric ages of returned lunar samples reveal that most volcanic eruptions stopped at approximately 3 Ga (Hörz et al. 1991). This finding was interpreted as evidence for an early cooling of the mantle below the temperature necessary to produce partial melts. However, this interpretation is inconsistent with crater counts on mare basalt surfaces, which indicate that some basalts erupted as 'recently' as about 1-2 Gyr ago (Hiesinger et al. 2003, 2011). Some geophysical models of the thermal evolution of the Moon suggest that the zone of partial melting necessary for the production of basaltic magmas migrated to depths too great for melts to reach the surface approximately 3.4-2.2 Gyr ago (e.g. Spohn et al. 2001). However, taking into account the insulating effects of a porous megaregolith, the interior can be kept warm enough to explain late-stage volcanic eruptions until about 2 Ga (Ziethe et al. 2009). Moreover, a non-uniform distribution of heat-producing elements in the mantle, as indicated by Lunar Prospector data, could extend the potential for melting to even more recent times.

Detailed crater size-frequency distribution measurements revealed that the two Gruithuisen domes in the northern Oceanus Procellarum region appear to be contemporaneous with the emplacement of the surrounding mare basalts, but post-date the formation of post-Imbrium crater Iridum

(Wagner et al. 1996, 2002). Head et al. (2000) interpreted this contemporaneity with the maria as evidence for a petrogenetic link; one possibility is that mare diapirs stalled at the base of, and partially remelted, the crust, which produced the more silicic viscous magmas of the domes. Crater sizefrequency distribution measurements were also performed for red spots in southern Oceanus Procellarum and Mare Humorum, and indicate a wide range of ages. For example, Hansteen Alpha is about 3.74-3.56 Ga old, and so is slightly younger than the Gruithuisen domes but post-dates craters Billy (3.88 Ga) and Hansteen (3.87 Ga). However, Hansteen Alpha is older than the surrounding mare materials (3.51 Ga) (Wagner et al. 2010). NE of Mare Humorum, red-spot light plains associated with a feature named 'The Helmet' (investigated in detail by Bruno et al. 1991) range in age from 3.94 Ga (Darney χ) to 2.08 Ga (Wagner *et al.* 2010). The ages of the Gruithuisen domes and of Hansteen Alpha show that high-silica, more viscous non-mare volcanism was active in a shorter time interval than mare volcanism activity, and appears to be restricted to more or less the Late Imbrian Epoch, at least in these two investigated areas (Wagner et al. 2002, 2010). However, a nonvolcanic origin for the red-spot light plains cannot be excluded on the basis of the data currently available (Wagner et al. 2010 and references therein).

Tectonism

The Moon is a so-called one-plate or stagnant-lid planetary body (e.g. Solomon & Head 1979, 1980; Spohn et al. 2001; Hiesinger & Head 2006). Crystallization of the magma ocean resulted in a globally continuous, low-density crust that may have hindered the development of plate tectonics early in lunar history. Once such a nearly continuous, low-density crust or stagnant lid was established, conductive cooling dominated the transfer of heat from the Moon's interior to its surface. This resulted in the production of a globally continuous lithosphere rather than multiple, moving and subducting plates as on Earth. The heat flows measured at some of the Apollo landing sites are much lower than those on Earth (e.g. Langseth et al. 1976), and are consistent with heat loss predominantly by conduction. The large ratio of surface area to volume has been very effective in cooling the Moon by conduction (i.e. by radiating heat into space). Thus, it is thought that the lithosphere of the Moon thickened rapidly, and so the Moon became a one-plate planet quickly, losing most of its heat through conduction (Solomon 1978). Support for this model comes from nearside seismic data that indicate the presence of a relative rigid, 800-1000 km-thick lithosphere (Nakamura et al. 1973; Spohn et al. 2001; Wieczorek *et al.* 2006). In summary, the crust of the Moon appears to be thick, rigid, immobile and cool, inhibiting large-scale motion. The lack of plate tectonics-style crustal deformation is consistent with the returned samples, which show virtually no textures typical of plastic deformation.

On the Moon, tectonic deformation is caused by: (1) impact-induced stress; (2) stress induced by the load of basaltic materials within impact basins; (3) thermal effects; and (4) tidal forces (e.g. Hiesinger & Head 2006), producing mostly extensional and contractional features (e.g. faults, graben, dykes and wrinkle ridges).

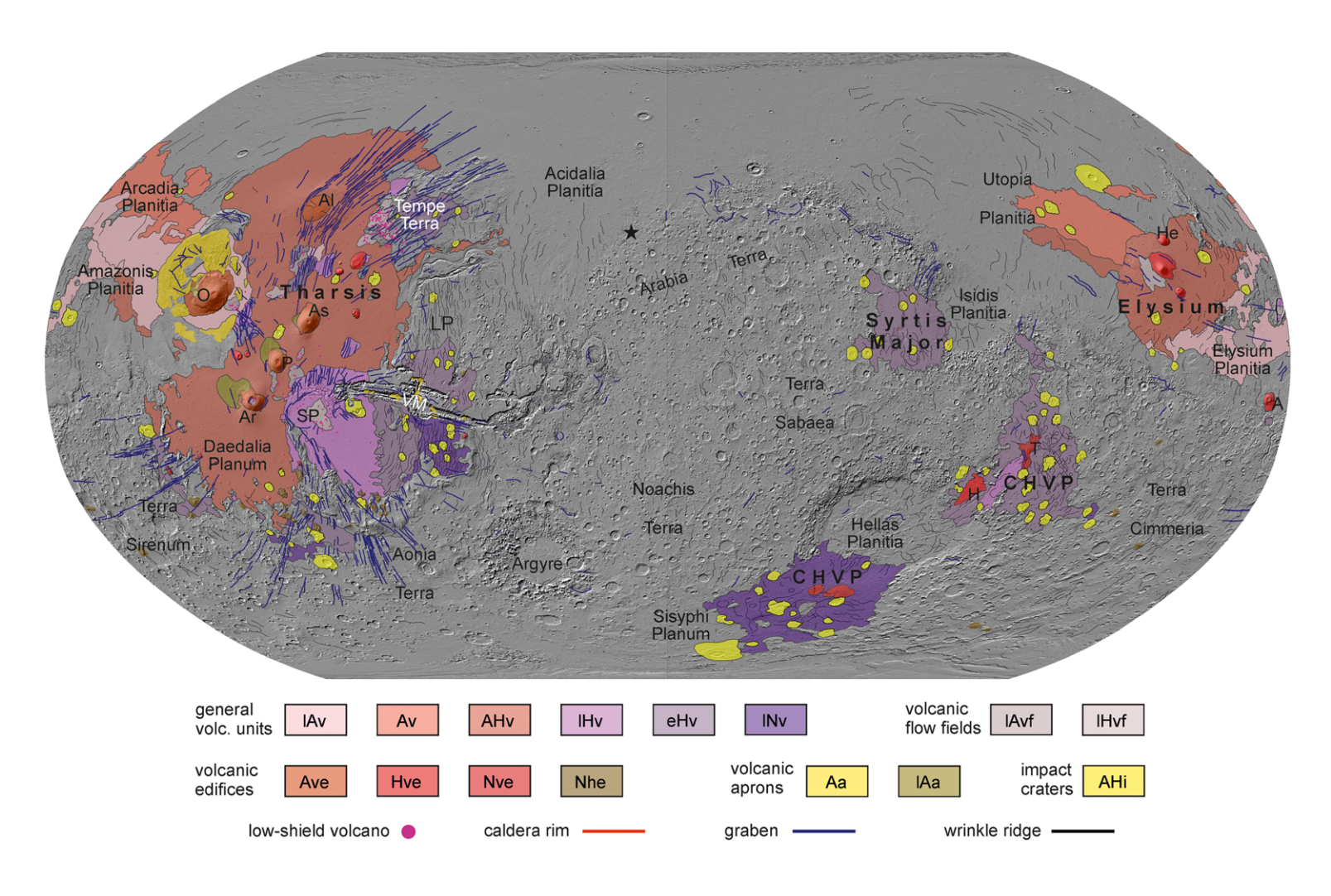
Models of lunar thermal evolution indicate that, during the first billion years, the lunar crust was subject to extensional stresses produced by thermal expansion, and that, during the following 3.5 Ga until the present, compressional stresses have dominated due to cooling and contraction (e.g. Solomon & Chaiken 1976). However, these thermal models have numerous unconstrained parameters that have influence on the model predictions for the evolution of the planetary radius and the resulting stress field (e.g. Pritchard & Stevenson 2000). Although the early stresses in the lunar crust are not accurately known, Solomon & Head (1979) proposed that graben that are related to the loading by basaltic flows of basin centres could only form in the presence of global, mildly tensile stresses. Pritchard & Stevenson (2000) pointed out that the end of graben formation at 3.6 Ga cannot be used to decipher the ancient global lunar stress field because local effects including flexure and magmatic activity (i.e. diapirism) could mask the signal. However, after about 3.6 Ga, the lunar stress field became compressional, and internally driven tectonic activity may have ceased for 2.5-3 Gyr, until sufficient stress (>1 kbar) had accumulated to produce small-scale thrust faults.

Tidal effects due to the Earth-Moon gravitational interaction would have been more intense early in lunar history, when the Moon was closer to Earth. In fact, early lunar tectonic activity may have been dominated by tidal stresses, and internally generated stresses may have been less important. However, the spatial distribution of lineaments mapped on the lunar surface is similar on the near- and farside, and thus is probably independent of tidal forces (e.g. the collapse of a tidal bulge) (Chabot et al. 2000). In particular, Watters et al. (2010) argued that the spatial distribution of small young lobate scarps is inconsistent with an origin related to tidal deformation. They concluded that a global contraction of the lunar radius by 100 m over the last 1 Gyr could explain the observed pattern and calculated stresses.

In the following paragraphs, we describe briefly some of the tectonic landforms on the Moon, including graben, wrinkle ridges, lobate scarps and floor-fractured craters.

Graben. Impacts are capable of creating radial and/ or concentric extensional troughs or graben (e.g. Ahrens & Rubin 1993), and impact-induced faults may be reactivated by seismic energy (e.g. Schultz & Gault 1975). Loading of impact basins with basaltic infill causes the development of extensional stresses at the edges of the basins and the formation of arcuate troughs or rilles there (e.g. Solomon & Head 1979, 1980; Wilhelms 1987) (Fig. 7e). Towards the basin interior, compressional stress due to downwarping of the basin centre leads to the formation of subradial and concentric ridges (Solomon & Head 1979, 1980; Freed et al. 2001) (Fig. 7f). Concentric graben around the Humorum basin are a few hundred kilometres long and are filled with basaltic lavas. Thus, they are evidence of early extensional forces in this area. Because these graben extend virtually unobstructed from the mare into the adjacent highlands and cut across pre-existing craters, their formation was possibly related to a substantial, deep-seated, basin-wide stress field.

Wrinkle ridges. Wrinkle ridges are common landforms on terrestrial planets (Figs 6 & 7f). On the Moon, the spatial dimensions of wrinkle ridges range from several kilometres up to 10 km in width, tens to hundreds of km in length and their average heights are of the order of 100 m (Wilhelms 1987). Lucchitta (1976) proposed that wrinkle ridges are caused by thrust faulting and folding, a model also favoured by Golombek (1999) and Golombek et al. (2000) on the basis of highresolution topographical data of Martian wrinkle ridges. Although wrinkle ridges on the Moon are commonly interpreted as thrust faults formed by compressive stresses (e.g. Hodges 1973; Lucchitta 1976; Solomon & Head 1979, 1980; Plescia & Golombek 1986; Schultz & Zuber 1994; Golombek 1999; Golombek et al. 2000; Hiesinger & Head 2006), some may have an origin linked to the emplacement of magma in the subsurface (e.g. Strom 1964; Hartmann & Wood 1971). Observed en echelon offsets of wrinkle ridges in Mare Serenitatis were interpreted as evidence of compressional stresses. The wrinkle ridges in Mare Serenitatis are concentric to the basin, and Muehlberger (1974) and Maxwell (1978) estimated a centrosymmetric foreshortening of approximately 0.5-0.8% in order to produce the ridges. Ground-penetrating radar (GPR) data from the Apollo Lunar Sounding Experiment (ALSE) revealed substantial upwarping, and possibly folding and faulting of the basaltic surface down to about 2 km below the wrinkle ridges. Recent work has shown that deep-seated faults that penetrate approximately 20 km into the lunar



lithosphere underlie wrinkle ridges in Mare Crisium (Byrne *et al.* 2014*c*).

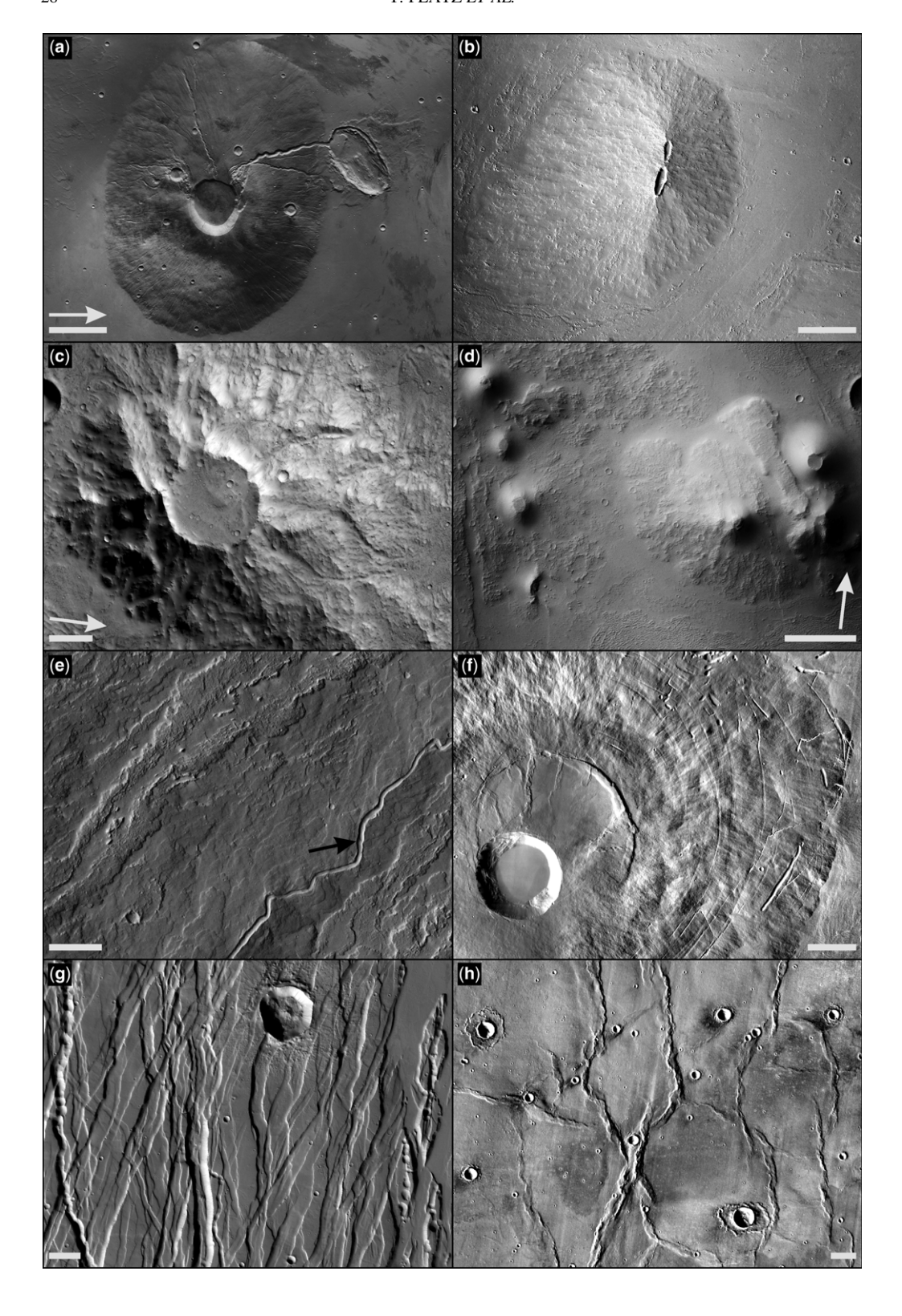
Lobate scarps. Although wrinkle ridges and graben dominate the tectonics of the nearside maria, lobate scarps are the dominant tectonic landform on the farside (Watters & Johnson 2010; Watters et al. 2010). Lunar lobate scarps are characterized by steep scarp faces and by linear or curvilinear asymmetric forms with arcuate fault surfaces, and consist of a series of smaller, connected structures that form complexes. Scarp complexes have lengths of up to about 10 km, occur in sets of up to 10 individual structures and commonly are less than approximately 100 m high (e.g. Binder 1982, 1986; Binder & Gunga 1985; Watters et al. 2010; Banks et al. 2012; Williams et al. 2013; Clark et al. 2014). Schultz (1972) realized that the scarps were very young and based on crater degradation measurements, Binder & Gunga (1985) estimated the ages of lobate scarps found in Apollo Panoramic Camera images to be <1 Ga. Such young ages are generally consistent with crater size-frequency measurements (van der Bogert et al. 2012), their relatively undegraded appearance and their crosscutting relationships with small craters (Watters & Johnson 2010: Watters et al. 2010). Thus, Watters et al. (2010) proposed that the lobate scarps are evidence of late-stage contraction of the Moon, and that the estimated strains accommodated by these small scarps are consistent with thermal history models that predict low-level compressional stresses and relatively small changes (100–1000 m) in lunar radius. Although thermal history models for either a nearly or totally molten early Moon, or an early Moon with an initially hot exterior (i.e. a magma ocean) and a cool interior, predict latestage compressional stresses in the upper crust and lithosphere, the timing of scarp formation and the estimated stress levels are more consistent with the magma-ocean hypothesis (e.g. Watters et al. 2010).

Floor-fractured craters. Numerous impact craters on the Moon exhibit an extensive system of fractures and graben on their floors (Fig. 6). Schultz (1976) proposed that fracturing of lava-filled crater floors (e.g. crater Gassendi) might be related to isostatic uplift of the floor materials and expansion due to the emplacement of sills below the crater floor. Support for this interpretation comes from the geophysical models of Wichman & Schultz (1995, 1996) and Dombard & Gillis (2001). Wichman & Schultz (1996) estimated the minimum depth of a 30 km-wide and 1900 m-thick intrusion beneath crater Tauruntius to be of the order of 1-5 km, resulting in an excess pressure of around 9 MPa. Similarly, on the basis of their model, Dombard & Gillis (2001) concluded that, compared with topographical relaxation, laccolith emplacement is the more viable formation process. More recent studies utilizing gravity data acquired by the Gravity Recovery and Interior Laboratory (GRAIL) mission demonstrated the presence and dynamics of magmatic intrusive bodies beneath floorfractured craters (Jozwiak et al. 2014; Thorey & Michaut 2014).

Mars

Early Mars exploration by flybys of the Mariner 4, 6 and 7 spacecraft, and orbital observations by the Mariner 9 and Viking Orbiter I and II missions, revealed extensive volcanic surfaces and large volcanic edifices on the Red Planet (McCauley *et al.* 1972; Greeley & Spudis 1981). In the seminal paper of Greeley & Spudis (1981), most of the volcanic landforms were categorized into large shield volcanoes (e.g. Olympus Mons and the three Tharsis Montes, Arsia, Pavonis and Ascraeus), steep-sided domes (e.g. Tharsis Tholus) and highland paterae (e.g. Tyrrhenus and Hadriacus Montes) (Fig. 8) – the latter being the only large-scale volcanic

Fig. 8. The distribution of volcanic units, edifices and tectonic structures on Mars (adopted from Tanaka et al. 2014). Unit names consist of (1) age, (2) unit group and (3) unit subtype; (1) stratigraphic periods include: A, Amazonian; H, Hesperian; N, Noachian; with epochs shown in lower case (i.e. e, Early; l, Late); (2) a, apron; h, highlands; i, impact; v, volcanic; (3) e, edifice; f, field. Note that only Amazonian – Hesperian impact craters are shown, which may superpose volcanic units. Units Aa and IAa located around Olympus Mons, and west of the Tharsis Montes, respectively, represent edifice-derived volcanic lastic material. Mapped Noachian highland edifices may be volcanic constructs; those located in Sisyphi Planum are not shown at this map scale. All unit contacts are displayed as certain contacts for clarity. Symbols for graben and wrinkle ridges have been modified from the source (Tanaka et al. 2014). The locations of low-shield volcanoes are from Hauber et al. (2011), Platz & Michael (2011), and Manfredi et al. (2012). Note there exist more low-shield volcanoes in Tharsis; those present in Elysium Planitia are not included. Major volcanic provinces are abbreviated as CHVP, Tharsis, Elysium and Syrtis Major. A, Apollinaris Mons; Al, Alba Mons; Ar, Arsia Mons; As, Ascraeus Mons; CHVP, Circum-Hellas Volcanic Province; H, Hadriacus Mons; He, Hecates Tholus; LP, Lunae Planum; O, Olympus Mons; P, Pavonis Mons; SP, Syria Planum; T, Tyrrhenus Mons; VM, Valles Marineris. The star shows the approximate location of Eden Patera (Michalski & Bleacher 2013). The map has a Robinson projection, centred at 0°E; the background image is a Mars Orbiter Laser Altimeter (MOLA)-derived shaded-relief image (0.46 km/px).



landforms attesting to explosive volcanism in early Mars history (Fig. 8). Extensive volcanic plains associated with large edifices were recognized and grouped into volcanic provinces, with Tharsis and Elysium being the largest, most active and longest-lived (e.g. Neukum *et al.* 2004, 2010; Hauber *et al.* 2011; Platz & Michael 2011). Greeley & Spudis (1981) found that volcanic activity on Mars spans the entire planet's history, and is recorded over large portions of its surface (Fig. 8). Major volcanic landforms, including large volcanic provinces and associated shield volcanoes, pyroclastic cones, lava flows, and fall-out deposits, are reviewed in the following subsections.

Volcanism

Volcanic provinces. The Tharsis region is the most dominant locus of volcanic activity on Mars, extending more than 6000 km (NNE-SSW) by 3500 km (east-west). This region has been mainly formed by five large volcanoes, with summit elevations of up to 21 km (Olympus Mons, Alba Mons and the Tharsis Montes). Several smaller volcanoes, known as paterae and tholi (Uraunius, Biblis, Ulysses Paterae and Tharsis, Ceraunius (Fig. 9a), Uraunius, and Jovis Tholi), are also present (Fig. 8). More than 700 small, low-shield volcanoes (Fig. 9b), vents and fissures located in summit calderas, on edifice flanks, at the periphery of large shield volcanoes or within fractured terrain have also been identified so far. Particularly noteworthy are two low-shield fields in Sinai Planum (Baptista et al. 2008; Hauber et al. 2011; Richardson et al. 2013) and Tempe Terra (Davis & Tanaka 1993; Hauber et al. 2011) (Fig. 8).

The majority of volcanic material in the Tharsis volcanic province was erupted in the Noachian Period (>3.71 Ga) to Early Hesperian Epoch (3.71 – 3.61 Ga), with infrequent eruptions thereafter scattered throughout the Late Hesperian Epoch (3.61-3.37 Ga) and Amazonian Period (3.37 Gapresent) (Neukum & Hiller 1981; Greeley & Schneid 1991: Neukum et al. 2004, 2010: Werner 2009) (Fig. 8). More recently, lava flows as young as 2 Ma were discovered, which are mostly related to low-shield volcanoes or late-stage effusive events (Neukum et al. 2004; Vaucher et al. 2009; Hauber et al. 2011; Platz & Michael 2011). Volcanic activity associated with partial caldera collapse at the summit of most large shield volcanoes has also occurred in the Middle-Late Amazonian (Werner 2009; Robbins et al. 2011). The total production of magma (i.e. intrusive and extrusive) within the Tharsis region is estimated to be about $3 \times 10^8 \text{ km}^3$ (Phillips *et al.* 2001). However, to date, no data exist on what percentage of that volume was erupted during each of the three Martian periods (i.e. the Noachian, Hesperian and Amazonian).

The Elysium volcanic province (Fig. 8) is located in the eastern hemisphere of Mars, and comprises the 14 km-tall Elysium Mons and the smaller Albor and Hecates Tholi, all of which are situated on the broad, >1200 km-wide Elysium rise. The Elysium rise itself developed on the SE rim of the approximately 3300 km-diameter Utopia impact basin, which is thought to have formed at approximately 4.1 Ga (Frey et al. 2007; Frey 2008). This province comprises lava flow plains and reworked volcaniclastic material, which together extend over an area of approximately 3.4×10^6 km² (Tanaka et al. 2005). The total minimum

Fig. 9. Examples of volcanic and tectonic features on Mars. (a) Ceraunius Tholus, a large shield volcano, located in the Tharsis region between Ascraeus Mons and Tempe Terra. It is a large shield volcano partially buried by the surrounding lava plains. From its central caldera a large valley emanates towards the north which formed a delta within the Rahe impact crater. Rahe's butterfly-shaped ejecta blanket is clearly visible. Scale bar is 25 km (HRSC image mosaic; ESA/ DLR/FU Berlin (Gerhard Neukum)). (b) Low-shield volcano located south of Ascraeus Mons at 3.1°N, 106.8°W. The edifice is partially buried by external lava flows; channel and levée morphologies are partially visible. The edifice's summit is marked by two aligned and elongated craters. Lava flows emanated radially from the vents. Scale bar is 2 km (context camera [CTX] image P06_003185_1824). (c) Zephyria Tholus, an ancient, degraded highland volcano located at 19.7°S, 172.9°E that hosts a filled central, circular caldera (scale bar: 4 km; CTX image B18_016743_1597). (d) Pyroclastic cones located in the Ulysses Fossae area north of Biblis Tholus. This image is centred at 5.8°N, 122.8°W. From two cones a thick lava flow emanates. At others an extended surrounding lava field is observed (scale bar: 4 km; CTX image P21_009198_1858). (e) Examples of different types of lava flow morphology, approximately 30 km NNE of Olympus Mons (22.1°N, 129.8°W). Bottom right: a sinuous channel atop a lava tube (black arrow). Top left: lava flows with either channel-levée or sheet-flow morphologies (scale bar: 1 km; CTX image P20_008684_2011). (f) Concentric graben at the lower flanks of Pavonis Mons, whose summit region is marked by a large filled caldera and a vounger, partially filled caldera. Note the radially oriented wrinkle ridges on the summit (THEMIS IR daytime mosaic centred at 1.3°N, 248.6°E; scale bar is 25 km). (g) A heavily fractured surface in Tharsis, located between Ceraunius Fossae and Tractus Catena. In some graben segments, classic pit chains developed; low-lying fractures have been flooded by Tharsis-sourced lava flows (upper left; HRSC image h9443_0000 centred at 26.0°N, 254.2°E; scale bar is 5 km). (h) Typical wrinkle ridges, here shown in Lunae Planum, with linear to concentric orientations. This image is centred at 18.9°N, 295.5°E (THEMIS IR daytime mosaic). Scale bar is 10 km. North is up in all images unless otherwise indicated by white arrow.

volume of erupted and reworked volcanic material is about $3.5 \times 10^6 \, \mathrm{km}^3$ (Platz *et al.* 2010). The eruption frequency for the province has been recently studied by dating lava flows and caldera segments across Elysium (Platz & Michael 2011). Main volcanic activity occurred between 2.5 and 1 Ga but decreased thereafter, however, with 12 less frequent eruptions recorded in the past 500 myr (Platz & Michael 2011).

To the south and SE of Elysium there is yet another volcanically active region known as Elysium Planitia or the Cerberus volcanic plains (Fig. 8), which contains one of the youngest lowshield volcanoes and lava flows known on Mars (Plescia 2003; Werner et al. 2003; Baratoux et al. 2009; Vaucher et al. 2009). Because these lava flows and low-shield volcanoes are mostly associated with or originate at the Cerberus Fossae fracture system, which also extends into the Elysium volcanic province, Platz & Michael (2011) argued that both regions share the same magma source at depth. Hence, Elysium Planitia is considered as part of the broader Elysium volcanic province.

The Syrtis Major volcanic province is located SW of the 1350 km-diameter Isidis impact basin, near the Martian highland-lowland boundary. It extends over $7.4 \times 10^6 \text{ km}^2$, and includes Syrtis Major Planum and the two edifices of Nili and Meroe Paterae (Fig. 8). The estimated thickness of erupted volcanic material in the province ranges from 0.5 to 1 km, with a total volume of about $1.6 \times 10^5 - 3.2 \times 10^5 \text{ km}^3$ (Hiesinger & Head 2004). The low-relief volcanoes each contain a northsouth-orientated caldera, whose formation ages are given as 3.73-2.33 Ga and 3.77-0.23 Ga for Meroe Patera caldera segments, and 3.55-1.61 Ga for Nili Patera (Werner 2009; Robbins et al. 2011). Based on geological mapping and observed areal densities for craters larger than 5 km in diameter, an Early-Late Hesperian age (i.e. 3.71-3.37 Ga) for Syrtis Major volcanism is suggested (Greeley & Guest 1987; Hiesinger & Head 2001; Tanaka et al. 2005, 2014). However, a recent study of mapping and dating of individual lava flows and volcanic crater infill clearly points to volcanic activity extending into the Early and Middle Amazonian Epochs across the province (Platz et al. 2014).

The Circum-Hellas Volcanic Province (CHVP) is located at the periphery of the large, approximately 2100 km-diameter Hellas impact basin (Fig. 8). The province consists of the two well-studied highland volcanoes Tyrrhenus and Hadriacus Montes, as well as the extensive volcanic plains of Hesperia Planum to the NE, and Malea Planum (including the putative volcanoes Amphitrites, Peneus, Malea and Pityusa Paterae) to the SW of Hellas (Greeley & Spudis 1981; Williams *et al.* 2007, 2008, 2009). The entire province covers more

than $2.1 \times 10^6 \, \mathrm{km}^2$ and formed after the Hellas basin-forming event at about $4.0-3.8 \, \mathrm{Ga}$ (Williams et al. 2009). Major volcanic activity throughout the CVHP appears to be restricted to the Noachian and Hesperian, between 3.9 and 3.6 Ga (Williams et al. 2009), although isolated activity at Hesperia Planum did occur during the Early Amazonian (Lehmann et al. 2012).

Apollinaris Mons and other ancient highland volcanoes. Apollinaris Mons is a low-relief, stand-alone volcanic edifice located near the highland-lowland transitional zone SE of the Elysium volcanic province, at 9.2°S, 174.8°E (Fig. 8). The edifice is about 180 km in diameter and rises up to 3.2 km. Based on its relief, surface texture and degraded friable materials, it is likely to be composed of pyroclastic material (Robinson *et al.* 1993; Crumpler *et al.* 2007). Apollinaris Mons appears to have been active during the Noachian and Hesperian periods (Werner 2009; Tanaka *et al.* 2014), which may have included long-lived hydrothermal activity (El Maarry *et al.* 2012).

Recently, some large, irregularly shaped depressions in Arabia Terra were interpreted to represent ancient volcanic constructs that together could form the putative Arabia Terra volcanic province (Michalski & Bleacher 2013). Of these possible volcanoes, Eden Patera (Fig. 8) is the best candidate, a large depression 55 × 85 km in size, located at 33.6°N, 348.9°E. Fine-grained, layered and often sulphate-bearing material exposed throughout Arabia Terra (Malin & Edgett 2000; Edgett & Malin 2002) may represent volcanic fall-out deposits sourced from Eden Patera and nearby presumptive volcanic constructs (Michalski & Bleacher 2013).

In the cratered highlands of Mars, further edifices have been identified that potentially resemble ancient Noachian, partially highly degraded or deformed volcanoes (e.g. Dohm & Tanaka 1999; Stewart & Head 2001; Ghatan & Head 2002; Xiao et al. 2012). Xiao et al. (2012) mapped 75 such edifices; most of them are located at the southern periphery of Daedalia Planum and the Thaumasia highlands, in Terra Sirenum, Sisyphi Planum (including Sisyphi Montes) and Terra Sabea (Fig. 8). However, the best-preserved potential volcanic edifice is Zephyria Tholus (Fig. 9c), located at 19.8°S, 172.9°E (Stewart & Head 2001; Ghatan & Head 2002) (Fig. 8).

Volcanic landforms

Volcano morphometry. Volcano morphology on Mars differs substantially in terms of edifice diameter, height and flank slopes relative to volcanoes on Earth. Martian volcanoes consist primarily of large and low-angle shield volcanoes, domes, pyroclastic cones (scoria/cinder cones and tuff rings) and putative stratovolcanoes. Edifice formation and evolution essentially depends on whether these volcanic constructs were formed during a single eruptive phase (i.e. they are monogenetic) or during repeated eruptions (i.e. polygenetic), and/or on the longevity of volcanism at certain sites, leading to the large shield volcanoes and stratovolcanoes. The large volcanoes known as Montes, Tholi and Paterae in the major volcanic provinces developed over millions to billions of years, punctuated with periods of quiescence of currently unknown durations (e.g. Werner 2009; Williams *et al.* 2010; Platz & Michael 2011).

Owing to the differing geological settings in which major volcanoes formed (e.g. on slopes along the highland-lowland transitional zone (Olympus, Alba, Apollinaris Montes), in tectonically active regions (Alba and Tharsis Montes), or near or on large impact basin rims (Nili and Mereo Paterae or Elysium and Hadriacus Montes, respectively), these edifices are rarely symmetrical in shape and structure. As a result, basal diameters and slopes vary across individual edifices. The giants among the Martian volcanoes, with respect to height and basal diameter, are Olympus Mons (21.2 km in height) and Alba Mons (c. 1100 km in diameter) (Plescia 2004), respectively. Generally, the large shield volcanoes in the Tharsis and Elysium volcanic provinces have flank slopes of about $1^{\circ}-6^{\circ}$, although a few Tholi exhibit flank slopes of up to 27° (Plescia 2004; Platz et al. 2011). Syrtis Major and the circum-Hellas shield volcanoes are characterized by flank slopes of less than 1° (Plescia 2004).

Small shield volcanoes are observed throughout the Tharsis region and in the Elysium volcanic province, and commonly occur in clusters or chains (Figs 8 & 9b). Their basal diameters range from a few kilometres to a few tens of kilometres, and they frequently have summit elevations of up to several hundred metres and flank slopes of less than 5° (Baratoux et al. 2009; Bleacher et al. 2009; Hauber et al. 2009; Richardson et al. 2013). These shield volcanoes are typical of plains-style volcanism (Greeley 1982). It is likely that the formation of low-shield volcanoes was common throughout the evolution of the Tharsis volcanic province, although most of the older edifices were probably buried by successive, subsequent volcanic activity (Hauber et al. 2011).

Pyroclastic cones (Fig. 9d), defined here as scoria/cinder and tephra cones and tuff rings, have only been observed on Mars since the availability of high-resolution imagery in the following areas: Pavonis Mons (Keszthelyi *et al.* 2008), Ascraeus Mons (Mouginis-Mark & Christensen 2005), Syria Planum (Hauber *et al.* 2009), Ulysses Fossae (Brož

& Hauber 2012), Utopia Planitia (Lanz et al. 2010), Nili Patera (Skok et al. 2010) and the Nephentes—Amenthes region (Skinner & Tanaka 2007; Brož & Hauber 2013). Nevertheless, their possible existence in some locations had been reported earlier (e.g. Carr et al. 1977; Frey & Jarosewich 1982; Edgett 1990; Hodges & Moore 1994; Plescia 1994). Morphometric analyses of Martian pyroclastic cones are sparse. However, Brož & Hauber (2012) studied 29 pyroclastic cones in the Ulysses Fossae area in detail (see the cover picture of this Special Publication); cone basal diameter, height and slope can be up to 3.9 km, 650 m and 27.5°, respectively.

Lava flows. Lava flows on Mars can be generally classified as channel fed and tube fed (Fig. 9e). Channel-fed lava flows are often narrow at proximal reaches, forming levées on either side of the flow with a confined inner channel. Further away, the levée-channel morphology can transition into a sheet flow, which is characterized by flat-topped, rough or smooth textured surfaces, steep flow margins and lobate escarpments. Sheet-flow width at distal reaches is often several times larger than the channelled lava flow near its source region. Tube-fed lava flows form curvilinear ridges up to several kilometres across. These long ridges exhibit either single, partially recognizable channels at their crests, or aligned isolated or coalesced pit-craters that formed after the encapsulated tubes had been drained (i.e. syn- or post-eruptive collapse). The tube morphology can transition into multiple overlapping, narrow, channelled to sheettype flows that in turn form a lava field or fan at the base of the tube. This type of tube-fed flow is best observed on the western flanks of Olympus Mons (Fig. 9e). Channel-fed sheet flows are probably best preserved on the relatively young, Middle-Late Amazonian lava plains in the Tharsis province (Fig. 9e). In each of the Martian volcanic provinces, channel-fed and tube-fed lava flows were formed, although their state of preservation differs. Moreover, pre-existing surface textures, channel confinement and slope, lava composition, and effusion rate result in differences in lava-flow morphology (e.g. ridged or platy texture, and channel sinuosity) and morphometry (e.g. width, height, runout distance and volume).

Fallout deposits. Volcanic fallout or tephra deposits generally consist of particles that have been transported ballistically from a source vent or settled from an eruption column. In the latter case, particles may have been transported over large distances before settling down from the atmosphere, forming air-fall deposits. Clast sizes within fallout deposits vary considerably. In proximal reaches, tephra deposits can be poorly sorted, and are comprised

of ash (<2 mm in width), lapilli (2-64 mm) and blocks/bombs fragments (i.e. wall rock/juvenile material; >64 mm). Further from the source, particles become increasingly better sorted, with tephra deposits continuously thinning out downrange of the volcanic plume and away from its apex.

On Mars, several fine-grained and friable deposits have been observed that probably have a volcanic origin. The largest deposits, collectively known as the Medusae Fossae Formation (Scott & Tanaka 1982; Mandt et al. 2008), are located along the highland-lowland transitional zone between 140°E and 230°E (i.e. the longitudinal range) and to the south of the Elysium rise through to Olympus Mons. The source for these large (potentially tephra) deposits has been attributed to either Apollinaris Mons (Kerber et al. 2011b) or to the Tharsis volcanic province (Bradley et al. 2002; Hynek et al. 2003). Interestingly, ground observations by the Mars Exploration Rover 'Spirit' in Gusev crater confirmed the presence of layered coarse and finegrained tephra at 'Home Plate' (Squyres et al. 2007).

Volcaniclastic deposits. The collective term 'volcaniclastic deposit' includes lahar, debris-flow and debri-avalanche (landslide) deposits, dunes, and rootless cones, which together resemble reworked primary volcanic deposits such as lava flows, as well as pyroclastic flow and tephra deposits. On Mars, debris avalanche deposits caused by flank edifice failure are observed in association with Olympus Mons and Tharsis Tholus. Olympus Mons is surrounded by aureole deposits known as Lycus. Cyane, and Gigas Sulci and Sulci Gordii, which represent large-scale landslide deposits that were probably sourced from the circumferential scarp (Lopes et al. 1982; McGovern et al. 2004; Byrne et al. 2013a). Tharsis Tholus also experienced several flank failure events, of which only remnants of the western flank collapse are preserved as mounds and rotated blocks (Platz et al. 2011). The best examples of lahar (and debris-flow) deposits are those associated with the sudden release of groundwater at the western flank of the Elysium rise (Christiansen 1989). During the outburst(s) of water, a substantial portion of the lower western Elysium flank was eroded, transported and deposited onto the plains of Utopia Planitia. Since the observed channels and channel networks of Granicus Valles and Hrad Vallis are confined by debris levées at proximal to medial reaches, a 'pure' fluvial origin with subsequent valley formation can be excluded.

Dark sediments and dunes are frequently observed in the highlands of Mars. They occur mostly within craters, calderas and intercrater plains. Their aeolian origin was suggested in earlier studies (e.g. Thomas 1984; Edgett & Blumberg 1994) and they

feature particle sizes ranging from medium to coarse sand, which appear coarser than their analogues on Earth (Edgett & Christensen 1991, 1994). Remotely sensed spectroscopic studies revealed that most of these dark dunes and sediments are composed of olivine and pyroxene, which suggests a volcanic origin (e.g. Poulet *et al.* 2007; Tirsch *et al.* 2011). Dark basaltic material is either deposited within craters by airfall or tephra layers are exposed by impact craters from which intracrater dunes formed (Tirsch *et al.* 2011). Probably the best examples of active, dark basaltic dunes are those exposed in the caldera Nili Patera (Silvestro *et al.* 2010), which are composed of abraded lava material and reworked tephra.

Rootless cones (or pseudocraters) form by explosive interactions between lava and external water (Thorarinsson 1953), either while lava is flowing over water-saturated strata or when it physically mingles with external water/ice. On Mars, there are abundant locations of so-called rootless cones – conical edifices with a summit depression – that have also been attributed to periglacial processes (i.e. pingos: e.g. Burr et al. 2005; Page 2007) and mud volcanism (Farrand et al. 2005). Recent detailed surveys have shown that small cone groups in Tartarus Colles (Hamilton et al. 2011), and in Athabasca Valles and Cerberus Palus (Keszthelyi et al. 2010), probably formed by rootless eruptions.

Composition of volcanic rocks

The morphology and morphometry of lava flows (e.g. Greeley 1974; Greeley & Spudis 1981; Keszthelyi et al. 2004), and their derived rheological parameters (e.g. Zimbelman 1985; Baloga et al. 2003; Garry et al. 2007; Baratoux et al. 2009; Hauber et al. 2011; Pasckert et al. 2012), together with the similarities between terrestrial (e.g. islands of Hawaii and Galapagos) and Martian shield volcanoes (e.g. Greeley & Spudis 1981; Hauber et al. 2009), suggest that volcanism on Mars is predominantly basaltic in nature. Geochemical analyses of Mars-sourced SNC (Shergottite, Nakhlite Chassignite) meteorites (e.g. McSween 1994, 2002) and in situ rover and lander investigations (e.g. Larsen et al. 2000; McSween et al. 2004) have also confirmed the dominant presence of basaltic rocks on Mars. Although andesitic rock compositions were also suggested to be present at rover/lander sites and across the northern plains (Bandfield et al. 2000; Larsen et al. 2000), Wyatt & McSween (2002) reanalysed mineral abundances from published work and attributed the 'andesite'-like signature to low-temperature, aqueous alteration of basalts. Igneous minerals such as olivine, pyroxene and feldspar, as well as volcanic glass present in the Martian regolith, have been detected by spectral analyses from orbital spacecraft (e.g. Bandfield *et al.* 2000; Christensen *et al.* 2003; Bibring *et al.* 2005). Rock compositional analyses at the Mars Exploration Rover 'Spirit' and Mars Science Laboratory 'Curiosity' landing sites provided evidence for a bulk-chemical, mineralogical and textural diversity of igneous samples (e.g. Squyres *et al.* 2006; Sautter *et al.* 2014).

Volcano-tectonics

Calderas. On all large shield and highland volcanoes across the main volcanic provinces, summit caldera(s) are observed, which attest to single or multiple cycles of large-scale magma storage, growth and replenishment within the edifices and subsequent summit collapse(s). Crumpler et al. (1996) studied Martian calderas and defined two distinct caldera types: (1) Olympus type and (2) Arsia type (Fig. 9a, f), which are characterized by complex/nested or by single summit calderas, respectively. Caldera dimensions vary substantially in diameter and depth. The largest caldera of the biggest shield volcanoes is hosted by Arsia Mons and measures 115 km in diameter, whereas, at highland volcanoes in the CHVP, calderas have formed with diameters up to 145 km (Crumpler et al. 1996). Caldera depths range from a few hundred metres up to 5 km (for Pavonis Mons: Fig. 9f). It has been noted that most of the 'smaller' volcanoes (Uraunius Mons and Tharsis, Ceraunius, Jovis, Biblis, and Ulysses Tholi) at the periphery of the Tharsis Montes exhibit greater caldera depths (i.e. between 1 and 3 km) than the calderas of most of the large shield volcanoes in Tharsis (Crumpler et al. 1996). Martian calderas show similar features to terrestrial calderas, including one or more of the following characteristics: steep, circular to elliptical caldera walls, terraced caldera margins, circumferential scarps, faults and graben, radially orientated ridges and faults, pit crater chains, linear arrangement of small vents, and volcanic flooding that has levelled caldera floors (e.g. Crumpler et al. 1996; Mouginis-Mark & Rowland 2001; Platz et al. 2011; Byrne et al. 2012).

Flank deformation. Volcanoes can experience tectonic deformation due to a number of exogenic processes (e.g. rifting) but gravitationally driven tectonism is one of the primary endogenic processes responsible for volcano flank deformation (Fig. 9f). Edifice spreading and sagging represent end members of a structural continuum along which a given volcano, subject to gravitational deformation, will lie; this continuum probably applies to Mars as equally as it does to Earth (Byrne et al. 2013a). Volcano spreading is characterized by the formation of a system of radial normal faults,

often forming 'leaf graben', on the flanks of the edifice and a concentric thrust belt at its base (Borgia *et al.* 2000). In contrast, volcano sagging will result in the development of concentric flank thrusts or 'terraces' (Byrne *et al.* 2009, 2013*a*), accompanied by the formation of a flexural moat and bulge (e.g. Comer *et al.* 1985).

There is little direct evidence for volcano spreading on Mars. This is because spreading requires that an edifice be mechanically detached from its underlying basement, such that the response to loading is accommodated in the main by the volcano itself (e.g. McGovern & Solomon 1993; Borgia 1994), and the conditions necessary for such decoupling (e.g. low-competency strata such as clays) are not widely observed on Mars. Nevertheless, the Tharsis Tholus edifice, in eastern Tharsis, does appear to have experienced sector collapse in a manner similar to volcanoes known to have spread on Earth (Platz et al. 2011). Spreading along phyllosilicates proximal to and beneath Olympus Mons has also probably played a role in shaping that volcano (Morgan & McGovern 2005; McGovern & Morgan 2009; Byrne et al. 2013a).

The effects of volcano sagging are seen much more widely across Mars. At least nine volcanoes (including Olympus Mons) show evidence of flank terraces, topographically subtle landforms that are difficult to see without the aid of topographical data (Byrne et al. 2009). These structures were observed on Olympus and on the Tharsis Montes initially (e.g. Thomas et al. 1990) but their prevalence on shields of a range of shapes and sizes indicates that their formation is likely to be tied to a process commonly experienced by volcanoes. Flank terraces were tied to lithospheric flexure by McGovern & Solomon (1993), an interpretation reinforced by more recent analogue modelling studies (e.g. Byrne et al. 2013a). Importantly, volcano sagging will serve to place an edifice into a state of net compression, which will impede or even inhibit magma ascent to its summit, and, in turn, will alter its eruptive behaviour and development (e.g. Byrne et al. 2012; McGovern et al. 2014).

Tectonic structures

It is widely accepted that Mars is a one-plate planet, although the prospect of plate tectonics having at some point operated on that planet has yet to be fully resolved (Sleep 1994; Yin 2012). This possibility was proposed because of the apparent hemispheric crustal dichotomy dividing Mars into the southern high-standing, cratered highlands and the northern lowlands, with the latter appearing, with Viking-based imagery, to be less cratered than the southern highlands. With new, high-resolution topographical data, however, large subdued basin

structures were discovered, which most probably makes the lowlands as old as the highlands (Frey 2008). There are currently two theories for how the dichotomy on Mars developed: (1) by a giant impact (e.g. Wilhelms & Squyres 1984; Andrews-Hanna *et al.* 2008; Marinova *et al.* 2008); or (2) by endogenic processes (convective overturn of the interior (Wise *et al.* 1979) or by degree-1 convection with north–south asymmetry (Zhong & Zuber 2001; Roberts & Zhong 2006)).

In the Martian lithosphere, a suite of faults has been identified with normal (e.g. Plescia & Saunders 1982; Schultz et al. 2007), reverse (e.g. Schultz & Tanaka 1994) and strike-slip senses of movement (Andrews-Hanna et al. 2008; Yin 2012) (Fig. 8). Extensional features include normal faults, halfgraben, graben and rift-like structures such as Acheron Fossae (Kronberg et al. 2007) (Figs 8 & 9g). As for other terrestrial worlds, most graben likely represent an hourglass-shaped subsurface pattern (Schultz et al. 2007). And as for Mercury and the Moon, wrinkle ridges (Figs 7f & 9h) are very common landforms on the Martian surface once more interpreted as arcuate, asymmetric ridges that have formed above an underlying, low-angle thrust fault. This type of faulting is thought to occur in layered rocks such as sedimentary sequences or successions of lava flows. Well-developed wrinkle-ridge systems are probably best preserved in Lunae, Solis and Syrtis Major Plana (Fig. 9h).

The global tectonic map of Mars (Knapmeyer et al. 2006) shows that the focus of activity is associated with the large Tharsis volcanic province. Here, large sets of normal faults, half-graben and graben radiate outwards (with minor occurrences of concentric faults) from the central Tharsis rise (Fig. 8). Plescia & Saunders (1982) studied in detail the tectonic evolution of Tharsis, and proposed four discrete centres of faulting that, from oldest to youngest, include the Thaumasia highlands, northern Syria Planum and two centres near Pavonis Mons.

The timing of the main tectonic activity on Mars was later determined by Anderson et al. (2001) to have peaked in five main phases. The oldest identified stage of activity occurred during the Noachian, when most of the graben in Syria Planum, Tempe Terra and Thaumasia formed. The Late Noachian-Early Hesperian (stage 2) and Early Hesperian (stage 3) tectonic phases formed extensional structures along the central Valles Marineris, and in Pavonis, Syria, Ulysses and Tempe Terra, respectively. Stage 3 tectonic activity is also associated with wrinkle-ridge formation in Lunae and Solis Plana, as well as in Thaumasia, Sirenum, Memnonia and Amazonis Planitia (Anderson et al. 2001). The tectonic structures formed in stage 4 (Late Hesperian-Early Amazonian)

developed around Alba Mons and the Tharsis Montes, whereas the latest activity (stage 5) occurred during the Middle–Late Amazonian with associated faults located around the large shield volcanoes (Anderson *et al.* 2001).

The main cause of extensional deformation within Tharsis and its periphery is its loading-induced stress on the lithosphere. It is thought that most graben are the surface expressions of giant dyke swarm intrusions (Ernst *et al.* 2001; Wilson & Head 2002; Schultz *et al.* 2004). Similar concentric and radial fault patterns (e.g. Cerberus Fossae), although far less numerous, are also observed in the Elysium volcanic province, where the mass and volume of the Elysium rise has also induced faulting.

Valles Marineris constitutes the largest, most spectacular and, perhaps, the most puzzling set of canyons in the solar system (Lucchitta et al. 1992). Although the linearity of canyon walls suggests a tectonic origin, differing driving mechanisms have been proposed for the canyons, including tectonic rifting associated with large-scale magmatism and/or extensive dyke emplacement (e.g. Blasius et al. 1977; Mège & Masson 1996; McKenzie & Nimmo 1999; Schultz & Lin 2001; Dohm et al. 2009), collapse along tectonic zones and subsequent catastrophic discharges (Sharp 1973; Tanaka & Golombek 1989; Spencer & Fanale 1990; Rodriguez et al. 2006), salt tectonics (Montgomery & Gillespie 2005; Adams et al. 2009), composite origins involving erosion (Lucchitta et al. 1994) and/or major distinct stages of collapse and normal faulting (Schultz 1998), and volcano-erosion where Tharsissourced lava tubes form pit chains due to roof collapse, which later evolve into fossae and chasmata (Leone 2014). A recent study by Andrews-Hanna (2012) showed that canyon formation occurred through displacement along steeply dipping faults, coupled with vertical subsidence.

Article summaries

P. Mancinelli, F. Minelli, A. Mondini, C. Pauselli & C. Federico

A downscaling approach for geological characterization of the Raditladi basin of Mercury

Through combining newly available photogeological, compositional and topographical data for Mercury, Mancinelli et al. (2014) first present a new synthesis of the surface units on the innermost planet. These authors then investigate an area of particularly diverse units in greater detail, an area that includes the 260 km-diameter Raditladi

impact basin. In investigating the geological history of the basin, they construct a geological cross-section that shows how the volcanic units inside the interior of Raditladi were emplaced upon impact-related units. The chapter ends with a call for further regional- and local-scale mapping of Mercury, to elucidate the origin of units observed globally but whose nature is currently unclear.

N. P. Lang & I. López

The magmatic evolution of three Venusian coronae

Lang & López (2013) argue that the volcanic products and forms associated with three case-study coronae, Zemire, Bhumidevi and Aramiti, may not be consistent with widely accepted models of corona formation. Instead, their evolution can be explained by the mass evacuation of a stratified, shallow magma chamber. This evacuation and collapse would account for the observed extensive lava flows emanating from the annular fractures surrounding these coronae, as well as the steep-sided domes and tholi that formed along these fractures at the latest stage of the corona evolution, when crystal-rich magmas (or basaltic foams) were squeezed up and forced to the surface.

R. C. Ghail & L. Wilson

A pyroclastic flow deposit on Venus

Ghail & Wilson (2013) describe the morphological characteristics of a semi-circular, doughnut-shaped deposit on Venus that is morphologically consistent with pyroclastic flow deposits on Earth. The hydrodynamic interaction of this deposit, named Scathach Fluctus, with a volcanic cone indicate flow velocities of up to 48 m s⁻¹. Estimated volatile abundances associated with the explosive eruption imply high CO₂ and SO₂ concentrations in the mantle. Because the radar characteristics of Scathach Fluctus are similar to many parts of the Venusian surface, these authors suggest that pyroclastic flow deposits are more widespread on the second planet than previously thought.

C. M. Meyzen, M. Massironi, R. Pozzobon & L. Dal Zilio

Are terrestrial plumes from motionless plates analogues to Martian plumes feeding the giant shield volcanoes?

Hawaiian intraplate volcanism has long been thought an apt analogue to the giant, long-lived volcanoes on Mars. However, Meyzen et al. (2014) argue for a revision of that view: that, instead, volcanoes on the slow-moving Nubian and Antarctic plates provide a better comparison. By comparing and contrasting the properties of volcanoes located on slow-moving plates on Earth with the large volcanoes in Mars' Tharsis region, these authors seek to understand more fully the nature and significance of the large-scale melting and differentiation processes of volcanoes on Mars.

T. Morota, Y. Ishihara, S Sasaki, S. Goossens, K. Matsumoto, H. Noda, H. Araki, H. Hanada, S. Tazawa, F. Kikuchi, T. Ishikawa, S. Tsuruta, S. Kamata, H. Otake, J. Haruyama & M. Ohtake

Lunar mare volcanism: lateral heterogeneities in volcanic activity and relationship with crustal structure

The asymmetry of lunar near- and farside maria is still under investigation. Here, **Morota** *et al.* **(2014)** study the relationship between mare distribution and crustal thickness on the Moon using remotely sensed geological and geophysical data. Their results show that magma extrusion is dominant in regions of relatively thin crust, which is consistent with previous studies. However, these authors also find lateral heterogeneities in the upper limits of crustal thickness, which would allow magma ascent to, and lava extrusion onto, the lunar surface. These heterogeneities may be due to lateral variations in melt/magma generation within the mantle and/or changes in crustal density.

C. Carli, G. Serventi & M. Sgavetti

VNIR spectral characteristics of terrestrial igneous effusive rocks: mineralogical composition and the influence of texture

Carli et al. (2014) discuss the utility of visible and near-infrared (VNIR) spectroscopy to map mineralogical variations across planetary surfaces. In particular, igneous rocks emplaced effusively have distinct crystal field absorption bands in the VNIR spectral range, bands that correspond to the rocks' constituent mineralogy. These authors review how petrological properties influence the interpretation of rock mineralogy using spectroscopy. Among other results, they show how grain and crystal size can influence the spectra of effusive rocks, and how glassy components in rock groundmass reduce or hide absorption bands of mafic minerals or feldspars. They also suggest that combining

geomorphic and spectral data is the most reliable method of mapping of volcanic material on planetary surfaces.

S. Ferrari, M. Massironi, S. Marchi, P. K. Byrne, C. Klimczak, E. Martellato & G. Cremonese

Age relationships of the Rembrandt basin and Enterprise Rupes, Mercury

The time-stratigraphic relationship between the 715 km-diameter Rembrandt impact basin and the Enterprise Rupes scarp system, which extends for over 800 km across the surface of Mercury, is the focus of the work by Ferrari et al. (2014). These authors find that the Rembrandt basin formed at about 3.8 Ga, with resurfacing of its interior by volcanic smooth plains occurring within 100–300 myr after basin formation. The most recent activity along Enterprise Rupes took place at about 3.6 Ga, cross-cutting (and therefore post-dating) the basin's volcanic infilling event(s). It is currently unclear whether the initiation of the Enterprise Rupes fault system pre- or post-dates the Rembrandt basin-forming event.

F. C. Lopes, A. T. Caselli, A. Machado & M. T. Barata

The development of the Deception Island volcano caldera under control of the Bransfield Basin sinistral strike-slip tectonic regime (NW Antarctica)

Deception Island is a small, volcanically active caldera volcano located in the Bransfield Strait, off the Antarctic Peninsula. **Lopes** *et al.* (2014) present evidence that the fractures that have shaped the edifice, and its elongate caldera, are the result of pervasive left-lateral simple shearing within the Bransfield Basin. They also review the formational history of the caldera, proposing that at least two phases of collapse have occurred: first in a small-volume event and, later, in a larger event that affected the flanks of the volcano itself

P. K. Byrne, E. P. Holohan, M. Kervyn, B. van Wyk de Vries & V. R. Troll

Analogue modelling of volcano flank terrace formation on Mars

Flank terraces are laterally extensive, topographically subtle landforms on the slopes of large Martian shield volcanoes. In this chapter, **Byrne** *et al.* (2014a) use a series of scaled analogue models to

test the hypothesis that flank terraces result from constriction of a volcano as it down-flexes its underlying lithospheric basement. They show that terrace formation on sagging edifices is largely independent of volcano slope, size or aspect ratio, but increasing lithospheric thickness will ultimately inhibit terrace development entirely. These authors conclude that understanding the structural evolution of large shields on Mars requires that these volcanoes be appraised within the context of lithospheric flexure.

R. Pozzobon, F. Mazzarini, M. Massironi & L. Marinangeli

Self-similar clustering distribution of structural features on Ascraeus Mons (Mars): implications for magma chamber depth

Pozzobon et al. (2014) use self-similar fractal clustering techniques to examine the distribution of pit craters on the Ascraeus Mons volcano on Mars. These pits are probably related to feeder dykes and, by understanding how the pits are distributed, the subsurface architecture of the magma system below Ascraeus can be understood. The authors find evidence for two discrete pit populations, indicative of two magma sources – one at shallow depths and the other deep below the volcano – and appraise this finding within the context of earlier studies of the volcano, suggesting that this analysis may provide insight into the deep structure of other large volcanoes on Mars.

P. J. McGovern, E. B. Grosfils, G. A. Galgana, J. K. Morgan, M. E. Rumpf, J. R. Smith & J. R. Zimbelman

Lithospheric flexure and volcano basal boundary conditions: keys to the structural evolution of large volcanic edifices on the terrestrial planets

McGovern et al. (2014) study the interplay between large volcanic edifices and the underlying lithosphere, which flexes in response to the exerted volcanic load. Lithospheric thickness influences the shape of the flexural response, and the associated stress states in turn can influence the structure and evolution of the overlying edifice – which in turn affects lithosphere response. The edifice–basement basal boundary condition (i.e. welded base or gliding basal plane) determines whether compression is transferred into the edifice, which can potentially inhibit magma ascent into the edifice. Volcanoes situated on a thick lithosphere and a clay-based

décollement can grow to enormous sizes, whereas the growth of an edifice welded to a thin lithosphere is likely to be limited.

E. B. Grosfils, P. J. McGovern, P. M. Gregg, G. A. Galgana, D. M. Hurwitz, S. M. Long & S. R. Chestler

Elastic models of magma reservoir mechanics: a key tool for investigating planetary volcanism

Exploring the mechanics of magma storage, its ascent to the surface, and the interplay of subsurface and surface volcano-tectonic processes is the main objective of this contribution by **Grosfils** *et al.* (2013). These authors use bespoke elastic numerical models that leverage field, laboratory and remotesensing observations to study volcanic processes on terrestrial worlds. Their models provide renewed insights into how subsurface magma reservoirs inflate and rupture, and how these processes relate to volcano growth, caldera formation, and the associated emplacement of circumferential and radial dykes.

M. Massironi, G. Di Achille, D. A. Rothery, V. Galluzzi, L. Giacomini, S. Ferrari, M. Zusi, G. Cremonese & P. Palumbo

Lateral ramps and strike-slip kinematics on Mercury

Massironi et al. (2014) investigate contractional features on Mercury for evidence of strike-slip deformation. Such evidence includes en echelon fold arrays, restraining bends, positive flower structures, stike-slip duplexes and crater rims that have been displaced by lobate scarps and high-relief ridges. These authors find that the strike-slip to transpressional motion along faults they observe is inconsistent with a globally homogenous stress field predicted to result from secular cooling-induced global contraction alone. They conclude that other processes, such as mantle convection, may have played a contributory role during the tectonic evolution of Mercury.

L. Giacomini, M. Massironi, S. Marchi, C. I. Fassett, G. Di Achille & G. Cremonese

Age dating of an extensive thrust system on Mercury: implications for the planet's thermal evolution

Mercury's surface is characterized by abundant contractional features such as lobate scarps and wrinkle ridges, which are principally attributed to the planet's secular cooling and resultant global contraction. Giacomini et al. (2014) study the formation age of an extensive fold and thrust belt of which Blossom Rupes is part, using different age determination techniques, including buffered crater counting. They find that thrust activity along this system terminated between 3.7 and 3.5 Ga. Should these techniques indicate that other large-scale contractional features on Mercury have similar ages, a revision of current thermal evolution models for Mercury, including an earlier onset of planetary contraction, is required.

V. Galluzzi, G. Di Achille, L. Ferranti, C. Popa & P. Palumbo

Faulted craters as indicators for thrust motions on Mercury

Is it possible to directly determine true dip angles and slip vectors for faults on other planets? **Galluzzi** *et al.* (2014) show that this can be accomplished by using digital terrain models of deformed craters on Mercury. In so doing, these authors demonstrate the broad range of dip angles and kinematics of Mercurian faults. This methodology, which allows for the quantitative structural characterization of remotely sensed faults, can be used to enhance our understanding of planetary geodynamics.

L. B. Harris & J. H. Bédard

Interactions between continent-like 'drift', rifting and mantle flow on Venus: gravity interpretations and Earth analogues

Harris & Bédard (2014b) identify major strikeslip shear zones at Ishtar and Afrodite Terrae and at Sedna Planitia, using offsets of Bouger gravity anomalies and gravity gradient edges. Their observations call for a new conceptual model capable of satisfying Venusian subduction-free geodynamics, dominant convective upwellings and the substantial horizontal tectonism required by the observed strike-slip belts. These authors suggest that mantle traction, generated and controlled by linear upwellings along rifts, has resulted in the substantial lateral motion of areas of continent-like crust on Venus, such as Lakshumi planum (in western Ishtar Terra). This process accounts for the fold-andthrust belt that bounds Lakshumi planum to the north, as well as the transpressive regimes recognized at its eastern and western margins. Harris & Bédard (2014b) conclude by proposing that this new perspective of Venus may provide insight into the tectonics of the Archaean Earth.

M. T. Barata, F. C. Lopes, P. Pina, E. I. Alves & J. Saraiya

Automatic detection of wrinkle ridges in Venusian Magellan imagery

Wrinkle ridges are common and widespread tectonic features on Venus. Barata et al. (2014) present an automated algorithm to detect wrinkle ridges using Magellan Synthetic Aperture Radar imagery, with which they characterize ridge morphology, including orientation, length and spacing. This procedure greatly enhances wrinkle ridge mapping and analysis. In addition, these authors also test an automated procedure to identify and characterize impact craters and their ejecta.

A. L. Nahm & R. A. Schultz

Rupes Recta and the geological history of the Mare Nubium region of the Moon: insights from forward mechanical modelling of the 'Straight Wall'

The Moon's famous Rupes Recta, or 'Straight Wall', situated in Mare Nubium on the lunar near-side has been known for more than three centuries. Nahm & Schultz (2013) investigate its fault characteristics. Detailed structural mapping and throw distribution measurements show that this structure has experienced bi-directional growth. Forward mechanical modelling of its topography indicates that the fault has a dip angle of 85°, almost 0.5 km of maximum displacement and penetrates over 40 km into the lunar lithosphere. These authors show that the development of Rupes Recta could have been strongly influenced by columnar cooling joints activated as shear planes during subsidence of Mare Nubium.

D. Y. Wyrick, A. P. Morris, M. K. Todt & M. J. Watson-Morris

Physical analogue modelling of Martian dyke-induced deformation

Dykes are commonly thought to form, and thus underlie, laterally extensive graben on planetary surfaces. Using analogue modelling techniques, Wyrick et al. (2014) demonstrate that dykes injected into an undisturbed crust cause ridges and related contractional features to develop at the surface, instead of extensional structures. This finding has important implications for graben sets on numerous worlds, including our understanding of Tharsis-radial graben, which should predate dyke emplacement, the evolution of Venusian radiating

fissure systems and, supposedly, dyke-induced graben on the Moon

L. Guallini, C. Pauselli, F. Brozzetti & L. Marinangeli

Physical modelling of large-scale deformational systems in the South Polar Layered Deposits (Promethei Lingula, Mars): new geological constraints and climatic implications

In a follow-on study of the Promethei Lingula ice sheet on Mars, **Guallini et al.** (2014) integrate structural analysis with thermal and mechanical models to quantify the deformation of part of the ice sheet's South Polar Layered Deposits. They show that parts of these deposits feature soft-sediment deformation and that internal compositions are dominated by CO₂ ice. Moreover, these authors determine that deformation of the layered deposits is unlikely to have occurred under present-day climatic conditions. Instead, warmer temperatures in the past were likely to have been responsible for soft-sediment deformation, and may even have triggered gravitational sliding of the entire ice sheet.

D. L. Buczkowski & D. Y. Wyrick

Tectonism and magmatism identified on asteroids

This contribution provides a review of linear features observed on a range of asteroids, including Gaspra, Eros and Itokawa. **Buczkowski & Wyrick** (2014) primarily focus on previous observations of tectonic structures, current models to explain linear feature formation and the implications for the internal structure of these small bodies. Even though Vesta is a unique and differentiated proto-planetary body, it hosts fractures and grooves that are morphologically similar to those observed on smaller asteroids, and is therefore also included in this review chapter. To date, no volcanic features have been identified on Vesta's surface, but these authors discuss the prospect that the geological history of Vesta may have included endogenic magmatism.

This volume would not have been possible without the assistance of all who willingly agreed to review these chapters. Thanks also go to the reviewer, D. A. Williams, of this chapter. The authors also wish to thank T. M. Hare (USGS Astrogeology Science Center, Flagstaff, AZ) for compiling global datasets in GIS-ready formats for Venus, the Moon and Mars. M. A. Ivanov (Russian Academy of Science, Moscow) kindly provided his geological map of Venus and assisted in simplifying the map units. P. K.

Byrne acknowledges support from the MESSENGER project, under contracts NASW-00002 to the Carnegie Institution of Washington and NAS5-97271 to The Johns Hopkins University Applied Physics Laboratory, and from the Department of Terrestrial Magnetism, Carnegie Institution of Washington. M. Massironi acknowledges the support from the Italian Space Agency (ASI) within the SIMBIOSYS Project (ASI-INAF agreement no. I/022/10/0) and from the University of Padua within the Ateneo Project CPDA112213/11. This research made use of NASA's Planetary Data System and Astrophysics Data System.

References

- ADAMS, J. B., GILLESPIE, A. R. ET AL. 2009. Salt tectonics and collapse of Hebes Chasma, Valles Marineris, Mars. Geology, 37, 691–694.
- AHRENS, T. J. & RUBIN, A. M. 1993. Impact-induced tensional failure in rock. *Journal of Geophysical Research*, 98, 1185–1203.
- AITTOLA, M. & KOSTAMA, V. 2000. Venusian novae and arachnoids: characteristics, differences and the effect of the geological environment. *Planetary Space Science*, 48, 1479–1489.
- AITTOLA, M. & KOSTAMA, V. P. 2002. Chronology of the formation process of Venusian novae and the associated coronae. *Journal of Geophysical Research*, 107, 5112.
- ANDERSON, D. L. 2007. New Theory of the Earth. Cambridge University Press, Cambridge.
- ANDERSON, F. S. & SMREKAR, S. E. 1999. Tectonic effects of climate change on Venus. *Journal of Geophysical Research*, **104**, 30 743–30 756.
- ANDERSON, R. C., DOHM, J. M. ET AL. 2001. Primary centers and secondary concentrations of tectonic activity through time in the western hemisphere of Mars. *Journal of Geophysical Research*, **106**, 20 563–20 585.
- ANDREWS-HANNA, J. C. 2012. The formation of Valles Marineris: 1. Tectonic architecture and the relative roles of extension and subsidence. *Journal of Geophy*sical Research, 117, E03006.
- ANDREWS-HANNA, J. C., ZUBER, M. T. & BANERDT, W. B. 2008. The Borealis basin and the origin of the Martian crustal dichotomy. *Nature*, 453, 1212–1215.
- ANSAN, V., VERGELY, P. & MASSON, P. 1996. Model of formation of Ishtar Terra, Venus. *Planetary and Space Science*, 44, 817–831.
- ANTONENKO, I., HEAD, J. W., MUSTARD, J. F. & HAWKE, B. R. 1995. Criteria for the detection of lunar cryptomaria. *Earth, Moon, and Planets*, 69, 141–172.
- ARKANI-HAMED, J. 1996. Analysis and interpretation of high-resolution topography and gravity of Ishtar Terra, Venus. *Journal of Geophysical Research*, 101, 4691–4710.
- Arndt, J. & von Engelhardt, W. 1987. Formation of Apollo 17 orange and black glass beads. *Journal of Geophysical Research*, 92, 372–376.
- ARVIDSON, R. E., BOYCE, J. ET AL. 1979. Standard techniques for the presentation and analysis of crater size-frequency data. *Icarus*, 37, 467–474.
- ARYA, A. S., THANGJAM, G. & RAJASEKHAR, R. P. 2011. Analysis of mineralogy of an effusive volcanic lunar

- dome in Marius Hills, Oceanus Procellarum. Abstract 1845 presented at the EPSC-DPS Joint Meeting 2011, 2–7 October 2011, Nantes, France.
- BAER, G., TERRA, L., BINDSCHADLER, D. L. & STOFAN, E. R. 1994. Spatial and temporal relations between coronae and extensional belts, northern Lada Terra, Venus. *Journal of Geophysical Research*, **99**, 8355–8369.
- BAKER, V. R., KOMATSU, G., GULICK, V. C. & PARKER, T. J. 1997. Channels and valleys. *In*: BOUGHER, S. W., HUNTEN, D. M. & PHILLIPS, R. J. (eds) *Venus II*: *Geology, Geophysics, Atmosphere, and Solar Wind Environment*. University of Arizona Press, Tucson, AZ, 757–793.
- BALDWIN, R. B. 1964. Lunar crater counts. *The Astronomical Journal*, **69**, 377–392.
- BALOGA, S. M., MOUGINIS-MARK, P. J. & GLAZE, L. S. 2003. Rheology of a long lava flow at Pavonis Mons, Mars. Journal of Geophysical Research, 108, E75066.
- BANDFIELD, J. L., HAMILTON, V. E. & CHRISTENSEN, P. R. 2000. A global view of Martian surface compositions from MGS-TES. *Science*, 287, 1626–1630.
- BANERDT, W. B., McGILL, G. E. & ZUBER, M. T. 1997. Plains tectonics on Venus. In: GOUGHER, S. W., HUNTEN, D. M. & PHILLIPS, R. J. (eds) Venus II: Geology, Geophysics, Atmosphere, and Solar Wind Environment. University of Arizona Press, Tucson, AZ, 901–930.
- BANKS, M. E., WATTERS, T. R., ROBINSON, M. S., TORNABENE, L. L., TRAN, T., OJHA, L. & WILLIAMS, N. R. 2012. Morphometric analysis of small-scale lobate scarps on the Moon using data from the Lunar Reconnaissance Orbiter. *Journal of Geophysical Research*, 117, E00H11, http://dx.doi.org/10.1029/2011JE00 3907
- BAPTISTA, A. R., MANGOLD, N. ET AL. 2008. A swarm of small shield volcanoes on Syria Planum, Mars. Journal of Geophysical Research, 113, E9010.
- BARATA, M. T., LOPES, F. C., PINA, P., ALVES, E. I. & SARAIVA, J. 2014. Automatic detection of wrinkle ridges in Venusian Magellan imagery. In: PLATZ, T., MASSIRONI, M., BYRNE, P. K. & HIESINGER, H. (eds) Volcanism and Tectonism Across the Inner Solar System. Geological Society, London, Special Publications, 401. First published online January 9, 2014, http://dx.doi.org/10.1144/SP401.5
- BARATOUX, D., PINET, P., TOPLIS, M. J., MANGOLD, N., GREELEY, R. & BAPTISTA, A. R. 2009. Shape, rheology and emplacement times of small Martian shield volcanoes. *Journal of Volcanology and Geothermal Research*, **185**, 47–68.
- BARSUKOV, V. L., BASILEVSKY, A. T. ET AL. 1986. The geology and geomorphology of Venus surface as revealed by the radar images obtained by Venera 15 and 16. Journal of Geophysical Research, 91, 378–398.
- BASALTIC VOLCANISM STUDY PROJECT 1981. Basaltic Volcanism on the Terrestrial Planets. Pergamon, New York.
- Basilevsky, A. T. & Head, J. W. 1995. Regional and global stratigraphy of Venus: a preliminary assessment and implications for the geological history of Venus. *Planetary Space Science*, **43**, 1523–1553.
- BASILEVSKY, A. T. & HEAD, J. W. 1998. The geologic history of Venus: a stratigraphic view. *Journal of Geo*physical Research, 103, 8531–8544.

- Basilevsky, A. T. & Head, J. W. 2000. Geologic units on Venus: evidence for their global correlation. *Planetary* and Space Science, **48**, 75–111.
- BASILEVSKY, A. T., PRONIN, A. A., RONCA, L. B., KRYUCHKOV, V. P., SUKHANOV, A. L. & MARKOV, M. S. 1986. Styles of tectonic deformation on Venus – Analysis of Venera-15 and Venera-16 data. *Journal of Geophysical Research*, 91, D399–D411.
- Basilevsky, A. T., Head, J. W., Schaber, G. G. & Strom, R. G. 1997. The resurfacing history of Venus. *In*: Bougher, S. W., Hunten, D. M. & Philleps, R. J. (eds) *Venus II: Geology, Geophysics, Atmosphere, and Solar Wind Environment*. University of Arizona Press, Tucson, AZ, 1047–1086.
- BASILEVSKY, A. T., AITTOLA, M., RAITALA, J. & HEAD, J. W. 2009. Venus astra/novae: estimates of the absolute time duration of their activity. *Icarus*, 203, 337–351.
- Basilevsky, A. T., Shalygin, E. V. *Et al.* 2012. Geologic interpretation of the near-infrared images of the surface taken by the Venus Monitoring Camera, Venus Express. *Icarus*, **217**, 434–450.
- BECKER, K. J., WELLER, L. A., EDMUNDSON, K. L., BECKER, T. L., ROBINSON, M. S., ENNS, A. C. & SOLOMON, S. C. 2012. Global controlled mosaic of Mercury from MESSENGER orbital images. Abstract 2654 presented at the 43rd Lunar & Planetary Science Conference, March 19–23, 2012, The Woodlands, Texas.
- BIBRING, J. P., LANGEVIN, Y. *ET AL.* 2005. Mars surface diversity as revealed by the OMEGA/Mars Express observations. *Science*, **307**, 1576–1581.
- BILOTTI, F. & SUPPE, J. 1999. The global distribution of wrinkle ridges on Venus. *Icarus*, **139**, 137–157.
- BINDER, A. B. 1982. Post-Imbrium global tectonism: evidence for an initially totally molten Moon. *Moon and Planets*, **26**, 117–133.
- BINDER, A. B. 1986. The initial thermal state of the Moon. *In*: HARTMANN, W. K., PHILLIPS, R. J. & TAYLOR, G. J. (eds) *Origin of the Moon*. Lunar and Planetary Institute, Houston, TX, 425–433.
- BINDER, A. B. & GUNGA, H. 1985. Young thrust-fault scarps in the highlands: evidence for an initially totally molten Moon. *Icarus*, **63**, 421–441.
- BINDSCHADLER, D. L. & HEAD, J. W. 1991. Tessera terrain, Venus: characterization and models for origin and evolution. *Journal of Geophysical Research*, 96, 5889–5907.
- BINDSCHADLER, D. L. & PARMENTIER, E. M. 1990. Mantle flow tectonics: the influence of a ductile lower crust and implications for the formation of topographic uplands on Venus. *Journal of Geophysical Research*, **95**, 21 329–21 344.
- BINDSCHADLER, D. L., SCHUBERT, G. & KAULA, W. M. 1992. Cold spots and hot spots: global tectonics and mantle dynamics of Venus. *Journal of Geophysical Research*, **97**, 13 495–13 532.
- BJONNES, E. E., HANSEN, V. L., JAMES, B. & SWENSON, J. B. 2012. Equilibrium resurfacing of Venus: results from new Monte Carlo modeling and implications for Venus surface histories. *Icarus*, 217, 451–461.
- BLAIR, D. M., FREED, A. M. ET AL. 2013. The origin of graben and ridges in Rachmaninoff, Raditladi, and Mozart basins, Mercury. Journal of Geophysical Research, 118, 47-58.

- BLASIUS, K. R., CUTTS, J. A., GUEST, J. E. & MASURSKY, H. 1977. Geology of the Valles Marineris: first analysis of imaging from the Viking 1 Orbiter primary mission. *Journal of Geophysical Research*, 82, 4067–4091.
- BLEACHER, J. E., GLAZE, L. S. *ET AL.* 2009. Spatial alignment analyses for a field of small volcanic vents south of Pavonis Mons and implications for the Tharsis province, Mars. *Journal of Volcanology and Geothermal Research*, **185**, 96–102.
- BLEWETT, D. T., HAWKE, B. R., LUCEY, P. G., TAYLOR, G. J., JAUMANN, R. & SPUDIS, P. D. 1995. Remote sensing and geologic studies of the Schiller-Schickard region of the Moon. *Journal of Geophysical Research*, 100, 16 959–16 978.
- Borg, L. E., Connelly, J. N., Boyet, M. & Carlson, R. W. 2011. Chronological evidence that the Moon is either young or did not have a global magma ocean. *Nature*, **477**, 70–72.
- Borgia, A. 1994. Dynamic basis of volcanic spreading. *Journal of Geophysical Research*, **99**, 17 791–17 804.
- Borgia, A., Delaney, P. T. & Denlinger, R. P. 2000. Spreading volcanoes. *Annual Review of Earth and Planetary Science*, **28**, 539–570.
- BRADEN, S. E., ROBINSON, M. S., TRAN, T., GENGL, H., LAWRENCE, S. J. & HAWKE, B. R. 2010. Morphology of Gruithuisen and Hortensius domes: Mare v. nonmare volcanism. Abstract 2677 presented at the 41st Lunar & Planetary Science Conference, March 1–5, 2010, The Woodlands, Texas.
- Bradley, B. A., Sakimoto, S. E. H., Frey, H. & Zimbelman, J. R. 2002. Medusae Fossae Formation: new perspectives from Mars Global Surveyor. *Journal of Geophysical Research*, **107**, 5058, http://dx.doi.org/10.1029/2001JE001537
- Brown, C. D. & Grimm, R. E. 1995. Tectonics of Artemis-Chasma – A Venusian plate boundary. *Icarus*, 117, 219–249
- BROŽ, P. & HAUBER, E. 2012. An unique volcanic field in Tharsis, Mars: pyroclastic cones as evidence for explosive eruptions. *Icarus*, 218, 88–99, http://dx.doi.org/ 10.1016/j.icarus.2011.11.030
- BROŽ, P. & HAUBER, E. 2013. Hydrovolcanic tuff rings and cones as indicators for phreatomagmatic explosive eruptions on Mars. *Journal of Geophysical Research*, 118, 1656–1675.
- BRUNO, B. C., LUCEY, P. G. & HAWKE, B. R. 1991. Highresolution UV-visible spectroscopy of lunar red spots. Proceedings of Lunar and Planetary Science, 21, 405–415.
- BUCZKOWSKI, D. L. & WYRICK, D. Y. 2014. Tectonism and magmatism identified on asteroids. *In*: PLATZ, T., MAS-SIRONI, M., BYRNE, P. K. & HIESINGER, H. (eds) *Volcanism and Tectonism Across the Inner Solar System*. Geological Society, London, Special Publications, 401. First published online July 28, 2014, http:// dx.doi.org/10.1144/SP401.18
- Burr, D. M., Soare, R. J., Wan Bun Tseung, J.-M. & Emery, J. P. 2005. Young (late Amazonian), near surface, ground ice features near the equator, Athabasca Valles, Mars. *Icarus*, **178**, 56–73.
- Bussey, D. B. J., Guest, J. E. & Sørensen, S.-A. 1997. On the role of thermal conductivity on thermal erosion by lava. *Journal of Geophysical Research*, **102**, 10 905–10 908.

- BYRNE, P. K., VAN WYK DE VRIES, B., MURRAY, J. B. & TROLL, V. R. 2009. The geometry of volcano flank terraces on Mars. Earth and Planetary Science Letters, 281, 1–13
- Byrne, P. K., van Wyk de Vries, B., Murray, J. B. & Troll, V. R. 2012. A volcanotectonic survey of Ascraeus Mons, Mars. *Journal of Geophysical Research*, **117**, E01004.
- Byrne, P. K., Holohan, E. P., Kervyn, M., van Wyk de Vries, B., Troll, V. R. & Murray, J. B. 2013a. A sagging-spreading continuum of large volcano structure. *Geology*, 41, 339–342.
- BYRNE, P. K., KLIMCZAK, C. ET AL. 2013b. The origin of Mercury's northern volcanic plains. *Geological Society of America, Abstracts with Programs*, **45**, 851.
- Byrne, P. K., Klimczak, C. *et al.* 2013c. An assemblage of lava flow features on Mercury. *Journal of Geophysical Research*, **118**, 1303–1322.
- BYRNE, P. K., KLIMCZAK, C. ET AL. 2013d. Tectonic complexity within volcanically infilled craters and basins on Mercury. Abstract 1261 presented at the 44th Lunar & Planetary Science Conference, March 18–22, 2013. The Woodlands, Texas.
- Byrne, P. K., Holohan, E. P., Kervyn, M., van Wyk de Vries, B. & Troll, V. R. 2014a. Analogue modelling of volcano flank terrace formation on Mars. In: Platz, T., Massironi, M., Byrne, P. K. & Hiesinger, H. (eds) Volcanism and Tectonism Across the Inner Solar System. Geological Society, London, Special Publications, 401. First published online May 8, 2014, http://dx.doi.org/10.1144/SP401.14
- BYRNE, P. K., KLIMCZAK, C., ŞENGÖR, A. M. C., SOLOMON, S. C., WATTERS, T. R. & HAUCK, S. A. 2014b. Mercury's global contraction greatly exceeds earlier measurements. *Nature Geoscience*, 7, 301–307.
- BYRNE, P. K., KLIMCZAK, C., SOLOMON, S. C., MAZARICO, E., NEUMANN, G. A. & ZUBER, M. T. 2014c. Deepseated contractional tectonics in Mare Crisium, the Moon. Abstract 2,396 presented at the 45th Lunar & Planetary Science Conference, March 17–21, 2014, The Woodlands, Texas.
- CAMPBELL, B. A. 1999. Surface formation rates and impact crater densities on Venus. *Journal of Geophysical Research*, **104**, 21 952–21 955.
- CAMPBELL, D. B., HEAD, J. W., HARMON, J. K. & HINE, A. A. 1984. Venus volcanism and rift formation in Beta Regio. *Science*, **226**, 167–170.
- CARLI, C., SERVENTI, G. & SGAVETTI, M. 2014. VNIR spectral characteristics of terrestrial igneous effusive rocks: mineralogical composition and the influence of texture. *In:* PLATZ, T., MASSIRONI, M., BYRNE, P. K. & HIESINGER, H. (eds) *Volcanism and Tectonism Across the Inner Solar System.* Geological Society, London, Special Publications, 401. First published online June 17, 2014, http://dx.doi.org/10. 1144/SP401.19
- CARR, M. H. 1966. Geologic Map of the Mare Serenitatis Region of the Moon. United States Geological Survey, Miscellaneous Geologic Investigations Series Map, I-489 (LAC-42).
- CARR, M. H., GREELEY, R., BLASIUS, K. R., GUEST, J. E. & MURRAY, J. B. 1977. Some martian volcanic features as viewed from the Viking Orbiters. *Journal of Geo*physical Research, 82, 3985–4015.

- Chabot, N. L., Hoppa, G. V. & Strom, R. G. 2000. Analysis of lunar lineaments: far side and polar mapping. *Icarus*, **147**, 301–308.
- CHARETTE, M. P., McCORD, T. B., PIETERS, C. & ADAMS, J. B. 1974. Application of remote spectral reflectance measurements to Lunar geology classification and determination of titanium content of lunar soils. *Journal of Geophysical Research*, 74, 1605–1613, http://dx.doi.org/10.1029/JB079i011p01605
- CHETTY, T. R. K., VENKATRAYUDU, M. & VENKATASI-VAPPA, V. 2010. Structural architecture and a new tectonic perspective of Ovda Regio, Venus. *Planetary* and Space Science, 58, 1286–1297.
- CHEVREL, S. D., PINET, P. C. & HEAD, J. W. 1999. Gruithuisen domes region: a candidate for an extended non-mare volcanism unit on the Moon. *Journal of Geophysical Research*, **104**, 16 515–16 529.
- CHRISTENSEN, P. R., BANDFIELD, J. L. ET AL. 2003. Morphology and composition of the surface of Mars: mars Odyssey THEMIS results. Science, 300, 2056–2061.
- Christiansen, E. H. 1989. Lahars in the Elysium region of Mars. *Geology*, 17, 203–206.
- CLARK, J. D., HURTADO, J. H., HIESINGER, H. & VAN DER BOGERT, C. H. 2014. Investigation of lobate scarps: Implications for the tectonic and thermal evolution of the Moon. Abstract 2048 presented at the 45th Lunar & Planetary Science Conference, March 17–21, 2014, The Woodlands, Texas.
- COHEN, B. A., SWINDLE, T. D. & KRING, D. A. 2000. Support for the Lunar Cataclysm Hypothesis from lunar meteorite impact melt ages. *Science*, **290**, 1754–1756, http://dx.doi.org/10.1126/science.290.5497.1754
- COMER, R. P., SOLOMON, S. C. & HEAD, J. W. 1985. Mars: thickness of the lithosphere from the tectonic response to volcanic loads. *Reviews of Geophysics*, 23, 61–92.
- COOMBS, C. R., HAWKE, B. R. & GADDIS, L. R. 1987. Explosive volcanism on the Moon. Abstract 197–198 presented at the 18th Lunar & Planetary Science Conference, Houston, Texas.
- COOMBS, C. R., HAWKE, B. R., PETERSON, C. A. & ZISK, S.
 H. 1990. Regional pyroclastic deposits in the north-central portion of the lunar nearside. Abstract 228–229 presented at the 21st Lunar & Planetary Science Conference, Houston, Texas.
- CRUMPLER, L. S. & AUBELE, J. 2000. Volcanismon Venus. In: SIGURDSON, H., HOUGHTON, B., RYMER, H., STIX, J. & McNutt, S. (eds) Encyclopedia of Volcanoes. Academic Press, New York, 727–770.
- CRUMPLER, L. S., HEAD, J. W. & AUBELE, J. C. 1996. Calderas on Mars: characteristics, structure, and associated flank deformation. *In*: McGuire, W. J., Jones, A. P. & Neuberg, J. (eds) *Volcano Instabilities on the Earth and Other Planets*. Geological Society, London, Special Publications, 110, 307–348.
- CRUMPLER, L. S., AUBELE, J. C. & ZIMBELMAN, J. R. 2007.
 Volcanic features of New Mexico analogous to volcanic features on Mars. *In:* CHAPMAN, M. G. (ed.) *The Geology of Mars.* Cambridge University Press, Cambridge, 95–125.
- DAVIS, P. A. & TANAKA, K. L. 1993. Small volcanoes in Tempe Terra, Mars: their detailed morphometry and inferred geologic significance. Abstract 379–380 presented at the Lunar & Planetary Science Conference, Houston, Texas.

DELANO, J. W. 1986. Pristine lunar glasses: criteria, data, and implications. *Journal of Geophysical Research*, 91, 201–213.

- DeLaughter, J. E. & Jurdy, D. M. 1999. Corona classification by evolutionary stage. *Icarus*, **139**, 81–92.
- DENEVI, B. W., ROBINSON, M. S. ET AL. 2009. The evolution of Mercury's crust: a global perspective from MESSENGER. Science, 324, 613–618.
- DENEVI, B. W., ERNST, C. M. ET AL. 2013. The distribution and origin of smooth plains on Mercury. *Journal of Geophysical Research*, 118, 891–907.
- DI ACHILLE, G., POPA, C., MASSIRONI, M., MAZZOTTA EPIFANI, E., ZUSI, M., CREMONESE, G. & PALUMBO, P. 2012. Mercury's radius change estimates revisited using MESSENGER data. *Icarus*, 221, 456–460.
- DOGLIONI, C., CARMINATI, E., CUFFARO, M. & SCROCCA, D. 2007. Subduction kinematics and dynamic constraints. *Earth Science Reviews*, 83, 125–175.
- DOGLIONI, C., CARMINATI, E., CRESPI, M., CUFFARO, M., PENATI, M. & RIGUZZI, F. 2014. Tectonically asymmetric Earth: from net rotation to polarized westward drift of the lithosphere. *Geoscience Frontiers*, first published online 18 February 2014, http://dx.doi.org/ 10.1016/j.gsf.2014.02.001
- DOHM, J. M. & TANAKA, K. L. 1999. Geology of the Thaumasia region, Mars: plataeu development, valley origin, and magmatic evolution. *Planetary and Space Science*, 47, 411–431.
- DOHM, J. M., WILLIAMS, J.-P. *ET AL*. 2009. New evidence for a magmatic influence on the origin of Valles Marineris, Mars. *Journal of Volcanology and Geothermal Research*, **185**, 12–27.
- DOMBARD, A. J. & GILLIS, J. J. 2001. Testing the viability of topographic relaxation as a mechanism for the formation of lunar floor-fractured craters. *Journal of Geophysical Research*, **106**, 27 901–27 910.
- DOMBARD, A. J. & HAUCK, S. A., II. 2008. Despinning plus global contraction and the orientation of lobate scarps on Mercury: predictions for MESSENGER. *Icarus*, **198**, 274–276.
- Dowty, E., Prinz, M. & Keil, K. 1974a. Ferroan anorthosite a widespread and distinctive lunar rock type. *Earth and Planetary Science Letters*, **24**, 15–25, http://dx.doi.org/10.1016/0012–821X (74)90003-X
- DOWTY, E., PRINZ, M. & KEIL, K. 1974b. 'Very High Alumina Basalt'. A mixture and not a magma type. *Science*, 183, 1214–1215, http://dx.doi.org/10. 1126/science.183.4130.1214
- DZURISIN, D. 1978. The tectonic and volcanic history of Mercury as inferred from studies of scarps, ridges, troughs, and other lineaments. *Journal of Geophysical Research*, 83, 4883–4906.
- EDGETT, K. & BLUMBERG, D. 1994. Star and linear dunes on Mars. *Icarus*, **112**, 448–464, http://dx.doi.org/10. 1006/icar.1994.1197
- EDGETT, K. & CHRISTENSEN, P. R. 1991. The particle size of Martian aeolian dunes. *Journal of Geophysical Research*, **96**, 22 762–22 776.
- EDGETT, K. & CHRISTENSEN, P. R. 1994. Mars aeolian sand: regional variations among dark-hued crater floor features. *Journal of Geophysical Research*, 99, 1997–2018.
- EDGETT, K. S. 1990. Possible cinder cones near the summit of Pavonis Mons, Mars. Abstract 311–312 presented

- at the 21st Lunar & Planetary Science Conference, Houston, Texas.
- EDGETT, K. S. & MALIN, M. C. 2002. Martian sedimentary rock stratigraphy: outcrops and interbedded craters of northwest Sinus Meridiani and southwest Arabia Terra. *Geophysical Research Letters*, **29**, 2179, http://dx.doi.org/10.1029/2002gl016515
- ELKINS-TANTON, L. T. & HAGER, B. H. 2005. Giant meteoroid impacts can cause volcanism. *Earth and Planetary Science Letters*, 239, 219–232.
- EL MAARRY, M. R., DOHM, J. M. *ET AL*. 2012. Searching for evidence of hydrothermal activity at Apollinaris Mons, Mars. *Icarus*, **217**, 297–314, http://dx.doi.org/10.1016/j.icarus.2011.10.022
- ERNST, R. E., HEAD, J. W., PARFITT, E., GROSFILS, E. & WILSON, L. 1995. Giant radiating dyke swarms on Earth and Venus. *Earth Science Reviews*, 39, 1–58.
- Ernst, R. E., Grosfils, E. B. & Mège, D. 2001. Giant dyke swarms: earth, Venus, and Mars. *Annual Review of Earth and Planetary Sciences*, **29**, 489–534.
- FAGENTS, S. A. & GREELEY, R. 2001. Factors influencing lava-substrate heat transfer and implications for thermomechanical erosion. *Bulletin of Volcanology*, 62, 519–532.
- FARRAND, W. H., GADDIS, L. R. & KESZTHELYI, L. 2005. Pitted cones and domes on Mars: observations in Acidalia Planitia and Cydonia Mensae using MOC, THEMIS, and TES data. *Journal of Geophysical Research*, 110, E05005, http://dx.doi.org/10.1029/ 2004/IE002297
- FASSETT, C. I., KADISH, S. J., HEAD, J. W., SOLOMON, S. C. & STROM, R. G. 2011. The global population of large craters on Mercury and comparison with the Moon. *Geophysical Research Letters*, 38, L10202, http://dx. doi.org/10.1029/2011GL047294
- FERNÀNDEZ, C., ANGUITA, F., RUIZ, J., ROMEO, I., MARTÍN-HERRERO, À., RODRÍGUE, A. & PIMENTEL, C. 2010. Structural evolution of Lavinia Planitia, Venus: implications for the tectonics of the lowland plains. *Icarus*, 206, 210–228.
- FERRARI, S., MASSIRONI, M., MARCHI, S., BYRNE, P. K., KLIMCZAK, C., MARTELLATO, E. & CREMONESE, G. 2014. Age relationships of the Rembrandt basin and Enterprise Rupes, Mercury. In: PLATZ, T., MASSIRONI, M., BYRNE, P. K. & HIESINGER, H. (eds) Volcanism and Tectonism Across the Inner Solar System. Geological Society, London, Special Publications, 401. First published online July 29, 2014, http://dx.doi.org/10. 1144/SP401.20
- FISCHER, K. M., FORD, H. A., ABT, D. L. & RYCHERT, C. A. 2010. The lithosphere – asthenosphere boundary. *Annual Reviews of Earth and Planetary Sciences*, 38, 551–575.
- FRANKEL, C. 2005. Worlds on Fire: Volcanoes on the Earth, the Moon, Mars, Venus and Io. Cambridge University Press, Cambridge.
- FREED, A. M., MELOSH, H. J. & SOLOMON, S. C. 2001. Tectonics of mascon loading: resolution of the strike-slip faulting paradox. *Journal of Geophysical Research*, 106, 20 603–20 620.
- Freed, A. M., Solomon, S. C., Watters, T. R., Phillips, R. J. & Zuber, M. T. 2009. Could Pantheon Fossae be the result of the Apollodorus crater-forming impact within the Caloris basin, Mercury? *Earth and Planetary Science Letters*, **285**, 320–327.

- FREED, A. M., BLAIR, D. M. ET AL. 2012. On the origin of graben and ridges within and near volcanically buried craters and basins in Mercury's northern plains. Journal of Geophysical Research, 117, E00L06, http://dx.doi.org/10.1029/2012JE004119
- FREY, H. 2008. Ages of very large impact basins on Mars: implications for the late heavy bombardment in the inner solar system. *Geophysical Research Letters*, 35, L13203.
- FREY, H. & JAROSEWICH, M. 1982. Subkilometer martian volcanoes—Properties and possible terrestrial analogs. *Journal of Geophysical Research*, 87, 9867–9879.
- FREY, H., EDGAR, L. & LILLIS, R. 2007. Very large visible and buried impact basins on Mars: implications for internal and crustal evolution and the late heavy bombardment in the inner solar system. Abstract 3070 presented at the 7th International Conference on Mars, July 9–13, 2007, California Institute of Technology (Caltech).
- GADDIS, L. R., PIETERS, C. M. & HAWKE, B. R. 1985. Remote sensing of lunar pyroclastic mantling deposits. *Icarus*, 61, 461–489.
- GADDIS, L., ROSANOVA, C., HARE, T., HAWKE, B. R., COOMBS, C. & ROBINSON, M. S. 1998. Small lunar pyroclastic deposits: a new global perspective. Abstract 1807–1808 presented at the 29th Lunar & Planetary Science Conference, March 16–20, 1998, The Woodlands. Texas.
- GALGANA, G. A., GROSFILS, E. B. & McGOVERN, P. J. 2013. Radial dike formation on Venus: insights from models of uplift, flexure and magmatism. *Icarus*, 225, 538–547.
- GALLUZZI, V., DI ACHILLE, G., FERRANTI, L., POPA, C. & PALUMBO, P. 2014. Faulted craters as indicators for thrust motions on Mercury. In: PLATZ, T., MASSIRONI, M., BYRNE, P. K. & HIESINGER, H. (eds) Volcanism and Tectonism Across the Inner Solar System. Geological Society, London, Special Publications, 401. First published online June 12, 2014, http://dx.doi.org/10.1144/SP401.17
- GARRY, W. B., ZIMBELMAN, J. R. & GREGG, T. K. P. 2007. Morphology and emplacement of a long channeled lava flow near Ascraeus Mons volcano, Mars. *Journal of Geophysical Research*, 112, E08007.
- GERYA, T. V. 2014. Plume-induced crustal convection: 3D thermomechanical model and implications for the origin of novae and coronae on Venus. Earth and Planetary Science Letters, 391, 183–192.
- GHAIL, R. C. & WILSON, L. 2013. A pyroclastic flow deposit on Venus. *In*: PLATZ, T., MASSIRONI, M., BYRNE, P. K. & HIESINGER, H. (eds) *Volcanism and Tectonism Across the Inner Solar System*. Geological Society, London, Special Publications, 401. First published online November 19, 2013, http://dx.doi.org/ 10.1144/SP401.1
- GHATAN, G. J. & HEAD, J. W., III. 2002. Candidate subglacial volcanoes in the south polar region of Mars: morphology, morphometry, and eruption conditions. *Journal of Geophysical Research*, **107**, 5048, http://dx.doi.org/10.1029/2001JE001519
- GHENT, R. & HANSEN, V. 1999. Structural and kinematic analysis of eastern Ovda Regio, Venus: implications for crustal plateau formation. *Icarus*, 139, 116–136.

- GIACOMINI, L., MASSIRONI, M., MARCHI, S., FASSETT, C. I., DI ACHILLE, G. & CREMONESE, G. 2014. Age dating of an extensive thrust system on Mercury: implications for the planet's thermal evolution. *In:* PLATZ, T., MASSIRONI, M., BYRNE, P. K. & HIESINGER, H. (eds) *Volcanism and Tectonism Across the Inner Solar System.* Geological Society, London, Special Publications, 401. First published online August 13, 2014, http://dx.doi.org/10.1144/SP401.21
- GIGUERE, T. A., TAYLOR, G. J., HAWKE, B. R. & LUCEY, P. G. 2000. The titanium contents of lunar mare basalts. *Meteoritics and Planetary Science*, **35**, 193–200, http://dx.doi.org/10.1111/j.1945-5100.2000.tb01985.x
- GIGUERE, T. A., HAWKE, B. R. ET AL. 2003. Remote sensing studies of the Lomonosov-Fleming region of the Moon. Journal of Geophysical Research, 108, 5118, http://dx.doi.org/10.1029/2003JE002069
- GILLIS-DAVIS, J. J., BLEWETT, D. T. ET AL. 2009. Pit-floor craters on Mercury: evidence of near-surface igneous activity. Earth and Planetary Science Letters, 285, 243–250.
- GILMORE, M. S. & HEAD, J. W. 2000. Sequential deformation of plains at the margin of Alpha Regio, Venus: implications for tessera formation. *Meteoritics and Planetary Science*, 35, 667–687.
- GILMORE, M. S., COLLINS, G. C., IVANOV, M. A., MARINAN-GELI, L. & HEAD, J. W. 1998. Style and sequence of extensional structures in tessera terrain, Venus. *Journal of Geophysical Research*, 103, 16 813–16 840.
- GLAZE, L. S., STOFAN, E. R., SMREKAR, S. E. & BALOGA, S. M. 2002. Insights into corona formation through statistical analyses. *Journal of Geophysical Research*, 107, 5135
- GLOTCH, T. D., HAGERTY, J. J. ET AL. 2011. The Mairan domes: silicic volcanic constructs on the Moon. Geophysical Research Letters, 38, L21204, http://dx.doi. org/10.1029/2011GL049548
- GOLOMBEK, M. 1999. Introduction to the special section: mars Pathfinder. *Journal of Geophysical Research*, **104**, 8521–8522, http://dx.doi.org/10.1029/1998JE 900032
- GOLOMBEK, M. P., PLESCIA, J. B. & FRANKLIN, B. J. 1991.Faulting and folding in the formation of planetary wrinkle ridges. *Proceedings of Lunar and Planetary Science*, 21, 679–693.
- GOLOMBEK, M. P., ANDERSON, F. S. & ZUBER, M. T. 2000. Martian wrinkle ridge topography: evidence for subsurface faults from MOLA. Abstract 1294 presented at the 31st Lunar & Planetary Science Conference, March 13–17, 2000, The Woodlands, Texas.
- GOLOMBEK, M. P., ANDERSON, F. S. & ZUBER, M. T. 2001. Martian wrinkle ridge topography: evidence for subsurface faults from MOLA. *Journal of Geophysical Research*, **106**, 23 811–23 822.
- GREELEY, R. 1971. Lava tubes and channels in the lunar Marius Hills. *The Moon*, **3**, 289–314.
- GREELEY, R. (ed.) 1974. Geologic Guide to the Island of Hawaii: A Field Guide for Comparative Planetary Geology. NASA CR-152416. NASA, Washington, DC.
- GREELEY, R. 1982. The Snake River Plains, Idaho: representative of a new category of volcanism. *Journal of Geophysical Research*, 87, 2705–2712.
- Greeley, R. & Guest, J. E. 1987. Geologic Map of the Eastern Equatorial Region of Mars, Scale

- 1:15,000,000. United States Geological Survey, Miscellaneous Geologic Investigations Series Map, I-1802-B
- GREELEY, R. & SCHNEID, B. D. 1991. Magma generation on Mars – amounts, rates, and comparisons with Earth, Moon, and Venus. Science, 254, 996–998.
- GREELEY, R. & SPUDIS, P. D. 1981. Volcanism on Mars. Reviews of Geophysics and Space Physics, 19, 13–41.
- GREELEY, R., KADEL, S. D. ET AL. 1993. Galileo imaging observations of lunar maria and related deposits. Journal of Geophysical Research, 98, 17 183–17 206.
- GRIMM, R. E. & PHILLIPS, R. J. 1991. Gravity anomalies, compensation mechanisms, and the geodynamics of western Ishtar Terra, Venus. *Journal of Geophysical Research*, 96, 8305–8324.
- Grinspoon, D. H. 1993. Implications of the high D/H ratio for the sources of water in Venus atmosphere. *Nature*, **363**, 428–431.
- GROSFILS, E. B. & HEAD, J. W. 1994. The global distribution of giant radiating dike swarms on Venus: implications for the global stress state. *Geophysical Research Letters*, **21**, 701–704.
- GROSFILS, E. B., AUBELE, J., CRUMPLER, L., GREGG, T. & SAKIMOTO, S. 1999. Volcanism on Venus and Earth's seafloor. In: GREGG, T. & ZIMBELMAN, J. (eds) Environmental Effects on Volcanic Eruptions: From Deep Ocean to Deep Space. Plenum, New York, 113–142.
- GROSFILS, E. B., McGOVERN, P. J., GREGG, P. M., GALGANA, G. A., HURWITZ, D. M., LONG, S. M. & CHESTLER, S. R. 2013. Elastic models of magma reservoir mechanics: a key tool for investigating planetary volcanism. *In:* PLATZ, T., MASSIRONI, M., BYRNE, P. K. & HIESINGER, H. (eds) *Volcanism and Tectonism Across the Inner Solar System*. Geological Society, London, Special Publications, 401. First published online December 11, 2013, http://dx.doi.org/10. 1144/SP401.2
- GUALLINI, L., PAUSELLI, C., BROZZETTI, F. & MARINAN-GELI, L. 2014. Physical modelling of large-scale deformational systems in the South Polar Layered Deposits (Promethei Lingula, Mars): new geological constraints and climatic implications. *In:* PLATZ, T., MASSIRONI, M., BYRNE, P. K. & HIESINGER, H. (eds) *Volcanism and Tectonism Across the Inner Solar System.* Geological Society, London, Special Publications, 401. First published online April 25, 2014, http://dx.doi.org/10.1144/SP401.13
- Guest, J. E. & Murray, J. B. 1976. Volcanic features of the nearside equatorial lunar maria. *Journal of the Geological Society, London*, **132**, 251–258.
- Guest, J. E. & Stofan, E. R. 1999. A new view of the stratigraphic history of Venus. *Icarus*, **139**, 56–66.
- GUNG, Y., PANNING, M. & ROMANOWICZ, B. 2003. Global anisotropy and the thickness of continents. *Nature*, **422**, 707–711.
- GUSTAFSON, J. O., BELL, J. F., GADDIS, L. R., HAWKE, B. R. & GIGUERE, T. A. 2012. Characterization of previously unidentified lunar pyroclastic deposits using Lunar Reconnaissance Orbiter Camera data. *Journal of Geophysical Research*, 117, E00H25, http://dx.doi.org/10.1029/2011JE003893
- HAGERTY, J. J., LAWRENCE, D. J., HAWKE, B. R., VANIMAN, D. T., ELPHIC, R. C. & FELDMAN, W. C. 2006. Refined thorium abundances for lunar red

- spots: implications for evolved, nonmare volcanism on the Moon. *Journal of Geophysical Research*, **111**, E06002, http://dx.doi.org/10.1029/2005JE002592
- HAMILTON, C. W., FAGENTS, S. A. & THORDARSON, T. 2011. Lava-ground ice interactions in Elysium Planitia, Mars: geomorphological and geospatial analysis of the Tartarus Colles cone groups. *Journal of Geophy*sical Research, 116, E03004.
- HAMILTON, V. & STOFAN, E. R. 1996. The geomorphology and evolution of Hecate Chasma, Venus. *Icarus*, 121, 171–104
- HANSEN, V. L. 2006. Geological constraints on crustal plateau surface histories, Venus: the lava pond and bolide impact hypotheses. *Journal of Geophysical Research*, 111, E11010.
- HANSEN, V. L. & LÓPEZ, I. 2010. Venus records a rich early history. *Geology*, **38**, 311–314.
- HANSEN, V. L. & OLIVE, A. 2010. Artemis, Venus: the largest tectonomagmatic feature in the solar system? *Geology*, 38, 467–470.
- HANSEN, V. L. & PHILLIPS, R. J. 1993. Tectonics and volcanism of eastern Aphrodite Terra, Venus No subduction, no spreading. *Science*, 260, 526–530.
- HANSEN, V. L. & WILLIS, J. J. 1996. Structural analysis of a sampling of tesserae: implications for Venus geodynamics. *Icarus*, 123, 296–312.
- HANSEN, V. L. & WILLIS, J. J. 1998. Ribbon terrain formation, southwestern Fortuna Tessera, Venus: implications for lithosphere evolution. *Icarus*, 132, 321–343.
- HANSEN, V. L. & YOUNG, D. A. 2007. Venus's evolution: A synthesis. In: CLOOS, M., CARLSON, W. D., GILBERT, M. C., LIOU, J. G. & SORENSEN, S. S. (eds) Convergent Margin Terranes and Associated Regions: A Tribute to W.G. Ernst. Geological Society of America Special Papers, 419, 255–273.
- HANSEN, V. L., BANKS, B. K. & GHENT, R. R. 1999. Tessera terrain and crustal plateaus, Venus. *Geology*, 27, 1071–1074.
- HANSEN, V. L., PHILLIPS, R. J., WILLIS, J. J. & GHENT, R. R. 2000. Structures in tessera terrain, Venus: issues and answers. *Journal of Geophysical Research*, **105**, 4135–4152.
- HARRIS, L. B. & BÉDARD, J. H. 2014a. Chapter 9: Crustal evolution and deformation in a non-plate tectonic Archaean Earth: comparisons with Venus. In: DILEK, Y. & FURNES, H. (eds) Evolution of Archean Crust and Early Life. Modern Approaches in Solid Earth Sciences, 7. Springer, Berlin, 215–288.
- HARRIS, L. B. & BÉDARD, J. H. 2014b. Interactions between continent-like 'drift', rifting and mantle flow on Venus: gravity interpretations and Earth analogues. In: Platz, T., Massironi, M., Byrne, P. K. & Hiesinger, H. (eds) Volcanism and Tectonism Across the Inner Solar System. Geological Society, London, Special Publications, 401. First published online May 19, 2014, http://dx.doi.org/10.1144/SP401.9
- HARTMANN, W. K. & WOOD, C. A. 1971. Moon: origin and evolution of multi-ring basins. *The Moon*, **3**, 3–78.
- HASHIMOTO, G. L., ROOS-SEROTE, M., SUGITA, S., GILMORE, M. S., KAMP, L. W., CARLSON, R. W. & BAINES, K. H. 2008. Felsic highland crust on Venus suggested by Galileo near infrared mapping spectrometer data. *Journal of Geophysical Research*, 113, E00B24, http://dx.doi.org/10.1029/2008JE003134

- HAUBER, E., BLEACHER, J., GWINNER, K., WILLIAMS, D. & GREELEY, R. 2009. The topography and morphology of low shields and associated landforms of plains volcanism in the Tharsis region of Mars. *Journal of Volcanol*ogy and Geothermal Research, 185, 69–95.
- HAUBER, E., BROŽ, P., JAGERT, F., JODŁOWSKI, P. & PLATZ, T. 2011. Very recent and wide-spread basaltic volcanism on Mars. Geophysical Research Letters, 38, L10201.
- HAWKE, B. R. & BELL, J. F. 1981. Remote sensing studies of lunar dark-halo craters. Bulletin of the American Astronomical Society, 13, 712.
- HAWKE, B. R. & SPUDIS, P. D. 1980. Geochemical anomalies on the eastern limb and farside of the moon. *Proceedings of the Conference on the Lunar Highlands Crust*, 14–16 November 1979, Houston, Texas. Pergamon Press, Oxford, 467–481.
- HAWKE, B. R., MACLASKEY, D., MCCORD, T. B., ADAMS, J. B., HEAD, J. W., PIETERS, C. M. & ZISK, S. 1979. Multispectral mapping of lunar pyroclastic deposits. *Bulle*tin of the American Astronomical Society, 12, 582.
- HAWKE, B. R., SPUDIS, P. D. & CLARK, P. E. 1985. The origin of selected lunar geochemical anomalies: implications for early volcanism and the formation of light plains. *Earth, Moon, and Planets*, **32**, 257–273.
- HAWKE, B. R., COOMBS, C. R., GADDIS, L. R., LUCEY, P. G. & OWENSBY, P. D. 1989. Remote sensing and geologic studies of localized dark mantle deposits on the Moon. *Proceedings of Lunar and Planetary Science*, 19, 255–268.
- HAWKE, B. R., LAWRENCE, D. J., BLEWETT, D. T., LUCEY, P. G., SMITH, G. A., SPUDIS, P. D. & TAYLOR, G. J. 2003. Hansteen Alpha: a volcanic construct in the lunar highlands. *Journal of Geophysical Research*, 108, 5069, http://dx.doi.org/10.1029/2002JE002013
- HAWKE, B. R., GILLIS, J. J. ET AL. 2005. Remote sensing and geologic studies of the Balmer-Kapteyn region of the Moon. *Journal of Geophysical Research*, 110, E06004, http://dx.doi.org/10.1029/2004JE002383
- Hawke, B. R., Giguerre, T. A. *et al.* 2011. Hansteen Apha: a silicic volcanic construct on the Moon. Abstract 1652 presented at the 42nd Lunar & Planetary Science Conference, March 7–11, 2011, The Woodlands, Texas.
- HEAD, J. W. 1976. Lunar volcanism in space and time. Reviews of Geophysics and Space Physics, 14, 265–300.
- HEAD, J. W. & CRUMPLER, L. S. 1987. Evidence for divergent plate boundary characteristics and crustal spreading on Venus. *Science*, 238, 1380–1385.
- HEAD, J. W. & GIFFORD, A. 1980. Lunar mare domes: classification and modes of origin. Earth, Moon, and Planets, 22, 235–258.
- HEAD, J. W. & WILSON, L. 1979. Alphonsus-type darkhalo craters: morphology, morphometry and eruption conditions. *Proceedings of Lunar and Planetary Science*, 10, 2861–2897.
- HEAD, J. W. & WILSON, L. 1980. The formation of eroded depressions around the sources of lunar sinuous rilles: observations. *Proceedings of Lunar and Planetary Science*, 11, 426–428.
- HEAD, J. W. & WILSON, L. 1986. Volcanic processes and landforms on Venus: theory, predictions, and observations. *Journal of Geophysical Research*, 91, 9407–9446.

- HEAD, J. W. & WILSON, L. 1992. Lunar mare volcanism. Stratigraphy, eruption conditions, and the evolution of secondary crusts. *Geochimica et Cosmochimica* Acta, 56, 2155–2175.
- HEAD, J. W., HESS, P. C. & McCORD, T. B. 1978. Geologic characteristics of lunar highland volcanic (Gruithuisen and Marina region) and possible eruption conditions. *Proceedings of Lunar and Planetary Science*, 9, 488–490.
- HEAD, J. W., CRUMPLER, L. S., AUBELE, J. C., GUEST, J. E. & SAUNDERS, R. S. 1992. Venus volcanism – classification of volcanic features and structures, associations, and global distribution from Magellan data. *Journal of Geophysical Research*, 97, 13 153–13 197.
- HEAD, J. W., MURCHIE, S. *ET AL.* 1993. Lunar impact basins: new data for the western limb and far side (Orientale and South Pole-Aitken basins) from the first Galileo flyby. *Journal of Geophysical Research*, **98**, 17 149–17 182.
- HEAD, J. W., WILSON, L., ROBINSON, M., HIESINGER, H., WEITZ, C. & YINGST, A. 2000. Moon and Mercury: volcanism in Early Planetary History. In: ZIMBELMAN, J. R. & GREGG, T. K. P. (eds) Environmental Effects on Volcanic Eruptions: From Deep Oceans to deep Space. Kluwer Academic, New York.
- HEAD, J. W., WILSON, L. & WEITZ, C. M. 2002. Dark ring in southwestern Orientale basin: origin as a single pyroclastic eruption. *Journal of Geophysical Research*, 107, 1-1-1-17, http://dx.doi.org/10.1029/ 2000JE001438
- Head, J. W., Murchie, S. L. *et al.* 2008. Volcanism on Mercury: evidence from the first MESSENGER flyby. *Science*, **321**, 69–72.
- HEAD, J. W., MURCHIE, S. L. ET AL. 2009. Volcanism on Mercury: evidence from the first MESSENGER flyby for extrusive and explosive activity and the volcanic origin of plains. Earth and Planetary Science Letters, 285, 227–242.
- HEAD, J. W., CHAPMAN, C. R. ET AL. 2011. Flood volcanism in the northern high latitudes of Mercury revealed by MESSENGER. Science, 333, 1853–1856.
- HEATHER, D. J., DUNKIN, S. K. & WILSON, L. 2003. Volcanism on the Marius Hills plateau: observational analyses using Clementine multispectral data. *Journal of Geophysical Research*, 108, 5017, http://dx.doi.org/10.1029/2002JE001938
- Heiken, G., McKay, D. S. & Brown, R. W. 1974. Lunar deposits of possible pyroclastic origin. *Geochimica et Cosmochimica Acta*, **38**, 1703–1718.
- HELBERT, J., MULLER, N., KOSTAMA, P., MARINANGELI, L., PICCIONI, G. & DROSSART, P. 2008. Surface brightness variations seen by VIRTIS on Venus Express and implications for the evolution of the Lada Terra region, Venus. Geophysical Research Letters, 35, 1–5.
- HERRICK, R. R. & PHILLIPS, R. J. 1992. Geological correlations with the interior density structure of Venus. Journal of Geophysical Research, 97, 16 017–16 034.
- HIESINGER, H. & HEAD, J. W., III. 2004. The Syrtis Major volcanic province, Mars: synthesis from Mars Global Surveyor data. *Journal of Geophysical Research*, 109, E01004.
- HIESINGER, H. & HEAD, J. W., III . 2006. New views of lunar geoscience: an introduction and overview. *Reviews in Mineralogy and Geochemistry*, 60, 1–81.

- HIESINGER, H. & JAUMANN, R. 2014. Chapter 23: The Moon. In: SPOHN, T., BREUER, D. & JOHNSON, T. (eds) Encyclopedia of the Solar System, 3rd edn. Elsevier, Amsterdam, 493–538.
- HIESINGER, H., JAUMANN, R., NEUKUM, G. & HEAD, J. W. 2000. Ages of mare basalts on the lunar nearside. *Journal of Geophysical Research*, 105, 29 239– 29 276, http://dx.doi.org/10.1029/2000JE001244
- HIESINGER, H., HEAD, J. W., III, WOLF, U. & NEUKUM, G. 2001. New age determinations of lunar mare basalts in Mare Cognitum, Mare Nubium, Oceanus Procellarum, and other nearside mare. Abstract 1815 presented at the 32nd Lunar & Planetary Science Conference, Houston, Texas
- HIESINGER, H., HEAD, J. W., WOLF, U., JAUMANN, R. & NEUKUM, G. 2003. Ages and stratigraphy of mare basalts in Oceanus Procellarum, Mare Nubium, Mare Cognitum, and Mare Insularum. *Journal of Geophysical Research*, **108**, 5065, http://dx.doi.org/10.1029/2002JE001985
- HIESINGER, H., HEAD, J. W., WOLF, U., JAUMANN, R. & NEUKUM, G. 2011. Ages and stratigraphy of lunar mare basalts: A synthesis. *In*: AMBROSE, W. A. & WILLIAMS, D. A. (eds) *Recent Advances and Current Research Issues in Lunar Stratigraphy*. Geological Society of America Special Papers, 477, 1–51.
- HIESINGER, H., VAN DER BOGERT, C. H. *ET Al.* 2012. How old are young lunar craters? *Journal of Geophysical Research*, **117**, E00H10, http://dx.doi.org/10.1029/2011JE003935
- HODGES, C. A. 1973. *Mare Ridges and Lava Lakes*. Apollo 17 Preliminary Science Report, NASA SP-330.
- HODGES, C. A. & MOORE, H. J. 1994. Atlas of Volcanic Features on Mars. United States Geological Survey, Professional Papers, 1534.
- HÖRZ, F., GRIEVE, R., HEIKEN, G., SPUDIS, P. & BINDER, A. 1991. Lunar surface processes. *In*: HEIKEN, G., VANIMAN, D. & FRENCH, B. (eds) *Lunar Source-book – A User Guide to the Moon*. Cambridge University Press, Cambridge, 61–120.
- HUANG, J., YANG, A. & ZHONG, S. 2013. Constraints of the topography, gravity and volcanism on Venusian mantle dynamics and generation of plate tectonics. *Earth and Planetary Science Letters*, 362, 207–214.
- HULME, G. 1973. Turbulent lava flows and the formation of lunar sinuous rilles. *Modern Geology*, **4**, 107–117.
- HURWITZ, D. M., HEAD, J. W., WILSON, L. & HIESINGER, H. 2012. Origin of lunar sinuous rilles: modeling effects of gravity, surface slope, and lava composition on erosion rates during the formation of Rima Prinz. *Journal of Geophysical Research*, 117, E00H14, http://dx.doi.org/10.1029/2011JE004000
- HURWITZ, D. M., HEAD, J. W. & HIESINGER, H. 2013a. Lunar sinuous rilles: distribution, characteristics, and implications for their origin. *Planetary and Space Science*, 79, 1–38, http://dx.doi.org/10.1016/j.pss. 2012.10.019
- HURWITZ, D. M., HEAD, J. W. ET AL. 2013b. Investigating the origin of candidate lava channels on Mercury with MESSENGER data: theory and observations. *Journal* of Geophysical Research, 118, 471–486, http://dx. doi.org/10.1029/2012JE004103
- HYNEK, B. M., PHILLIPS, R. J. & ARVIDSON, R. E. 2003. Explosive volcanism in the Tharsis region: global

- evidence in the Martian geologic record. *Journal of Geophysical Research*, **108**, 5111, http://dx.doi.org/10.1029/2003JE002062
- ISACKS, B., OLIVER, J. & SYKES, L. R. 1968. Seismology and the new global tectonics. *Journal of Geophysical Research*, 73, 5855–5899.
- IVANOV, B. A. & MELOSH, H. J. 2003. Impacts do not initiate volcanic eruptions: eruptions close to the crater. *Geology*, 31, 869–872.
- IVANOV, M. A. & HEAD, J. W. 1996. Tessera terrain on Venus: a survey of the global distribution, characteristics and relation to surrounding units from Magellan data. *Journal of Geophysical Research*, 101, 14 861–14 908.
- IVANOV, M. A. & HEAD, J. W., III. 2001. Geologic map of the Lavinia Planitia Quadrangle (V-55), Venus. United States Geological Survey, Miscellaneous Geologic Investigations Series, I-2684.
- IVANOV, M. A. & HEAD, J. W. 2008. Formation and evolution of Lakshmi Planum, Venus: assessment of models using observations from geological mapping. Planetary and Space Science, 56, 1949–1966.
- IVANOV, M. A. & HEAD, J. W. 2011. Global geological map of Venus. *Planetary Space Science*, 59, 1559–1600.
- IVANOV, M. A. & HEAD, J. W. 2013. The history of volcanism on Venus. *Planetary Space Science*, **84**, 66–92.
- JAUMANN, R., HIESINGER, H. ET AL. 2012. Geology, geochemistry, and geophysics of the Moon: status of current understanding. *Planetary and Space Science*, 74, 15–41, http://dx.doi.org/10.1016/j.pss.2012.08.019
- JOHNSON, C. L. & SANDWELL, D. T. 1992. Joints in Venusian lava flows. *Journal of Geophysical Research*, 97, 13 601–13 610.
- JOHNSON, J. R., LARSON, S. M. & SINGER, R. B. 1991.
 A reevaluation of spectral ratios for lunar mare TiO₂ mapping. *Geophysical Research Letters*, 18, 2153–2156, http://dx.doi.org/10.1029/91GL02094
- JOLLIFF, B. L., GILLIS, J. J., HASKIN, L. A., KOROTEV, R. L. & WIECZOREK, M. W. 2000. Major lunar crustal terranes: surface expressions and crust-mantle origins. *Journal of Geophysical Research*, 105, 4197–4216.
- JOLLIFF, B. L., WISEMAN, S. A. ET AL. 2011. Non-mare silicic volcanism on the lunar farside at Compton-Belkovich. Nature Geoscience, 4, 566–571, http:// dx.doi.org/10.1038/NGEO1212
- JOZWIAK, L. M., HEAD, J. W., ZUBER, M. T., SMITH, D. E. & NEUMANN, G. A. 2012. Lunar floor-fractured craters: classification, distribution, origin and implications for magmatism and shallow crustal structure. *Journal of Geophysical Research*, 117, E11005.
- JOZWIAK, L. M., HEAD, J. W. ET AL. 2014. Lunar floor-fractured craters: intrusion emplacement and associated gravity anomalies. Abstract 1464 presented at the 45th Lunar & Planetary Science Conference, March 17–21, 2014, The Woodlands, Texas.
- JULL, M. G. & ARKANI-HAMED, J. 1995. The implications of basalt in the formation and evolution of mountains on Venus. *Physics of Earth and Planetary Interiors*, 89, 163–175.
- KADDISH, S. J., FASSETT, C. I., HEAD, J. W., SMITH, D. E., ZUBER, M. T., NEUMANN, G. A. & MAZARICO, E. 2011. A global catalog of large lunar craters (≥20 km) from the Lunar Orbiter Laser Altimeter. Abstract 1006 presented at the 42nd Lunar & Planetary Science Conference, March 7–11, 2011, The Woodlands, Texas.

- KARGEL, J. S., KIRK, R. L., FEGLEY, B., JR. & TREIMAN, A. H. 1994. Carbonate-sulfate volcanism on Venus? *Icarus*, 112, 219–252.
- KAULA, W. M. 1990. Venus: a contrast in evolution to Earth. Science, 247, 1191–1196.
- KEDDIE, S. & HEAD, J. 1994. Sapas Mons, Venus: evolution of a large shield volcano. *Earth, Moon, and Planets*, 65, 129–190.
- KERBER, L., HEAD, J. W., SOLOMON, S. C., MURCHIE, S. L., BLEWETT, D. T. & WILSON, L. 2009. Explosive volcanic eruptions on Mercury: eruption conditions, magma volatile content, and implications for interior volatile abundances. *Earth and Planetary Science Letters*, 285, 263–271.
- KERBER, L., HEAD, J. W., MADELEINE, J.-B., FORGET, F. & WILSON, L. 2011a. The dispersal of pyroclasts from Apollinaris Patera, Mars: implications for the origin of the Medusae Fossae Formation. *Icarus*, 216, 212– 220. http://dx.doi.org/10.1016/j.icarus.2011.07.035
- KERBER, L., HEAD, J. W. ET AL. 2011b. The global distribution of pyroclastic deposits on Mercury: the view from MESSENGER flybys 1–3. Planetary and Space Science, 59, 1895–1909.
- KESZTHELYI, L., THORDARSON, T., McEWEN, A., HAACK, H., GUILBAUD, M. N., SELF, S. & ROSSI, M. J. 2004. Icelandic analogs to Martian flood lavas. Geochemistry Geophysics Geosystems, 5, Q11014.
- KESZTHELYI, L., JAEGER, W., MCEWEN, A., TORNABENE, L., BEYER, R. A., DUNDAS, C. & MILAZZO, M. 2008. High Resolution Imaging Science Experiment (HiRISE) images of volcanic terrains from the first 6 months of the Mars Reconnaissance Orbiter Primary Science Phase. *Journal of Geophysical Research*, 113, E04005, http://dx.doi.org/10.1029/2007JE002968
- Keszthelyi, L. P., Jaeger, W. L., Dundas, C. M., Martínez-Alonso, S., McEwen, A. S. & Milazzo, M. P. 2010. Hydrovolcanic features on Mars: preliminary observations from the first Mars year of HiRISE imaging. *Icarus*, **205**, 211–229.
- KIDDER, J. G. & PHILLIPS, R. J. 1996. Convection-driven subsolidus crustal thickening on Venus. *Journal of Geophysical Research*, **101**, 23 181–23 194.
- KIEFER, W. S. & HAGER, B. H. 1991. A mantle plume model for the equatorial highlands of Venus. *Journal* of Geophysical Research, 96, 20 947–20 966.
- KIEFER, W. S. & MURRAY, B. C. 1987. The formation of Mercury's smooth plains. *Icarus*, 72, 477–491.
- KLIMCZAK, C. 2013. Igneous dikes on the Moon: evidence from Lunar Orbiter Laser Altimeter topography. Abstract 1391 presented at the 44th Lunar & Planetary Science Conference, March 18–22, 2013, The Woodlands, Texas.
- KLIMCZAK, C., WATTERS, T. R. ET AL. 2012. Deformation associated with ghost craters and basins in volcanic smooth plains on Mercury: strain analysis and implications for plains evolution. *Journal of Geophysical Research*, 117, E00L03, http://dx.doi.org/10.1029/ 2012JE004L03
- KLIMCZAK, C., ERNST, C. M. ET AL. 2013. Insights into the subsurface structure of the Caloris basin, Mercury, from assessments of mechanical layering and changes in long-wavelength topography. *Journal of Geophysical Research*, 118, 2030–2044, http://dx. doi.org/10.1002/jgre.20157

- KNAPMEYER, M., OBERST, J., HAUBER, E., WÄHLISCH, M., DEUCHLER, C. & WAGNER, R. 2006. Working models for spatial distribution and level of Mars' seismicity. *Journal of Geophysical Research*, 111, E11006.
- KOENIG, E. & AYDIN, A. 1998. Evidence for large-scale strike-slip faulting on Venus. Geology, 26, 551–554.
- KOHLSTEDT, D. L. & MACKWELL, S. J. 2010. Strength and deformation of planetary lithospheres. *In:* WATTERS, T. R. & SCHULTZ, R. A. (eds) *Planetary Tectonics*. Cambridge University Press, Cambridge, 397–456.
- KOMATSU, G., GULICK, V. C. & BAKER, V. R. 2001. Valley networks on Venus. *Geomorphology*, **37**, 225–240.
- KOROTEV, R. L. 1996. On the relationship between the Apollo 16 ancient regolith breccias and feldspathic fragmental breccias, and the composition of the prebasin crust in the central highlands of the Moon. *Meteoritics & Planetary Science*, **31**, 403–412.
- KOROTEV, R. L. 1997. Some things we can infer about the Moon from the composition of the Apollo 16 regolith. *Meteoritics & Planetary Science*, **32**, 447–478.
- KOROTEV, R. L. 2000. A retrospective look at KREEP. *Meteoritics & Planetary Science*, **35**, A91.
- KOROTEV, R. L., JOLIFF, B. L., ZEIGLER, R. A., GILLIS, J. J. & HASKIN, L. A. 2003. Feldspathic lunar meteorites and their implications for compositional remote sensing of the lunar surface and the composition of the lunar crust. *Geochimica et Cosmochimica Acta*, 67, 4895– 4923, http://dx.doi.org/10.1016/j.gca.2003. 08.001
- KRASSILNIKOV, A. S. & HEAD, J. W. 2003. Novae on Venus: geology, classification, and evolution. *Journal* of Geophysical Research, 108, 5108, http://dx.doi. org/10.1029/2002JE001983
- KRONBERG, P., HAUBER, E. ET AL. 2007. Acheron Fossae, Mars: tetonic rifting, volcanism, and implications for lithospheric thickness. Journal of Geophysical Research, 112, E04005.
- KUCINSKAS, A. B., TURCOTTE, D. L. & ARKANI-HAMED, J. 1996. Isostatic compensation of Ishtar Terra, Venus. Journal of Geophysical Research, 101, 4725–4736.
- KUMAR, P. S. 2005. An alternative kinematic interpretation of Thetis Boundary Shear Zone, Venus: evidence for strike-slip ductile duplexes. *Journal of Geophysical Research*, **110**, E07001, http://dx.doi.org/10.1029/ 2004JE002387
- LANG, N. P. & HANSEN, V. L., 2006. Venusian channel formation as a subsurface process. *Journal of Geophysical Research*, 111, E04001, http://dx.doi.org/10.1029/2005JF002629
- LANG, N. P. & LÓPEZ, I. 2013. The magmatic evolution of three Venusian coronae. *In*: PLATZ, T., MASSIRONI, M., BYRNE, P. K. & HIESINGER, H. (eds) *Volcanism and Tectonism Across the Inner Solar System*. Geological Society, London, Special Publications, 401. First published online December 16, 2013, http://dx.doi.org/ 10.1144/SP401.3
- LANGSETH, M. G., KEIHM, S. J. & PETERS, K. 1976. Revised lunar heat-flow values. *Proceedings of Lunar and Planetary Science*, 3, 3143–3171.
- Lanz, J. K., Wagner, R., Wolf, U., Kröchert, J. & Neukum, G. 2010. Rift zone volcanism and associated cinder cone field in Utopia Planitia, Mars. *Journal of Geophysical Research*, **115**, E12019, http://dx.doi.org/10.1029/2010JE003578

- LARSEN, K. W., ARVIDSON, R. E., JOLLIFF, B. L. & CLARK, B. C. 2000. Correspondence and least squares analyses of soil and rock compositions for the Viking Lander 1 and pathfinder landing sites. *Journal of Geophysical Research*, **105**, 29 207–29 221.
- LAWRENCE, D. J., ELPHIC, R. C., FELDMAN, W. C., PRETTYMAN, T. H., GASNAULT, O. & MAURICE, S. 2003. Small-area thorium features on the lunar surface. *Journal of Geophysical Research*, **108**, 5102, http://dx.doi.org/10.1029/2003JE002050
- LAWRENCE, D. J., HAWKE, B. R., HAGERTY, J. J., ELPHIC, R. C., FELDMAN, W. C., PRETTYMAN, T. H. & VANIMAN, D. T. 2005. Evidence for a high-Th, evolved lithology on the Moon at Hansteen Alpha. *Geophysical Research Letters*, **32**, L07201, http://dx.doi.org/10.1029/2004GL022022
- LAWRENCE, S. J., STOPAR, J. D. *ET Al.* 2010. LROC observations of the Marius Hills. Abstract 1906 presented at the 41st Lunar & Planetary Science Conference, March 1–5, 2010, The Woodlands, Texas.
- LEHMANN, T. R., PLATZ, T. & MICHAEL, G. G. 2012. Ages of lava flows in the Hesperia volcanic province, Mars. Abstract 2526 presented at the 43rd Lunar & Planetary Science Conference, March 19–23, 2012, The Woodlands, Texas.
- LENARDIC, W., KAULA, W. M. & BINDSCHADLER, D. L. 1995. Some effects of a dry crustal flow law on numerical simulations of coupled crustal deformation and mantle convection on Venus. *Journal of Geophysical Research.* 100, 16 949–16 957.
- LEONE, G. 2014. A network of lava tubes as the origin of Labyrinthus Noctic and Valles Marineris on Mars. *Journal of Volcanology and Geothermal Research*, **277**, 1–8.
- Lewis, J. S. 2004. *Physics and Chemistry of the Solar System*. 2nd edn. Elsevier, Amsterdam.
- Lingenfelter, R. E., Peale, S. J. & Schubert, G. 1968. Lunar rivers. *Science*, **161**, 266–269.
- Longhi, J. 1980. Lunar crust, Achondrites. *Geotimes*, **25**, 19–20.
- Longhi, J. 2003. A new view of lunar ferroan anorthosites: postmagma ocean petrogenesis. *Journal of Geophysical Research*, **108**, 5083, http://dx.doi.org/10.1029/2002JE001941
- LONGHI, J. & ASHWAL, L. D. 1985. Two-stage models for lunar and terrestrial anorthosites: petrogenesis without a magma ocean. *Journal of Geophysical Research*, 90, C571–C584.
- Lopes, F. C., Caselli, A. T., Machado, A. & Barata, M. T. 2014. The development of the Deception Island volcano caldera under control of the Bransfield Basin sinistral strike-slip tectonic regime (NW Antarctica). *In*: Platz, T., Massironi, M., Byrne, P. K. & Hiesinger, H. (eds) *Volcanism and Tectonism Across the Inner Solar System*. Geological Society, London, Special Publications, 401. First published online February 6, 2014, http://dx.doi.org/10.1144/SP401.6
- LOPES, R., GUEST, J. E., HILLER, K. & NEUKUM, G. 1982. Further evidence for a mass movement origin of the Olympus Mons aureole. *Journal of Geophysical Research*, 87, 9917–9928.
- Lucchitta, B. K. 1976. Analysis of scarps on the rim of mare Serenitatis. Abstract 507–508 presented at the 7th Lunar & Planetary Science Conference, Houston, TX.

- Lucchitta, B. K., McEwen, A. S., Clow, G. D., Geissler, P. E., Singer, R. B., Schultz, R. A. & Squyres, S. W. 1992. The canyon system on Mars. *In*: Kieffer, H. H., Jakosky, B. M., Snyder, C. W. & Matthews, M. S. (eds) *Mars*. University of Arizona Press, Tucson, AZ, 453–492.
- LUCCHITTA, B. K., ISBELL, N. K. & HOWINGTON-KRAUS, A. 1994. Topography of Valles Marineris: implications for erosional and structural history. *Journal of Geophysical Research*, 99, 3783–3798.
- LUCEY, P., KOROTEV, R. L. *ET AL.* 2006. Understanding the lunar surface and space—Moon interactions. *Reviews in Mineralogy & Geochemistry*, **60**, 83–219.
- LUCEY, P. G., BLEWETT, D. T. & JOLLIFF, B. L. 2000. Lunar iron and titanium abundance algorithms based on final processing of Clementine ultravioletvisible images. *Journal of Geophysical Research*, 105, 20 297–20 306, http://dx.doi.org/10.1029/19 99JE0011117
- MAGEE, K. P. & HEAD, J. W. 2001. Large flow fields on Venus: implications for plumes, rift associations, and resurfacing. In: Ernst, R. E. & Buchan, K. L. (eds) Mantle Plumes: Their Identification Through Time. Geological Society of America Special Papers, 352, 81–101.
- MALIN, M. 1974. Lunar red spots: possible pre-mare materials. Earth and Planetary Science Letters, 21, 331–341.
- MALIN, M. C. & EDGETT, K. S. 2000. Sedimentary rocks of early Mars. Science, 290, 1927–1937.
- MANCINELLI, P., MINELLI, F., MONDINI, A., PAUSELLI, C. & FEDERICO, C. 2014. A downscaling approach for geological characterization of the Raditladi basin of Mercury. *In:* PLATZ, T., MASSIRONI, M., BYRNE, P. K. & HIESINGER, H. (eds) *Volcanism and Tectonism Across the Inner Solar System*. Geological Society, London, Special Publications, 401. First published online March 11, 2014, http://dx.doi.org/10.1144/SP401.10
- Mandt, K. E., de Silva, S. L., Zimbelman, J. R. & Crown, D. A. 2008. Origin of the Medusae Fossae Formation, Mars: insights from a synoptic approach. *Journal of Geophysical Research*, **113**, E12011.
- MANFREDI, L., PLATZ, T., CLARKE, A. B. & WILLIAMS, D. A. 2012. Volcanic history of the Tempe Volcanic Province. Paper presented at the American Geophysical Union, Fall Meeting 2012, Abstract V33B-2873.
- MANGOLD, N., ALLEMAND, P. & THOMAS, P. G. 1998. Wrinkle ridges of Mars: structural analysis and evidence for shallow deformation controlled by ice-rich décollements. *Planetary and Space Science*, 46, 345–356.
- MARCHI, S., MASSIRONI, M., CREMONESE, G., MARTEL-LATO, E., GIACOMINI, L. & PROCKTER, L. M. 2011. The effects of the target material properties and layering on the crater chronology: the case of Raditladi and Rachmaninoff basins on Mercury. *Planetary and Space Science*, 59, 1968–1980.
- MARCHI, S., CHAPMAN, C. R., FASSETT, C. I., HEAD, J. W., BOTTKE, W. F. & STROM, R. G. 2013. Global resurfacing of Mercury 4.0–4.1 billion years ago by heavy bombardment and volcanism. *Nature*, 499, 59–61.
- MARINANGELI, L. & GILMORE, M. S. 2000. Geologic evolution of the Akna Montes-Atropos Tessera

- region, Venus. *Journal of Geophysical Research*, **105**, 12 053–12 075.
- MARINOVA, M. M., AHARONSON, O. & ASPHAUG, E. 2008.
 Mega-impact formation of the Mars hemispheric dichotomy. *Nature*, 453, 1216–1219.
- MASSIRONI, M., DI ACHILLE, G. ET AL. 2014. Lateral ramps and strike-slip kinematics on Mercury. In: PLATZ, T., MASSIRONI, M., BYRNE, P. K. & HIESINGER, H. (eds) Volcanism and Tectonism Across the Inner Solar System. Geological Society, London, Special Publications, 401. First published online June 5, 2014, http://dx.doi.org/10.1144/SP401.16
- MAXWELL, T. A. 1978. Origin of multi-ring basin ridge systems: an upper limit to elastic deformation based on a finite-element model. *Proceedings of Lunar and Planetary Science*, 9, 3541–3559.
- McCauley, J. F., Carr, M. H. Et al. 1972. Preliminary Mariner-9 report on the geology of Mars. *Icarus*, 17, 289–327.
- McGill, G. E. 1993. Wrinkle ridges, stress domains, and kinematics of Venusian plains. *Geophysical Research Letters*, **20**, 2407–2410.
- McGill, G. E. 2004. Tectonic and stratigraphic implications of the relative ages of Venusian plains and wrinkle ridges. *Icarus*, **172**, 603–612.
- McGill, G. E., Stofan, E. R. & Smrekar, S. E. 2010. Venus tectonics. *In*: Watters, T. R. & Schultz, R. A. (eds) *Planetary Tectonics*. Cambridge University Press, Cambridge, 81–120.
- McGovern, P. J. & Morgan, J. K. 2009. Volcanic spreading and lateral variations in the structure of Olympus Mons, Mars. *Geology*, **37**, 139–142.
- McGovern, P. J. & Solomon, S. C. 1993. State of stress, faulting, and eruption characteristics of large volcanoes on Mars. *Journal of Geophysical Research*, 98, 23 553–23 579.
- McGovern, P. J., Smith, J. R., Morgan, J. K. & Bulmer, M. H. 2004. The Olympus Mons aureole deposits: new evidence for a flank-failure origin. *Journal of Geophy*sical Research, 109, E08008, http://dx.doi.org/10. 1029/2004JE002258
- McGovern, P. J., Grosfils, E. B., Galgana, G. A., Morgan, J. K., Rumpf, M. E., Smith, J. R. & Zimbelman, J. R. 2014. Lithospheric flexure and volcano basal boundary conditions: keys to the structural evolution of large volcanic edifices on the terrestrial planets. *In*: Platz, T., Massironi, M., Byrne, P. K. & Hiesinger, H. (eds) *Volcanism and Tectonism Across the Inner Solar System*. Geological Society, London, Special Publications, 401. First published online March 17, 2014, http://dx.doi.org/10.1144/SP401.7
- McKenzie, D. & Nimmo, F. 1999. The generation of Martian floods by the melting of ground ice above dikes. *Nature*, 397, 231–233.
- McKenzie, D. P. 1967. Some remarks on heat flow and gravity anomalies. *Journal of Geophysical Research*, **72**, 6261–6273.
- McKinnon, W. B., Zahnle, K. J., Ivanov, B. A. & Melosh, H. J. 1997. Cratering on Venus: models and observations. *In*: Gougher, S. W., Hunten, D. M. & Phillips, R. J. (eds) *Venus II: Geology, Geophysics, Atmosphere, and Solar Wind Environment*. University of Arizona Press, Tucson, AZ, 969–1014.

- McSween, H. Y. 1994. What we have learned about Mars from SNC meteorites. *Meteoritics*, **29**, 757–779.
- McSween, H. Y. 2002. The rocks of Mars, from far and near. *Meteoritics and Planetary Science*, **37**, 7–25.
- McSween, H. Y., Arvidson, R. E. *Et al.* 2004. Basaltic rocks analyzed by the Spirit rover in Gusev Crater. *Science*, **305**, 842–845.
- Mège, D. & Masson, P. 1996. A plume tectonics model for the Tharsis province, Mars. *Planetary and Space Sciences*, 44, 1499–1546.
- Melendrez, D. E., Johnson, J. R., Larson, S. M. & Singer, R. B. 1994. Remote sensing of potential lunar resources. 2: high spatial resolution mapping of spectral reflectance ratios and implications for nearside mare TiO₂ content. *Journal of Geophysical Research*, **99**, 5601–5619, http://dx.doi.org/10.1029/93JE03430
- Melosh, H. J. 1978. The tectonics of mascon loading. *Proceedings of Lunar and Planetary Science*, 9, 3513–3525.
- MELOSH, H. J. & DZURISIN, D. 1978. Mercurian global tectonics: a consequence of tidal despinning? *Icarus*, **35**, 227–236.
- MELOSH, H. J. & MCKINNON, W. B. 1988. The tectonics of Mercury. *In*: VILAS, F., CHAPMAN, C. R. & MAT-THEWS, M. S. (eds) *Mercury*. University of Arizona Press, Tucson, AZ, 374–400.
- MEYZEN, C. M., MASSIRONI, M., POZZOBON, R. & DAL ZILIO, L. 2014. Are terrestrial plumes from motionless plates analogues to Martian plumes feeding the giant shield volcanoes? *In:* PLATZ, T., MASSIRONI, M., BYRNE, P. K. & HIESINGER, H. (eds) *Volcanism and Tectonism Across the Inner Solar System.* Geological Society, London, Special Publications, **401**. First published online February 21, 2014, http://dx.doi.org/10. 1144/SP401.8
- MICHALSKI, J. R. & BLEACHER, J. E. 2013. Supervolcanoes within an ancient volcanic province in Arabia Terra, Mars. *Nature*, **502**, 47–52, http://dx.doi.org/10.1038/nature12482
- MONTÉSI, L. G. & ZUBER, M. T. 2003. Clues to the lithospheric structure of Mars from wrinkle ridge sets and localization instability. *Journal of Geophysi*cal Research, 108, 5048, http://dx.doi.org/10.1029/ 2002JE001974
- Montgomery, D. R. & Gillespie, A. 2005. Formation of Martian outflow channels by catastrophic dewatering of evaporite deposits. *Geology*, **33**, 625–628.
- Moresi, L. N. & Solomatov, V. S. 1998. Mantle convection with a brittle lithosphere: thoughts on the global tectonic style of the Earth and Venus. *Geophysical Journal*, **133**, 669–682.
- MORGAN, J. K. & MCGOVERN, P. J. 2005. Discrete element simulations of gravitational volcanic deformation:
 1. Deformation structures and geometries. *Journal of Geophysical Research*, 110, B05402.
- MORGAN, J. W. 1968. Rises trenches, great faults and crustal blocks 1968. *Journal of Geophysical Research*, 73, 1959–1982.
- MORGAN, P. & PHILLIPS, R. J. 1983. Hot spot heat transfer: its application to Venus and implications to Venus and Earth. *Journal of Geophysical Research*, **88**, 8305–8317.

MOROTA, T., HARUYAMA, J. ET AL. 2011. Timing and characteristics of the latest mare eruption on the Moon. Earth and Planetary Science Letters, 302, 255–266.

- MOROTA, T., ISHIHARA, Y. ET AL. 2014. Lunar mare volcanism: lateral heterogeneities in volcanic activity and relationship with crustal structure. In: PLATZ, T., MASSIRONI, M., BYRNE, P. K. & HIESINGER, H. (eds) Volcanism and Tectonism Across the Inner Solar System. Geological Society, London, Special Publications, 401. First published online March 20, 2014, http://dx.doi.org/10.1144/SP401.11
- MOUGINIS-MARK, P. J. & CHRISTENSEN, P. R. 2005. New observations of volcanic features on Mars from THEMIS instrument. *Journal of Geophysical Research*, **110**, E08007, http://dx.doi.org/10.1029/2005JE002421
- MOUGINIS-MARK, P. J. & ROWLAND, S. K. 2001. The geomorphology of planetary calderas. *Geomorphology*, 37, 201–223.
- MUEHLBERGER, W. R. 1974. Structural history of southeastern Mare Serenitatis and adjacent highlands. Proceedings of Lunar and Planetary Science, 5, 101–110.
- MUELLER, K. & GOLOMBEK, M. 2004. Compressional structures on Mars. Annual Review of Earth and Planetary Science, 32, 435–464.
- MUELLER, N., HELBERT, J., HASHIMOTO, G. L., TSANG, C. C. C., ERARD, S., PICCIONI, G. & DROSSART, P. 2008. Venus surface thermal emission at 1 μm in VIRTIS imaging observations: evidence for variation of crust and mantle differentiation conditions. *Journal of Geophysical Research*, **113**, E00B17.
- MURCHIE, S. L., WATTERS, T. R. ET AL. 2008. Geology of the Caloris Basin, Mercury: a View from MESSEN-GER. Science, 321, 73–76.
- MURRAY, B. C., STROM, R. G., TRASK, N. J. & GAULT, D. E. 1975. Surface history of Mercury: implications for terrestrial planets. *Journal of Geophysical Research*, 80, 2508–2514.
- MUSTARD, J. F. & HEAD, J. W. 1996. Buried stratigraphic relationships along the southwestern shores of Oceanus Procellarum: implications for early lunar volcanism. *Journal of Geophysical Research*, 101, 18 913–18 926.
- NAHM, A. L. & SCHULTZ, R. A. 2013. Rupes Recta and the geological history of the Mare Nubium region of the Moon: insights from forward mechanical modelling of the 'Straight Wall'. *In*: PLATZ, T., MASSIRONI, M., BYRNE, P. K. & HIESINGER, H. (eds) *Volcanism and Tectonism Across the Inner Solar System*. Geological Society, London, Special Publications, **401**. First published online December 16, 2013, http://dx.doi.org/10.1144/SP401.4
- NAKAMURA, Y., LAMMLEIN, D., LATHAM, G., EWING, M., DORMAN, J., PRESS, F. & TOKSÖZ, M. N. 1973. New seismic data on the state of the deep lunar interior. *Science*, 181, 49–51.
- NEAL, C. R. & TAYLOR, L. A. 1992. Using Apollo 17 High-Ti Mare Basalts as Windows to the Lunar Mantle. Workshop on Geology of the Apollo 17 Landing Site. Lunar Science Institute, Houston, TX, 40–44.
- Neukum, G. & Hiller, K. 1981. Martian ages. *Journal of Geophysical Research*, **86**, 3097–3121.

- NEUKUM, G. & IVANOV, B. A. 1994. Crater size distributions and impact probabilities on Earth from lunar, terrestrial-planet, and asteroid cratering data. *In:* GEHRELS, T. (ed.) *Hazard Due to Comets and Asteroids*. University of Arizona Press, Tucson, AZ, 359–416.
- Neukum, G., König, B. & Arkani-Hamed, J. 1975a. A study of lunar impact crater size distributions. *The Moon*, **12**, 201–229.
- Neukum, G., König, B., Fechtig, H. & Storzer, D. 1975b. Cratering in the Earth–Moon system. Consequences for age determination by crater counting. *Proceedings of Lunar and Planetary Science*, **6**, 2597–2620.
- Neukum, G., Ivanov, B. A. & Hartmann, W. K. 2001. Cratering records in the inner solar system in relation to the lunar reference system. *Space Science Reviews*, **96**, 55–86.
- Neukum, G., Jaumann, R. *et al.* 2004. Recent and episodic volcanic and glacial activity on Mars revealed by the High Resolution Stereo Camera. *Nature*, **432**, 971–979.
- Neukum, G., Basilevsky, A. T. *Et al.* 2010. The geologic evolution of Mars: episodicity of resurfacing events and ages from cratering analysis of image data and correlation with radiometric ages of Martian meteorites. *Earth and Planetary Science Letters*, **294**, 204–220.
- NIKOLAEVA, O., IVANOV, M. & BOROZDIN, V. 1992. Evidence on the crustal dichotomy of Venus. In: Venus Geology, Geochemistry, and Geophysics Research Results from the USSR. University of Arizona Press, Tueson A7
- NIMMO, F. & MCKENZIE, D. 1998. Volcanism and tectonics on Venus. Annual Review of Earth and Planetary Sciences. 26, 23–51.
- NITTLER, L. R., STARR, R. D. ET AL. 2011. The majorelement composition of Mercury's surface from MESSENGER X-Ray Spectrometer. Science, 333, 1847–1850.
- OBERBECK, V. R., QUAIDE, W. L., ARVIDSON, R. E. & AGGARWAL, H. R. 1977. Comparative studies of lunar, Martian, and Mercurian craters and plains. *Journal of Geophysical Research*, 82, 1681–1698.
- OHTAKE, M., MATSUNAGA, T. ET AL. 2009. The global distribution of pure anorthosite on the Moon. *Nature*, **461**, 236–240, http://dx.doi.org/10.1038/nature08317
- ÖPIK, E. 1960. The lunar surface as an impact counter. Monthly Notices of the Royal Astronomical Society, 120, 404–411.
- O'ROURKE, J. G. & KORENAGA, J. 2012. Terrestrial planet evolution in the stagnant-lid regime: size effects and the formation of self-destabilizing crust. *Icarus*, **221**, 1043–1060.
- Page, D. P. 2007. Recent low-latitude freeze-thaw on Mars. *Icarus*, **189**, 83-117.
- Papike, J. J. 1998. Comparative planetary mineralogy: chemistry of melt-derived pyroxene, feldspar, and olivine. Abstract 1008 presented at the 27th Lunar & Planetary Science Conference, Houston, TX.
- Papike, J. J. & Vaniman, D. T. 1978. The lunar mare basalt suite. *Geophysical Research Letters*, **5**, 433–436.
- Papike, J. J., Hodges, F. N., Bence, A. E., Cameron, M. & Rhodes, J. M. 1976. Mare basalts Crystal

- chemistry, mineralogy, and petrology. Reviews of Geophysics and Space Physics, 14, 475-540.
- Parmentier, E. M. & Hess, P. C. 1992. Chemical differentiation of a convecting planetary interior: consequences for a one-plate planet. *Geophysical Research Letters*, 19, 2015–2018.
- PASCKERT, J. H., HIESINGER, H. & REISS, D. 2012. Rheologies and ages of lava flows on Elysium Mons, Mars. *Icarus*, 219, 443–457.
- PASCKERT, J. H., HIESINGER, H. & VAN DER BOGERT, C. H. 2014. Lunar mare basalts in- and outside of the South Pole-Aitken basin. Abstract 1968 presented at the 45th Lunar & Planetary Science Conference, March 17–21, 2014, The Woodlands, Texas.
- PAVRI, B., HEAD, J. W., KLOSE, K. B. & WILSON, L. 1992. Steep-sided domes on Venus: characteristics, geologic settings, and eruption conditions from Magellan data. *Journal of Geophysical Research*, 97, 13 445–13 478.
- Peale, S., Schubert, G. & Lingenfelter, R. E. 1968. Distribution of sinuous rilles and water on the Moon. *Nature*, **220**, 1222–1225.
- PHILLIPS, R. J. & HANSEN, V. L. 1998. Geological evolution of Venus: rises, plains, plumes, and plateaus. Science, 279, 1492–1497.
- PHILLIPS, R. J. & MALIN, M. C. 1983. The interior of Venus and tectonic implications. *In*: Hunten, D. M., Colin, L., Donahue, T. M. & Moroz, V. I. (eds) *Venus*. University of Arizona Press, Tucson, AZ, 159–214.
- PHILLIPS, R. J., GRIMM, R. E. & MALIN, M. C. 1991. Hot-spot evolution and the global tectonics of Venus. *Science*, 252, 651–658.
- PHILLIPS, R. J., RAUBERTAS, R. F., ARVIDSON, R. E., SARKAR, I. C., HERRICK, R. R., IZENBERG, N. & GRIMM, R. E. 1992. Impact craters and Venus resurfacing history. *Journal of Geophysical Research*, 97, 15 923–15 948.
- PHILLIPS, R. J., ZUBER, M. T. ET AL. 2001. Ancient geodynamics and global-scale hydrology on Mars. Science, 291, 2587–2591.
- PIETERS, C. M. 1978. Mare basalt types on the front side of the moon a summary of spectral reflectance data. *Proceedings of Lunar and Planetary Science*, **9**, 2825–2849.
- PIETERS, C. M., HEAD, J. W., WHITFORD-STARK, J. L.,
 ADAMS, J. B., McCORD, T. B. & ZISK, S. H. 1980.
 Late high-titanium basalts of the western maria –
 Geology of the Flamsteed region of Oceanus Procellarum. *Journal of Geophysical Research*, 85, 3913–3938, http://dx.doi.org/10.1029/JB085iB07 p03913
- PLATZ, T. & MICHAEL, G. G. 2011. Eruption history of the Elysium Volcanic Province, Mars. Earth and Planetary Science Letters, 312, 140–151.
- PLATZ, T., KNEISSL, T., HAUBER, E., LE DEIT, L., MICHAEL, G. G. & NEUKUM, G. 2010. Total volume estimates of volcanic material and outgassing in the Elysium Volcanic Region. Abstract 2476 presented at the 41st Lunar & Planetary Science Conference, March 1–5, 2010, The Woodlands, Texas.
- PLATZ, T., MÜNN, S., WALTER, T. R., McGUIRE, P. C., DUMKE, A. & NEUKUM, G. 2011. Vertical and lateral collapse of Tharsis Tholus, Mars. *Earth and Planetary Science Letters*, **305**, 445–455, http://dx.doi.org/10.1016/j.epsl.2011.03.012

- PLATZ, T., JODLOWSKI, P., FAWDON, P., MICHAEL, G. G. & TANAKA, K. L. 2014. Amazonian volcanic activity at the Syrtis Major volcanic province, Mars. Abstract 2524 presented at the 45th Lunar & Planetary Science Conference, March 17–21, 2014, The Woodlands, Texas.
- PLESCIA, J. B. 1993. Wrinkle ridges of Arcadia Planitia, Mars. *Journal of Geophysical Research*, 98, 15 049–15 059.
- PLESCIA, J. B. 1994. Geology of the small Tharsis volcanoes: Jovis Tholus, Ulysses Patera, Biblis Patera, Mars. *Icarus*, 111, 246–269.
- PLESCIA, J. 2003. Cerberus fossae, Elysium, Mars: a source for lava and water. *Icarus*, **164**, 79–95.
- PLESCIA, J. B. 2004. Morphometric properties of Martian volcanoes. *Journal of Geophysical Research*, **109**, E03003.
- PLESCIA, J. B. & GOLOMBEK, M. P. 1986. Origin of planetary wrinkle ridges based on the study of terrestrial analogs. *Geological Society of America Bulletin*, **97**, 1289–1299.
- PLESCIA, J. B. & SAUNDERS, R. S. 1982. Tectonic history of the Tharsis Region, Mars. *Journal of Geophysical Research*, 87, 9775–9791.
- Poulet, F., Gomez, C. *et al.* 2007. Martian surface mineralogy from Observatoire pour la Minéralogie, l'Eau, les Glaces et l'Activité on board the Mars Express spacecraft (OMEGA/MEX): global mineral maps. *Journal of Geophysical Research*, **112**, E08S02, http://dx.doi.org/10.1029/2006JE002840
- POZZOBON, R., MAZZARINI, F., MASSIRONI, M. & MARINANGELI, L. 2014. Self-similar clustering distribution of structural features on Ascraeus Mons (Mars): implications for magma chamber depth. In: PLATZ, T., MASSIRONI, M., BYRNE, P. K. & HIESINGER, H. (eds) Volcanism and Tectonism Across the Inner Solar System. Geological Society, London, Special Publications, 401. First published online March 25, 2014, http://dx.doi.org/10.1144/SP401.12
- PRICE, M. & SUPPE, J. 1995. Constraints on the resurfacing history of Venus from the hypsometry and distribution of volcanism, tectonism and impact craters. *Earth, Moon, and Planets*, **71**, 99–145.
- PRITCHARD, M. E. & STEVENSON, D. J. 2000. The thermochemical history of the Moon: constraints and major questions. Abstract 1878 presented at the 31st Lunar & Planetary Science Conference, March 13–17, 2000, The Woodlands, Texas.
- PROCKTER, L. M., ERNST, C. M. *ET Al.* 2010. Evidence for young volcanism on Mercury from the third MESSENGER flyby. *Science*, **329**, 668–671.
- RAITALA, J. 1994. Main fault tectonics of Meshkenet Tessera on Venus. *Earth, Moon and Planets*, **65**, 55–70.
- RANALLI, G. 1995. *Rheology of the Earth*. Chapman & Hall, London.
- RANALLI, G. 1997. Rheology of the lithosphere in space and time. *In*: BURG, J.-P. & FORD, M. (eds) *Orogeny Through Time*. Geological Society, London, Special Publications, **121**, 19–37.
- REESE, C. C., SOLOMATOV, V. S. & MORESI, L. N. 1999. Non-Newtonian stagnant lid convection and magmatic resurfacing on Venus. *Icarus*, 80, 67–80.
- RICHARDSON, J. A., BLEACHER, J. E. & GLAZE, L. S. 2013. The volcanic history of Syria Planum, Mars.

Journal of Volcanology and Geothermal Research, **252**, 1–13.

- ROBBINS, S. J., DI ACHILLE, G. & HYNEK, B. M. 2011. The volcanic history of Mars: high-resolution crater-based studies of the calderas of 20 volcanoes. *Icarus*, **211**, 1179–1203.
- ROBERTS, J. H. & ZHONG, S. 2006. Degree-1 convection in the Martian mantle and the origin of the hemispheric dichotomy. *Journal of Geophysical Research*, 111, F06013
- ROBINSON, M. S. & LUCEY, P. G. 1997. Recalibrated Mariner 10 color mosaics: implications for Mercurian volcanism. *Science*, **275**, 197–200.
- ROBINSON, M. S., MOUGINIS-MARK, P. J., ZIMBELMAN, J. R., Wu, S. S. C., ABLIN, K. K. & HOWINGTON-KRAUS, A. E. 1993. Chronology, eruption duration, and atmospheric contribution of the Martian volcano Apollinaris Patera. *Icarus*, 104, 301–323.
- RODRIGUEZ, J. A. P., KARGEL, J. ET AL. 2006. Head-ward growth of chasmata by volatile outbursts, collapse, and drainage: evidence from Ganges Chaos, Mars. Geophysical Research Letters, 33, L18203.
- ROMEO, I. & TURCOTTE, D. L. 2008. Pulsating continents on Venus: an explanation for crustal plateaus and tessera terrains. *Earth and Planetary Science Letters*, **276**, 85–97.
- ROMEO, I., CAPOTE, R. & ANGUITA, F. 2005. Tectonic and kinematic study of a strike-slip zone along the southern margin of Central Ovda Regio, Venus: geodynamical implications for crustal plateaux formation and evolution. *Icarus*, **175**, 320–334.
- ROSENBERG, E. & McGILL, G. E. 2001. Geologic Map of the Pandrosos Dorsa Quadrangle (V-5), Venus. United States Geological Survey, Miscellaneous Geologic Investigations Series, I-2721.
- ROTHERY, D. A., THOMAS, R. J. & KERBER, L. 2014. Prolonged eruptive history of a compound volcano on Mercury: volcanic and tectonic implications. *Earth and Planetary Science Letters*, **385**, 59–67.
- RYAN, M. R. 1987. Elasticity and contractancy of Hawaiian olivine tholeiite and its role in the stability and structural evolution of subcaldera magma reservoirs and rift systems. *In*: DECKER, I. R. W., WRIGHT, T. L. & STAUFFER, P. H. (eds) *Volcanism in Hawaii*. United States Geological Survey, Professional Papers, **1350**, 1395–1447.
- SANDWELL, D. T., JOHNSON, C. L., BILOTTI, F. & SUPPE, J. 1997. Driving forces for limited tectonics on Venus. *Icarus*, **129**, 232–244.
- Sautter, V., Fabre, C. *et al.*, 2014. Igneous mineralogy at Bradbury Rise: the first ChemCam campaign at Gale crater. *Journal of Geophysical Research*, **119**, 30–46.
- SCHABER, G. 1982. Limited extension and volcanism along zones of lithospheric weakness. *Geophysical Research Letters*, **9**, 499–502.
- SCHABER, G. G. 1973. Lava flows in Mare Imbrium: geologic evaluation from Apollo orbital photography. *Proceedings of Lunar and Planetary Science*, **4**, 73–92
- SCHABER, G. G., BOYCE, J. M. & MOORE, H. J. 1976. The scarcity of mappable flow lobes on the lunar maria: unique morphology of the Imbrium flows. *Proceedings* of Lunar and Planetary Science, 7, 2783–2800.

- SCHABER, G. G., STROM, R. G. ET AL. 1992. Geology and distribution of impact craters on Venus: what are they telling us? *Journal of Geophysical Research*, **97**, 13 257–13 301.
- Schubert, G., Lingenfelter, R. E. & Peale, S. J. 1970. The morphology, distribution and origin of lunar sinuous rilles. *Reviews of Geophysics and Space Physics*, **8**, 199–224.
- SCHUBERT, G., ROSS, M. N., STEVENSON, D. J. & SPOHN, T. 1988. Mercury's thermal history and the generation of its magnetic field. *In*: VILAS, F., CHAPMAN, C. R. & MATTHEWS, M. S. (eds) *Mercury*. University of Arizona Press, Tucson, AZ, 429–460.
- SCHUBERT, G., SOLOMATOV, V. S., TACKLEY, P. J. & TURCOTTE, D. L. 1997. Mantle convection and the thermal evolution of Venus. In: BROUGHER, S. W., HUNTEN, D. M. & PHILLIPS, R. J. (eds) Venus II: Geology, Geophysics, Atmosphere, and Solar Wind Environment. University of Arizona Press, Tucson, AZ, 1245–1287.
- SCHULTZ, P. H. 1972. A preliminary morphologic study of the lunar surface. PhD thesis, University of Texas at Austin, Austin, TX.
- SCHULTZ, P. H. 1976. Floor-fractured lunar craters. *The Moon*, **15**, 241–273.
- Schultz, P. H. & Gault, D. E. 1975. Seismic effects from major basin formations on the Moon and Mercury. *The Moon*, **12**, 159–177.
- Schultz, P. H. & Spudis, P. D. 1979. Evidence for ancient mare volcanism. *Proceedings of Lunar and Planetary Science*, **10**, 2899–2918.
- SCHULTZ, P. H. & SPUDIS, P. D. 1983. Beginning and end of lunar mare volcanism. *Nature*, **302**, 233–236.
- Schultz, R. A. 1998. Multiple-process origin of Valles Ma-rineris basins and troughs, Mars. *Planetary and Space Sciences*, **46**, 827–834.
- SCHULTZ, R. A. 2000. Localization of bedding plane slip and backthrust faults above blind thrust faults: keys to wrinkle ridge structure. *Journal of Geophysical Research*, **105**, 12 035–12 052.
- SCHULTZ, R. A. & LIN, J. 2001. Three-dimensional normal faulting models of the Valles Marineris, Mars, and geodynamic implications. *Journal of Geophysical Research*, **106**, 16 549–16 566.
- SCHULTZ, R. A. & TANAKA, K. L. 1994. Lithospheric-scale buckling and thrust structures on Mars: the Coprates rise and south Tharsis ridge belt. *Journal of Geophysi*cal Research, 99, 8371–8385.
- SCHULTZ, R. A. & ZUBER, M. T. 1994. Observations, models, and mechanisms of failure of surface rocks surrounding planetary surface loads. *Journal of Geophysical Research*, 99, 14691–14702, http://dx.doi.org/10.1029/94JE01140
- SCHULTZ, R. A., OKUBO, C. H., GOUDY, C. L. & WILKINS, S. J. 2004. Igneous dikes on Mars revealed by Mars Orbiter Laser Altimeter topography. *Geology*, **32**, 889–892.
- SCHULTZ, R. A., MOORE, J. M., GROSFILS, E. B., TANAKA, K. L. & MèGE, D. 2007. The Canyonlands model for planetary grabens: revised physical basis and implications. *In*: CHAPMAN, M. G. (ed.) *The Geology of Mars*. Cambridge University Press, Cambridge, 371–399.
- Scoppola, B., Boccaletti, D., Bevis, M., Carminati, E. & Doglioni, C. 2006. The westward drift of the

- lithosphere: a rotational drag? Geological Society of America Bulletin, 118, 199–209.
- SCOTT, D. H. & TANAKA, K. L. 1982. Ignimbrites of Amazonis Planitia region of Mars. *Journal of Geophysical Research*, 87, 1179–1190.
- SENSKE, D. A., SCHABER, G. G. & STOFAN, E. R. 1992. Regional topographic rises on Venus: geology of western Eistla Regio and comparisons to Beta Regio and Atla Regio. *Journal of Geophysical Research*, 97, 13 395–13 420.
- SHARP, R. P. 1973. Mars: troughed terrain. *Journal of Geophysical Research*, **78**, 4063–4072.
- SHEARER, C. K. & NEWSOM, H. E. 2000. W-Hf abundances and the early origin and evolution of the Earth–Moon system. *Geochimica et Cosmochimica Acta*, **64**, 3599–3613.
- SHEARER, C. K., HESS, P. C. ET AL. 2006. Thermal and magmatic evolution of the Moon. Reviews in Mineralogy & Geochemistry, 60, 365–518.
- SHELLNUTT, J. G. 2013. Petrological modeling of basaltic rocks from Venus: a case for the presence of silicic rocks. *Journal of Geophysical Research*, 118, 1350–1364.
- SHKURATOV, Y. G., KAYDASH, V. G. & OPANASENKO, N. V. 1999. Iron and titanium abundance and maturity degree distribution on the lunar nearside. *Icarus*, 137, 222–234, http://dx.doi.org/10.1006/icar.1999. 6046
- SHOEMAKER, E. M. & HACKMAN, R. 1962. Stratigraphic basis for a lunar time scale. *In: The Moon. Proceedings of Symposium No. 14 of the International Astronomical Union held at Pulkovo Observatory, Leningrad, December 1960.* Academic Press, San Diego, CA, 289–300.
- SILVESTRO, S., FENTON, L. K., VAZ, D. A., BRIDGES, N. T. & ORI, G. G. 2010. Ripple migration and dune activity on Mars: evidence for dynamic wind processes. *Geo-physical Research Letters*, 37, L20203.
- SIMONS, M., SOLOMON, S. C. & HAGER, B. H. 1997. Localization of gravity and topography: constraints on the tectonics and mantle dynamics of Venus. *Geophysical Journal International*, **131**, 24–44.
- SKINNER, J. A. & TANAKA, K. L. 2007. Evidence for and implications of sedimentary diapirism and mud volcanism in the southern Utopia highland-lowland boundary plain, Mars. *Icarus*, 186, 41–59, http://dx. doi.org/10.1016/j.icarus.2006.08.013
- SKOK, J. R., MUSTARD, J. F., EHLMANN, B. L., MILLIKEN, R. E. & MURCHIE, S. L. 2010. Silica deposits in the Nili Patera caldera on the Syrtis Major volcanic complex on Mars. *Nature Geoscience*, 3, 838–841.
- SLEEP, N. H. 1994. Martian plate tectonics. *Journal of Geophysical Research*, 99, 5639–5655.
- SMITH, J. V., ANDERSON, A. T. ET AL. 1970. Petrologic history of the Moon inferred from petrography, mineralogy, and petrogenesis of Apollo 11 rocks. In: Levinson, A. A. (ed.) Proceedings of the Apollo 11 Lunar Science Conference, Volume 1. Pergamon Press, New York, 897–925.
- SMREKAR, S. E. 1994. Evidence for active hotspots on Venus from analysis of Magellan gravity data. *Icarus*, 112, 2–26
- SMREKAR, S. E. & PARMENTIER, E. M. 1996. Interactions of mantle plumes with thermal and chemical boundary

- layers: application to hotspots on Venus. *Journal of Geophysical Research*, **101**, 5397–5410.
- SMREKAR, S. E. & PHILLIPS, R. J. 1991. Venusian highlands – geoid to topography ratios and their implications. Earth and Planetary Science Letters, 107, 582–597.
- SMREKAR, S. E. & SOTIN, C. 2012. Constraints on mantle plumes on Venus: implications for volatile history. *Icarus*, 217, 510–523.
- SMREKAR, S. E. & STOFAN, E. R. 1999. Origin of coronadominated topographic rises on Venus. *Icarus*, 139, 100–115
- SMREKAR, S. E., STOFAN, E. R. & KIEFER, W. S. 1997. Large volcanic rises on Venus. In: BROUGHER, S. W., HUNTEN, D. M. & PHILLIPS, R. J. (eds) Venus II: Geology, Geophysics, Atmosphere, and Solar Wind Environment. University of Arizona Press, Tucson, AZ, 845–878.
- SMREKAR, S. E., MOREELS, P. & FRANKLIN, J. B. 2002. Characterization and formation of polygonal fractures on Venus. *Journal of Geophysical Research*, 107, 5098.
- SMREKAR, S. E., ELKINS-TANTON, L. ET AL. 2007. Tectonic and thermal evolution of Venus and the role of volatiles: implications for understanding the terrestrial planets. In: ESPOSITO, L. W., STOFAN, E. R. & CRAVENS, T. E. (eds) Exploring Venus as a Terrestrial Planet. American Geophysical Union, Geophysical Monograph Series, 176, 45-71.
- SODERBLOM, L. A., BOYCE, J. M. & ARNOLD, J. R. 1977. Regional variations in the lunar maria – Age, remanent magnetism, and chemistry. *Proceedings of Lunar and Planetary Science*, 8, 1191–1199.
- SOLOMATOV, V. S. & MORESI, L. N. 2000. Scaling of time-dependent stagnant lid convection: application to small-scale convection on Earth and other terrestrial planets. *Journal of Geophysical Research*, **105**, 21 795–21 817.
- SOLOMON, S. C. 1977. The relationship between crustal tectonics and internal evolution in the Moon and Mercury. *Physics of the Earth and Planetary Interiors*, **15**, 135–145.
- SOLOMON, S. C. 1978. The nature of isostasy on the Moon: how big of a Pratt-fall for Airy methods. *Proceedings of Lunar and Planetary Science*, **9**, 3499–3511.
- SOLOMON, S. C. 1993. The geophysics of Venus. *Physics Today*, **46**, 48–55.
- SOLOMON, S. C. & CHAIKEN, J. 1976. Thermal expansion and thermal stress in the moon and terrestrial planets Clues to early thermal history. *Proceedings of Lunar and Planetary Science*, **7**, 3229–3243.
- SOLOMON, S. C. & HEAD, J. W. 1979. Vertical movement in mare basins: relation to mare emplacement, basin tectonics, and lunar thermal history. *Journal of Geophysical Research*, 84, 1667–1682.
- SOLOMON, S. C. & HEAD, J. W. 1980. Lunar mascon basins: lava filling, tectonics, and evolution of the lithosphere. *Reviews of Geophysics and Space Physics*, **18**, 107–141.
- SOLOMON, S. C. & HEAD, J. W. 1982. Mechanisms for lithospheric heat transport on Venus: implications for tectonic style and volcanism. *Journal of Geophysical Research*, 87, 9236–9246.

SOLOMON, S. C. & LONGHI, J. 1977. Magma oceanography. I-Thermal evolution. *Proceedings of Lunar and Planetary Science*, 8, 583–599.

- SOLOMON, S. C., HEAD, J. W. *ET AL*. 1991. Venus tectonics: initial analysis from Magellan. *Science*, **252**, 297–312.
- SOLOMON, S. C., SMREKAR, S. E. ET AL. 1992. Venus tectonics: an overview of Magellan observations. *Journal of Geophysical Research*, 97, 13 199–13 255.
- SPENCER, J. R. & FANALE, F. P. 1990. New models for the origin of Valles Marineris closed depressions. *Journal* of Geophysical Research, 95, 14 301–14 313.
- SPOHN, T., KONRAD, W., BREUER, D. & ZIETHE, R. 2001. The longevity of lunar volcanism. implications of thermal evolution calculations with 2D and 3D mantle convection models. *Icarus*, 149, 54–65.
- SPUDIS, P. D., McGOVERN, P. J. & KIEFER, W. S. 2013. Large shield volcanoes on the Moon. *Journal of Geophysical Research*, 118, 1–19, http://dx.doi.org/10.1002/jgre.20059
- SQUYRES, S. W., AHARONSON, O. *ET AL.* 2007. Pyroclastic activity at Home Plate in Gusev crater, Mars. *Science*, **316**, 738–742.
- SQUYRES, S. W., JANES, D. M., BINDSCHADLER, L., SHARP-TON, V. L. & STOFAN, R. 1992. The morphology and evolution of coronae on Venus. *Journal of Geophysical Research*, **97**, 13 611–13 634.
- SQUYRES, S. W., ARVIDSON, R. E. ET AL. 2006. Rocks of Columbia Hills. *Journal of Geophysical Research*, 111, E02S11.
- STEWART, E. M. & HEAD, J. W. 2001. Ancient Martian volcanoes in the Aeolis region: new evidence from MOLA data. *Journal of Geophysical Research*, **106**, 17 505–17 513.
- STOCKSTILL-CAHILL, K. R., McCOY, T. J., NITTLER, L. R., WEIDER, S. Z. & HAUCK, S. A., II. 2012. Magnesiumrich crustal compositions on Mercury: implications for magmatism from petrologic modeling. *Journal of Geophysical Research*, 117, E00L15, http://dx.doi. org/10.1029/2012JE004140
- Stofan, E. R., Bindschadler, D. L., Head, J. W. & Parmentier, E. M. 1991. Corona structures on Venus: models of origin. *Journal of Geophysical Research*, **96**, 20 933–20 946.
- STOFAN, E. R., SHARPTON, V. L., SCHUBERT, G., BAER, G., BINDSCHADLER, D. L., JANES, D. M. & SQUYRES, S. W. 1992. Global distribution and characteristics of coronae and related features on Venus: implications for origin and relation to mantle processes. *Journal* of Geophysical Research, 97, 13 347–13 378.
- STOFAN, É. R., SMREKAR, S. E., BINDSCHADLER, D. L. & SENSKE, D. A. 1995. Large topographic rises on Venus: implications for mantle upwellings. *Journal of Geophysical Research*, 100, 23 317–23 327.
- STOFAN, E. R., BINDSCHADLER, D. L., HAMILTON, V. E., JANES, D. M. & SMREKAR, S. E. 1997. Coronae on Venus: morphology and origin. In: BROUGHER, S. W., HUNTEN, D. M. & PHILLIPS, R. J. (eds) Venus II: Geology, Geophysics, Atmosphere, and Solar Wind Environment. University of Arizona Press, Tucson, AZ, 931–965.
- STOFAN, E. R., ANDERSON, W., CROWN, A. & PLAUT, J. 2000. Emplacement and composition of steep-sided domes on Venus. *Journal of Geophysical Research*, 105, 26 757–26 771.

- STOFAN, E. R., TAPPER, S. V., GUEST, J. E., GRINROD, P. & SMREAKAR, S. E. 2001. Preliminary analysis of an expanded corona database for Venus. *Geophysical Research Letters*, 28, 4267–4270.
- STROM, G., SCHABER, G. & DAWSON, D. D. 1994. The global resurfacing of Venus. *Journal of Geophysical Research*, **99**, 10 899–10 926.
- STROM, R. G. 1964. Analysis of lunar lineaments, I: tectonic maps of the Moon. *University of Arizona Lunar and Planetary Laboratory Communications*, 2, 205–216.
- STROM, R. G. & NEUKUM, G. 1988. The cratering record on Mercury and the origin of impacting objects. *In*: VILAS, F., CHAPMAN, C. R. & MATTHEWS, M. S. (eds) *Mercury*. University of Arizona Press, Tucson, AZ, 336–373.
- STROM, R. G., TRASK, N. J. & GUEST, J. E. 1975. Tectonism and volcanism on Mercury. *Journal of Geophysical Research*, **80**, 2478–2507.
- STUDD, D., ERNST, R. E. & SAMSON, C. 2011. Radiating graben-fissure systems in the Ulfrun Regio area, Venus. *Icarus*, **215**, 279–291.
- SULLIVAN, K. & HEAD, J. W. 1984. Geology of the Venus lowlands: Guinevere and Sedna Planitia. *Proceedings* of the 15th Lunar and Planetary Science Conference, 12–16 March 1984, Houston, Texas. 836–837.
- Surkov, Y. A. 1983. Studies of Venus rocks by Veneras 8, 9 and 10. *In*: Hunten, D. M., Colin, L., Donahue, T. M. & Moroz, V. I. (eds) *Venus*. University of Arizona Press, Tucson, 154–158.
- Tanaka, K. L. & Golombek, M. P. 1989. Martian tension fractures and the formation of grabens and collapse features at Valles Marineris. *Proceedings of Lunar and Planetary Science*, **19**, 383–396.
- Tanaka, K. L., Senske, D. A., Price, M. & Kirk, R. L. 1997. Physiography, geomorphic/geologic mapping, and stratigraphy of Venus. *In*: Brougher, S. W., Hunten, D. M. & Phillips, R. J. (eds) *Venus II: Geology, Geophysics, Atmosphere, and Solar Wind Environment*. University of Arizona Press, Tucson, AZ, 667–694.
- TANAKA, K. L., SKINNER, J. A., JR & HARE, T. M. 2005. Geologic Map of the Northern Plains of Mars. United States Geological Survey, Miscellaneous Geologic Investigations Series Map, SIM-2888.
- TANAKA, K. L., SKINNER, J. A., JR. ET AL. 2014. Geologic Map of Mars, Scale 1:20,000,000. United States Geological Survey, Miscellaneous Geologic Investigations Series Map, SIM 3292, http://dx.doi.org/10.3133/ sim3292
- TAYLOR, G. J., WARREN, P., RYDER, G., DELANO, J., PIETERS, C. & LOFGREN, G. 1991. Lunar rocks. In: HEIKEN, G., VANIMAN, D. & FRENCH, B. (eds) The Lunar Source Book: A User's Guide to the Moon. Cambridge University Press, New York, 183–284.
- Taylor, L. A. 1982. Lunar and terrestrial crusts A contrast in origin and evolution. *Physics of the Earth and Planetary Interiors*, **29**, 233–241.
- Taylor, S. R., Norman, M. D. & Esat, T. 1993. The lunar highland crust: The origin of the Mg suite. *Meteoritics*, 28, 448
- TERADA, K., ANAND, M., SOKOL, A., BISCHOFF, A. & SANO, Y. 2007. Cryptomare magmatism 4.35 Gyr ago recorded in lunar meteorite Kalahari 009. *Nature*, 450, 849–852, http://dx.doi.org/10.1038/nature 06356

- THOMAS, P. 1984. Martian intracrater spotches: occurrence, morphology, and colors. *Icarus*, **57**, 205–227.
- THOMAS, P. J., SQUYRES, S. W. & CARR, M. H. 1990. Flank tectonics of Martian volcanoes. *Journal of Geophysical Research*, **95**, 14 345–14 355.
- THORARINSSON, S. 1953. The crater groups in Iceland. *Bulletin of Volcanology*, **14**, 3–44.
- THOREY, C. & MICHAUT, C. 2014. A model for the dynamics of crater-centered intrusion: application to lunar floor-fractured craters. *Journal of Geophysical Research*, 119, 286–312.
- TIRSCH, D., JAUMANN, R., PACIFICI, A. & POULET, F. 2011. Dark aeolian sediments in Martian craters: composition and sources. *Journal of Geophysical Research*, 116, E03002.
- Tran, T., Robinson, M. S. *et al.* 2011. Morphometry of lunar volcanic domes from LROC. Abstract 2228 presented at the 42nd Lunar & Planetary Science Conference, March 7–11, 2011, The Woodlands, Texas.
- TRASK, N. J. & GUEST, J. E. 1975. Preliminary geologic terrain map of Mercury. *Journal of Geophysical Research*, 80, 2461–2477.
- Tuckwell, G. W. & Ghail, R. C. 2003. A 400-km-scale strike-slip zone near the boundary of Thetis Regio, Venus. *Earth and Planetary Science Letters*, **211**, 45–45.
- TURCOTTE, D. L. 1993. An episodic hypothesis for Venusian tectonics. *Journal of Geophysical Research*, **98**, 17 061–17 068.
- TURCOTTE, D. L., MOREIN, G., ROBERTS, D. & MALAMUD, B. D. 1999. Catastrophic resurfacing and episodic subduction on Venus. *Icarus*, **139**, 49–54.
- VAN DER BOGERT, C. H., HIESINGER, H., BANKS, M. E., WATTERS, T. R. & ROBINSON, M. S. 2012. Derivation of absolute model ages for lunar lobate scarps. Abstract 1847 presented at the 43rd Lunar & Planetary Science Conference, March 19–23, 2012, The Woodlands, Texas.
- VAUCHER, J., BARATOUX, D., MANGOLD, N., PINET, P., KURITA, K. & GREGOIRE, M. 2009. The volcanic history of central Elysium Planitia: implications for Martian magmatism. *Icarus*, 204, 418–442.
- WAGNER, R. J., HEAD, J. W., WOLF, U. & NEUKUM, G. 1996. Age relations of geologic units in the Gruithuisen region of the moon based on crater sizefrequency measurements. 27th Lunar & Planetary Science Conference, 18–22 March 1996, Houston, Texas, 1367–1368, http://www.lpi.usra.edu/meetings/ lpsc1996/pdf/1684.pdf
- WAGNER, R., HEAD, J. W., III, WOLF, U. & NEUKUM, G. 2002. Stratigraphic sequence and ages of volcanic units in the Gruithuisen region of the Moon. *Journal* of Geophysical Research, 107, 14-1–14-15.
- WAGNER, R., HEAD, J. W., III, WOLF, U. & NEUKUM, G. 2010. Lunar red spots: stratigraphic sequence and ages of domes and plains in the Hansteen and Helmet regions on the lunar nearside. *Journal of Geophysical Research*, 115, E06015, http://dx.doi.org/10.1029/2009JE003359
- Walker, G. 1983. Ignimbrite types and ignimbrite problems. *Journal of Volcanology and Geothermal Research*, **17**, 65–88, http://dx.doi.org/10.1016/0377-0273(83)90062-8

- WARNER, J. L., SIMONDS, C. H. & PHINNEY, W. C. 1976. Genetic distinction between anorthosites and Mg-rich plutonic rocks: new data from 76255. *In:* Abstracts of the Lunar and Planetary Science Conference, Volume 7. Lunar and Planetary Institute, Houston, TX, 915–917.
- WARREN, P. H. 1990. Lunar anorthosites and the magmaocean plagioclase-flotation hypotheses: importance of FeO enrichment in the parent magma. *American Mineralogist*, **75**, 46–58.
- Warren, P. H. 1993. A concise compilation of petrologic information on possibly pristine nonmare moon rocks. *American Mineralogist*, **78**, 360–376.
- Warren, P. H. & Wasson, J. T. 1979. The origin of KREEP. Reviews of Geophysics and Space Physics, 17, 73–88.
- WATTERS, T. R. 1991. Origin of periodically spaced wrinkle ridges on the Tharsis Plateau of Mars. *Journal of Geophysical Research*, **96**, 15 599–15 616.
- WATTERS, T. R. & JOHNSON, C. L. 2010. Lunar tectonics. In: WATTERS, T. R. & SCHULTZ, R. A. (eds) Planetary Tectonics. Cambridge University Press, New York, 121–182.
- Watters, T. R., Robinson, M. S. & Cook, A. C. 1998. Topography of lobate scarps on Mercury: new constraints on the planet's contraction. *Geology*, **26**, 991–994.
- WATTERS, T. R., NIMMO, F. & ROBINSON, M. S. 2005. Extensional troughs in the Caloris basin of Mercury: evidence of lateral crustal flow. *Geology*, 33, 669–672.
- WATTERS, T. R., SOLOMON, S. C. ET AL. 2009. The tectonics of Mercury: the view after MESSENGER's first flyby. Earth and Planetary Science Letters, 285, 283–296.
- WATTERS, T. R., ROBINSON, M. S. ET AL. 2010. Evidence of recent thrust faulting on the Moon revealed by the Lunar Reconnaissance Orbiter Camera. Science, 329, 936–940.
- WATTERS, T. R., SOLOMON, S. C. ETAL. 2012. Extension and contraction within volcanically buried impact craters and basins on Mercury. Geology, 40, 1123–1126.
- WEIDER, S. Z., NITTLER, L. R. ET AL. 2012. Compositional heterogeneity on Mercury's surface revealed by the MESSENGER X-Ray Spectrometer. Journal of Geophysical Research, 117, E00L05, http://dx.doi.org/ 10.1029/2012JE004153
- WEITZ, C. & HEAD, J. W. 1999. Spectral properties of the Marius Hills volcanic complex and implications for the formation of lunar domes and cones. *Journal* of Geophysical Research, 104, 18 933–18 956.
- Weitz, C. M., Head, J. W. & Pieters, C. M. 1998. Lunar regional dark mantle deposits: geologic, multispectral, and modeling studies. *Journal of Geophysical Research*, **103**, 22 725–22 760.
- WERNER, S. C. 2009. The global Martian volcanic evolutionary history. *Icarus*, **201**, 44–68.
- Werner, S. C., van Gasselt, S. & Neukum, G. 2003. Continual geological activity in Athabasca Valles, Mars. *Journal of Geophysical Research*, **108**, E128081, http://dx.doi.org/10.1029/2002JE002020
- WICHMAN, R. W. & SCHULTZ, P. H. 1995. Floor-fractured impact craters on Venus: implications for igneous crater modification and local mechanism. *Journal of Geophysical Research*, **100**, 3233–3244.

- WICHMAN, R. W. & SCHULTZ, P. H. 1996. Crater-centered laccoliths on the Moon: modeling intrusion depth and magmatic pressure at the crater Taruntius. *Icarus*, 122, 193–199.
- WIECZOREK, M. A., JOLLIFF, B. L. ET AL. 2006. The constitution and structure of the lunar interior. Reviews in Mineralogy and Geochemistry, 60, 221–364, http://dx.doi.org/10.2138/rmg.2006.60.3, 2006
- WILHELMS, D. E. 1976. Mercurian volcanism questioned. *Icarus*, **28**, 551–558.
- WILHELMS, D. E. 1987. The Geologic History of the Moon. United States Geological Survey, Professional Papers, 1348.
- WILHELMS, D. E. 1979. *Relative Ages of Lunar Basins*. Reports of the Planetary Geology Program.
- WILHELMS, D. E. & McCauley, J. F. 1971. Geologic Map of the Near Side of the Moon. United States Geological Survey, Miscellaneous Geologic Investigations Series Map, 1-703.
- WILHELMS, D. E. & SQUYRES, S. W. 1984. The martian hemispheric dichotomy may be due to a giant impact. *Nature*, 309, 138–140.
- WILLIAMS, D. A., FAGENTS, S. A. & GREELEY, R. 2000. A reevaluation of the emplacement and erosional potential of turbulent, low-viscosity lavas on the Moon. *Journal of Geophysical Research*, **105**, 20 189–20 206.
- WILLIAMS, D. A., GREELEY, R. ET AL. 2007. Hadriaca Patera: insights into its volcanic history from Mars Express High Resolution Stereo Camera. Journal of Geophysical Research, 112, E10004, http://dx.doi. org/10.1029/2007JE002924
- WILLIAMS, D. A., GREELEY, R., WERNER, S. C., MICHAEL, G., CROWN, D. A., NEUKUM, G. & RAITALA, J. 2008. Tyrrhena Patera: geologic history derived from Mars Express High Resolution Stereo Camera. *Journal of Geophysical Research*, 113, E11005, http://dx.doi. org/10.1029/2008JE003104
- WILLIAMS, D. A., GREELEY, R. *Et al.* 2009. The Circum-Hellas volcanic province: overview. *Planetary and Space Science*, **57**, 895–916, http://dx.doi.org/10.1016/j.pss.2008.08.010
- WILLIAMS, D. A., GREELEY, R., MANFREDI, L., RAITALA, J. & NEUKUM, G. 2010. The Circum-Hellas volcanic province, Mars: assessment of wrinkle-ridged plains. *Earth and Planetary Science Letters*, 294, 492–505.
- WILLIAMS, N. R., WATTERS, T. R., PRITCHARD, M. E., BANKS, M. E. & BELL, J. F. 2013. Fault dislocation modeled structure of lobate scarps from Lunar Reconnaissance Orbiter Camera digital terrain models. *Journal of Geophysical Research*, 118, 224–233, http://dx.doi.org/10.1002/jgre.20051
- WILLIAMS-JONES, G., WILLIAMS-JONES, A. E. & STIX, J. 1998. The nature and origin of Venusian canali. Journal of Geophysical Research, 103, 8545–8555.
- WILSON, L. & HEAD, J. W. 1981. Ascent and eruption of basaltic magma on the earth and moon. *Journal of Geo*physical Research, 86, 2971–3001.
- WILSON, L. & HEAD, J. W. 1983. A comparison of volcanic eruption processes on Earth, Moon, Mars, Io, and Venus. *Nature*, 302, 663–669.
- WILSON, L. & HEAD, J. W. 1990. Factors controlling the structures of magma chambers in basaltic volcanoes.

- Abstract 1343 1344 presented at the 21st Lunar & Planetary Science Conference, Houston, Texas.
- WILSON, L. & HEAD, J. W. 2002. Tharsis-radial graben systems as the surface manifestations of plumerelated dike intrusion complexes: models and implications. *Journal of Geophysical Research*, 107, 5019.
- WILSON, L. & HEAD, J. W. 2003. Lunar Gruithuisen and Mairan domes: rheology and mode of emplacement. *Journal of Geophysical Research*, 108, 5012, http://dx.doi.org/10.1029/2002JE001909
- WISE, D. U., GOLOMBEK, M. P. & McGILL, G. E. 1979. Tectonic evolution of Mars. *Journal of Geophysical Research*, 84, 7934–7939.
- WOOD, C. A. & HEAD, J. W. 1975. Geologically setting and provenance of spectrally distinct pre-mare material of possible volcanic origin. Paper presented at the Conference on Origins of Mare Basalts and their Implications for Lunar Evolution, November 17–19, 1975, Houston, Texas.
- WOOD, J. A., DICKEY, J. S., MARVIN, U. B. & POWELL, B. N. 1970. Lunar anorthosites and a geophysical model of the Moon. *In*: LEVINSON, A. A. (ed.) *Proceedings* of the Apollo 11 Lunar Science Conference, Volume 1. Pergamon Press, New York, 965–988.
- WYATT, M. B. & McSween, H. Y. 2002. Spectral evidence for weathered basalt as an alternative to andesite in the northern lowlands of Mars. *Nature*, 417, 263–266.
- WYRICK, D. Y., MORRIS, A. P., TODT, M. K. & WATSON-MORRIS, M. J. 2014. Physical analogue modelling of Martian dyke-induced deformation. *In:* PLATZ, T., MASSIRONI, M., BYRNE, P. K. & HIESINGER, H. (eds) *Volcanism and Tectonism Across the Inner Solar System*. Geological Society, London, Special Publications, 401. First published online June 23, 2014, http://dx.doi.org/10.1144/SP401.15
- XIAO, L., HUANG, J., CHRISTENSEN, P. R., GREELEY, R., WILLIAMS, D. A., ZHAO, J. & HE, Q. 2012. Ancient volcanism and its implication for thermal evolution on Mars. Earth and Planetary Science Letters, 323–324, 9–18.
- YIN, A. 2012. Structural analysis of the Valles Marineris fault zone: possible evidence for large-scale strike-slip faulting on Mars. *Lithosphere*, 4, 286–330.
- ZHONG, S. & ZUBER, M. T. 2001. Degree-1 mantle convection and the crustal dichotomy on Mars. *Earth and Planetary Science Letters*, **189**, 75–84.
- ZIETHE, R., SEIFERLEIN, K. & HIESINGER, H. 2009. Duration and extent of lunar volcanism: comparison of 3D convection models to mare basalt ages. *Planetary and Space Science*, **57**, 784–796.
- ZIMBELMAN, J. R. 1985. Estimates of rheologic properties for flows on the Martian volcano Ascraeus Mons. *Journal of Geophysical Research*, **90**, 157–162.
- ZUBER, M. T. 1995. Wrinkle ridges, reverse faulting, and the depth penetration of lithospheric strain in Lunae Planum, Mars. *Icarus*, **114**, 80–92.
- ZUBER, M. T. & MOUGINIS-MARK, P. J. 1992. Caldera subsidence and magma chamber depth of the Olympus Mons volcano, Mars. *Journal of Geophysical Research*, 97, 18 295–18 307.